

Proceedings of the Mini-Workshop
Effective Quark-Quark Interaction

Bled, Slovenia, July 7-14, 2003

Edited by

Bojan Golli
Mitja Rosina
Simon Širca

University of Ljubljana and Jožef Stefan Institute

DMFA – ZALOŽNIŠTVO
LJUBLJANA, NOVEMBER 2003

The Mini-Workshop *Effective Quark-Quark Interaction*

was organized by

Jožef Stefan Institute, Ljubljana

Department of Physics, Faculty of Mathematics and Physics, University of Ljubljana

and sponsored by

Ministry of Education, Science and Sport of Slovenia

Department of Physics, Faculty of Mathematics and Physics, University of Ljubljana

Society of Mathematicians, Physicists and Astronomers of Slovenia

Organizing Committee

Simon Širca

Mitja Rosina

Bojan Golli

List of participants

Katharina Berger, Graz, katharina.berger@uni-graz.at

Michael Beyer, Rostock, beyer@topas.physik2.uni-rostock.de

Veljko Dmitrašinović, Belgrade, dmitrasin@yahoo.com

Leonid Glozman, Graz, leonid.glozman@uni-graz.at

Dubravko Horvatic, Zagreb, davorh@phy.hr

Mariana Kirchbach, San Luis Potosi, Mexico, mariana@ifisica.uaslp.mx

Dubravko Klabučar, Zagreb, klabucar@phy.hr

Willibald Plessas, Graz, plessas@bkfug.kfunigraz.ac.at

Bianka Sengl, Graz, bianka.sengl@uni-graz.at

Ica Stancu, Liege, fstancu@ulg.ac.be

Daniele Treleani, Trieste, daniel@ts.infn.it

Robert Wagenbrunn, Graz, robert.wagenbrunn@uni-graz.at

Bojan Golli, Ljubljana, bojan.golli@ijs.si

Damijan Janc, Ljubljana, damijan.janc@ijs.si

Borut Tone Oblak, Ljubljana, b_oblak@hotmail.com

Mitja Rosina, Ljubljana, mitja.rosina@ijs.si

Simon Širca, Ljubljana, simon.sirca@fmf.uni-lj.si

Electronic edition

<http://www-fl.ijs.si/BledPub/>

Contents

Preface	V
Point-Form and Instant-Form Calculations of Electromagnetic Form Factors	
<i>K. Berger</i>	1
Light front field theory of quark matter at finite temperature	
<i>M. Beyer</i>	11
Scalar mesons in the Gaussian approximation to the linear Σ model	
<i>V. Dmitrašinović</i>	19
Quark-meson model in a Tamm-Dancoff inspired approximation	
<i>D. Horvat, D. Horvatić, D. Tadić</i>	29
Autoclustering in baryon spectra	
<i>M. Kirchbach</i>	37
$\langle A^2 \rangle$-condensate and Dyson-Schwinger approach to mesons	
<i>D. Klabučar, D. Kekez</i>	47
Relativistic Constituent Quark Models: Theory and Applications	
<i>W. Plessas</i>	57
Effective Quark-Quark Interaction in Baryons	
<i>B. Sengl</i>	61
The role of a three-body confinement interaction in pentaquarks	
<i>Fl. Stancu</i>	69
$b\bar{b}b\bar{b}$ production in NN and NA interactions at the LHC	
<i>A. Del Fabbro and D. Treleani</i>	75
Covariant electromagnetic and axial form factors in a constituent quark model	
<i>R.F. Wagenbrunn</i>	79
Calculation of electroproduction amplitudes in the K-matrix formalism	
<i>B. Golli</i>	83

Double Charmed Tetraquarks

D. Janc, M. Rosina 89

A simplified collective model of pion

B. T. Oblak 95

Is the $cc\bar{u}\bar{d}$ tetraquark bound?

M. Rosina, D. Janc 103

Structure of the nucleon and the Δ from pion electro-production experiments at MAMI

S. Širca 107

Preface

The beautiful environment of Lake Bled and the cosy Villa Plemely have once again proven to be the stimuli that brightened up the atmosphere at this year's Mini-Workshop on Effective Quark-Quark Interaction. In spite of its title, the Workshop was general enough to include confrontations of meson-exchange and gluon-exchange forces, to question the need for three-body forces, as well as to discuss the restoration of chiral symmetry, deconfinement, and diquark clustering. We were eager to hear about the new experimental evidence of tetraquarks and pentaquarks, and latest results which will help us understand the nucleon and Δ form-factors and, to a large extent, the importance of relativity.

The series of Mini-Workshops at Bled which started in 1987, has established its peculiar character of friendly yet critical exchange of ideas. The scope of these small-scale meetings therefore remains to confront people working on closely related problems in hadronic physics, and to engage participants in comprehensive discussions without the time constraints of "official" meetings. This format and spirit of the Workshop has by now become traditional, and we are pleased to see that our guests invariably enjoy it. The Proceedings, initially published only in a web-edition, have also evolved into a full-fledged serial publication. We issue this booklet to help you better remember the flavour of the discussions, the impressive results, some credible and some less credible conclusions, and to help you see which gaps you would like to fill at the next Mini-Workshop.

Ljubljana, November 2003

B. Golli
M. Rosina
S. Širca

Workshops organized at Bled

- ▷ *What Comes beyond the Standard Model* (June 29–July 9, 1998)
Bled Workshops in Physics **0** (1999) No. 1
- ▷ *Hadrons as Solitons* (July 6-17, 1999)
- ▷ *What Comes beyond the Standard Model* (July 22–31, 1999)
- ▷ *Few-Quark Problems* (July 8-15, 2000)
Bled Workshops in Physics **1** (2000) No. 1
- ▷ *What Comes beyond the Standard Model* (July 17–31, 2000)
- ▷ *Statistical Mechanics of Complex Systems* (August 27–September 2, 2000)
- ▷ *Selected Few-Body Problems in Hadronic and Atomic Physics* (July 7-14, 2001)
Bled Workshops in Physics **2** (2001) No. 1
- ▷ *What Comes beyond the Standard Model* (July 17–27, 2001)
Bled Workshops in Physics **2** (2001) No. 2
- ▷ *Studies of Elementary Steps of Radical Reactions in Atmospheric Chemistry*
- ▷ *Quarks and Hadrons* (July 6-13, 2002)
Bled Workshops in Physics **3** (2002) No. 3
- ▷ *What Comes beyond the Standard Model* (July 15–25, 2002)
Bled Workshops in Physics **3** (2002) No. 4
- ▷ *Effective Quark-Quark Interaction* (July 7-14, 2003)
Bled Workshops in Physics **4** (2003) No. 1
- ▷ *What Comes beyond the Standard Model* (July 17-27, 2003)

Also published in this series

- ▷ Book of Abstracts, *XVIII European Conference on Few-Body Problems in Physics*, Bled, Slovenia, September 8–14, 2002, Edited by Rajmund Krivec, Bojan Golli, Mitja Rosina, and Simon Širca
Bled Workshops in Physics **3** (2002) No. 1–2



Point-Form and Instant-Form Calculations of Electromagnetic Form Factors*

K. Berger

Institut für Theoretische Physik, Universität Graz, Universitätsplatz 5, A-8010 Graz,
Austria

1 Introduction

In the nonperturbative regime of quantum chromodynamics (QCD), low-energy phenomena of hadrons are suitably described by constituent quark models (CQMs). These models incorporate relativity and the relevant properties of QCD such as, e.g., the spontaneous breaking of chiral symmetry ($SB\chi S$), which can be considered as being responsible for the appearance of (nearly) massless Goldstone bosons and constituent quarks. The latter can be viewed as relativistic quasi-particles with a dynamically generated mass, and - together with the Goldstone bosons - they represent the new degrees of freedom at low energies [11].

Based on this observation the Graz group constructed the so-called Goldstone-boson-exchange (GBE) CQM [9]. The three-quark Hamiltonian of this model consists of a relativistic kinetic-energy operator, a linear confinement potential and a hyperfine interaction derived from GBE.

The GBE CQM turned out to be rather successful in describing the spectra of all light and strange baryons in a unified framework [8], thereby resolving some long-standing problems in baryon spectroscopy, such as the level ordering of positive- and negative-parity nucleon excitations.

Beyond spectroscopy, the validity of any CQM has to be tested with regard to other observables, e.g., the electroweak nucleon structure. Up till now the GBE CQM has been found to be very adequate for the description of electromagnetic and axial form factors of the nucleons [17,6,10], baryon electric radii and magnetic moments [4,5]. The direct predictions obtained in the point-form approach to relativistic quantum mechanics agree surprisingly well with phenomenology in all cases where experimental data exist. Furthermore the GBE CQM has been successfully applied in studies of tetraquarks, pentaquarks [15], the N-N interaction [3] as well as mesonic resonance decays [14].

The performance of the GBE CQM with respect to the covariant description of the electroweak nucleon structure along the point form is critically discussed by Robert Wagenbrunn in his contribution to this Workshop [16]. Here we concentrate on a comparison of the point-form approach to the one along the instant form. We shortly outline the differences in the two formulations and provide a

* This work was supported by the Austrian Science Fund, project no. P14806-TPH.

quantitative comparison of the corresponding results for a two-body toy model and for the realistic case of the nucleons (using the wave functions of the GBE CQM).

2 Formalisms of the Calculation of Form Factors

In order to reach a reasonable description of the three-quark system, relativistic effects have to be properly taken into account. The demand of Lorentz covariance can be satisfied in the framework of Poincaré-invariant quantum mechanics. Among the several possibilities already outlined by Dirac [7], we consider in the first instance the point-form approach [12].

2.1 Point Form

The point form is characterized by the property that the interactions are contained only in the generators of the space-time translations, namely, the four-momentum operator P^μ . The fundamental operator equations – known as the point-form equations – are written in terms of the four-momentum operator as

$$[P^\mu, P^\nu] = 0 \quad (1)$$

$$U_\Lambda P^\mu U_\Lambda^{-1} = (\Lambda^{-1})^\mu_\nu P^\nu, \quad (2)$$

with U_Λ a unitary operator representing the Lorentz transformation Λ . Since the Lorentz boost transformations and the spatial rotations remain purely kinematic, the theory is manifestly covariant. Starting out from the free mass operator $M_{\text{free}} = \sqrt{P_{\text{free}}^\mu P_{\text{free},\mu}}$ the interaction can be introduced into the theory via the Bakamjian-Thomas construction [2] defining the full mass operator by

$$M = \sqrt{P^\mu P_\mu} = M_{\text{free}} + M_{\text{int}}. \quad (3)$$

The interacting mass operator M_{int} is obtained by replacing the free Hamiltonian H_{free} by the full Hamiltonian $H = H_{\text{free}} + H_{\text{int}}$, where H_{int} is the quark-quark potential. Then the four-momentum operator takes the following form

$$P^\mu = P_{\text{free}}^\mu + P_{\text{int}}^\mu = M V^\mu = (M_{\text{free}} + M_{\text{int}}) V^\mu \quad (4)$$

with V^μ the free four-velocity operator. The eigenstates Ψ and eigenvalues M_B of the system can be obtained by solving the eigenvalue equation of the full mass operator

$$M\Psi = M_B\Psi. \quad (5)$$

Velocity States The free three-body states (as simultaneous eigenstates of the operators P_{free}^μ , M_{free} , and H_{free})

$$|p_1 \sigma_1; p_2 \sigma_2; p_3 \sigma_3\rangle \quad (6)$$

of three spin- $\frac{1}{2}$ particles with masses m_i , four-momenta p_i , and z-projections σ_i of the spins (with $i = 1, 2, 3$) can be constructed as direct products of single-particle states just as in nonrelativistic quantum mechanics. The Lorentz transformations of these states

$$\begin{aligned} U_\Lambda |p_1 \sigma_1; p_2 \sigma_2; p_3 \sigma_3\rangle = \\ \prod_{k=1}^3 D_{\sigma'_k \sigma_k}^{\frac{1}{2}} [R_W(p_i, \Lambda)] |(\Lambda p_1) \sigma'_1; (\Lambda p_2) \sigma'_2; (\Lambda p_3) \sigma'_3\rangle \end{aligned} \quad (7)$$

involve three different Wigner rotations $R_W(p_i, \Lambda) = B^{-1}(\Lambda p_i) \Lambda B(p_i)$. Here, $B(p_i)$ is a canonical (i.e. rotationless) spin boost.

For the calculation of the invariant form factors it is convenient to introduce so-called velocity states defined by

$$\begin{aligned} |v; \mathbf{k}_1 \mu_1; \mathbf{k}_2 \mu_2; \mathbf{k}_3 \mu_3\rangle = U_{B(v)} |k_1 \mu_1; k_2 \mu_2; k_3 \mu_3\rangle \\ = \sum_{\sigma_1, \sigma_2, \sigma_3} \prod_{i=1}^3 D_{\sigma_i \mu_i}^{\frac{1}{2}} [R_W(k_i, B(v))] |p_1 \sigma_1; p_2 \sigma_2; p_3 \sigma_3\rangle, \end{aligned} \quad (8)$$

where $|k_1 \mu_1; k_2 \mu_2; k_3 \mu_3\rangle$ are three-body states satisfying the constraint $\sum_i \mathbf{k}_i = 0$. The action of general Lorentz transformations on these velocity states is given by

$$\begin{aligned} U_\Lambda |v; \mathbf{k}_1 \mu_1; \mathbf{k}_2 \mu_2; \mathbf{k}_3 \mu_3\rangle = U_\Lambda U_{B(v)} |k_1 \mu_1; k_2 \mu_2; k_3 \mu_3\rangle \\ = U_{B(\Lambda v)} U_{R_W} |k_1 \mu_1; k_2 \mu_2; k_3 \mu_3\rangle \\ = \sum_{\mu'_1, \mu'_2, \mu'_3} \prod_{i=1}^3 D_{\mu'_i \mu_i}^{\frac{1}{2}} (R_W) |(\Lambda v); (R_W \mathbf{k}_1) \mu'_1; (R_W \mathbf{k}_2) \mu'_2; (R_W \mathbf{k}_3) \mu'_3\rangle. \end{aligned} \quad (9)$$

It is significant that each individual quark momentum in the velocity states is rotated by the same Wigner rotation $R_W = B^{-1}(\Lambda v) \Lambda B(v)$. This fact allows the treatment of spin and orbital angular momentum in the same way as in non-relativistic quantum mechanics. The individual-particle momenta p_i and k_i are related by $p_i = B(v) k_i$ with $\sum_i \mathbf{k}_i = 0$. It should be noted that velocity states are simultaneous eigenstates of the (interaction-free) operators M_{free} , V^μ , and P_{free}^μ , respectively.

In detail we write the baryon eigenstates $|\Psi\rangle$ in any arbitrary frame $\mathbf{P} = M_B \mathbf{v}$ as

$$|\Psi\rangle = |v, M_B, J, \Sigma\rangle, \quad (10)$$

from where it is evident that they are simultaneous eigenstates of the full mass operator M , the linear-momentum operator P^μ , the total-angular-momentum operator J^2 , and its z-component J_z . Evidently they are also eigenstates of the four-velocity operator V^μ .

Matrix Elements of Invariant Form Factors In order to calculate the electromagnetic form factors one has to evaluate the matrix elements of the current

operator $\mathcal{J}^\mu(x)$ sandwiched between eigenstates of the four-momentum operator P^μ . Using a generalized Wigner-Eckart theorem one can decompose these current matrix elements into Clebsch-Gordan coefficients times reduced matrix elements [12]. The latter can be identified with the invariant form factors. In the standard Breit frame the initial and final four-momenta of the system are given by $P_{\text{in}} = M_B(\cosh \frac{\Delta}{2}, 0, 0, -\sinh \frac{\Delta}{2})$ and $P_f = M_B(\cosh \frac{\Delta}{2}, 0, 0, \sinh \frac{\Delta}{2})$, respectively. The invariant momentum transfer along the z-axis can be written as

$$q^2 = -Q^2 = (P_f - P_{\text{in}})^2 = -4M_B^2(\sinh \frac{\Delta}{2})^2. \quad (11)$$

In the (standard) Breit frame the invariant form factor is given by

$$2\sqrt{M'_B M_B} F_{\Sigma', \Sigma}^\mu(Q^2) = \langle v'(st), M'_B, J', \Sigma' | \mathcal{J}^\mu(0) | v(st), M_B, J, \Sigma \rangle. \quad (12)$$

Here Σ', Σ are the invariant spin-projection labels and $|v(st), M_B, J, \Sigma\rangle$ the baryon eigenstates; in our case $v(st)$ is the nucleon velocity. In the elastic case ($M'_B = M_B$) the invariant form factors in the Breit frame can be expressed in terms of the electric (G_E) and magnetic (G_M) Sachs form factors of the nucleon

$$F_{\Sigma', \Sigma}^{\mu=0} = G_E \delta_{\Sigma', \Sigma} \quad (13)$$

$$F_{\Sigma', \Sigma} = i \frac{Q}{2M_B} G_M \chi_{\Sigma'}^\dagger (\boldsymbol{\sigma} \times \hat{z}) \chi_\Sigma \quad (14)$$

with χ_Σ the nucleon Pauli spinor.

PFSA Current For the practical calculation of the nucleon form factors defined in Eq. (12) one has to use a suitable representation of the nucleon eigenstates in the Hilbert space. For this purpose we employ the velocity states introduced in Eq. (8). As a result the current matrix elements are then expressed in terms of the individual quark coordinates. The corresponding integrals cannot be solved, however, for any general three-body current operator. At this point one has to make some simplification.

Here we assume the electromagnetic current to be a single-particle operator $\mathcal{J}_{[1]}^\mu(x)$, i.e. the virtual photon interacts only with one single quark and the other two are spectators. Therefore this is called point-form spectator approximation (PFSA). It can also be seen as a relativistic impulse approximation but specifically in point form. It is characterized by the fact that the momentum $q^2 = (P_f - P_{\text{in}})^2$ transferred to the nucleon is different from the momentum transfer \tilde{q}^2 felt by the struck constituent quark:

$$\tilde{q}^2 = (p'_i - p_i)^2 = (B[v'(st)]k'_i - B[v(st)]k_i)^2 = -\tilde{Q}^2 \neq q^2. \quad (15)$$

In PFSA the matrix element of the single-particle current operator can then be expressed as

$$\begin{aligned} & \langle p'_1 \sigma'_1, p'_2 \sigma'_2, p'_3 \sigma'_3 | \mathcal{J}_{[1]}^\mu(0) | p_1 \sigma_1, p_2 \sigma_2, p_3 \sigma_3 \rangle = 2E_2 2E_3 \\ & \times \delta^3(\mathbf{p}'_2 - \mathbf{p}_2) \delta^3(\mathbf{p}'_3 - \mathbf{p}_3) \delta_{\sigma'_2 \sigma_2} \delta_{\sigma'_3 \sigma_3} \langle p'_1 \sigma'_1 | j^\mu(0) | p_1 \sigma_1 \rangle \end{aligned} \quad (16)$$

with $E_i = \sqrt{\mathbf{p}_i^2 + m_i^2}$. For the quark current j^μ we take the standard form for the electromagnetic current operator of a pointlike Dirac particle with charge e_i

$$\langle p'_i \sigma'_i | j^\mu(0) | p_i \sigma_i \rangle = e_i \bar{u}(p'_i, \sigma'_i) \gamma^\mu u(p_i, \sigma_i). \quad (17)$$

The invariant form factors of the nucleon in PFSA can then be calculated by solving the multiple integrals

$$\begin{aligned} F_{\Sigma', \Sigma}^\mu(Q^2) = & 3 \int d\mathbf{k}_1 d\mathbf{k}_2 d\mathbf{k}_3 dk'_1 dk'_2 dk'_3 \delta(\mathbf{k}_1 + \mathbf{k}_2 + \mathbf{k}_3) \delta(\mathbf{k}'_1 + \mathbf{k}'_2 + \mathbf{k}'_3) \\ & \times \delta^3[k'_2 - B^{-1}(v_{\text{out}})B(v_{\text{in}})k_2] \delta^3[k'_3 - B^{-1}(v_{\text{out}})B(v_{\text{in}})k_3] \\ & \times \psi_{\Sigma'}^*(\mathbf{k}'_1, \mathbf{k}'_2, \mathbf{k}'_3; \mu'_1, \mu'_2, \mu'_3) \psi_{\Sigma}(\mathbf{k}_1, \mathbf{k}_2, \mathbf{k}_3; \mu_1, \mu_2, \mu_3) \\ & \times \sqrt{\frac{\omega'_2 \omega'_3}{\omega_2 \omega_3}} \frac{1}{2\sqrt{\omega_1 \omega'_1}} D_{\lambda'_1 \mu'_1}^{1/2} [R_W(k'_1, B(v_{\text{out}}))] \\ & \times \langle p'_1 \lambda'_1 | j^\mu(0) | p_1 \lambda_1 \rangle D_{\lambda_1 \mu_1}^{1/2} [R_W(k_1, B(v_{\text{in}}))] \\ & \times D_{\mu'_2 \mu_2}^{1/2} [R_W(k_2, B^{-1}(v_{\text{out}})B(v_{\text{in}}))] \\ & \times D_{\mu'_3 \mu_3}^{1/2} [R_W(k_3, B^{-1}(v_{\text{out}})B(v_{\text{in}}))] . \end{aligned} \quad (18)$$

Here, v_{in} and v_{out} are the initial and final four-velocities in the Breit frame, defined by the nucleon total momentum as $M_B v_{\text{in}} = P_{\text{in}}$ and $M_B v_{\text{out}} = P_f$, respectively, with M_B the nucleon mass. The center-of-momentum wave function ψ_{Σ} (with Σ the nucleon total spin projection) depends on the individual intrinsic quark momenta \mathbf{k}_i and on the spin projections μ_i . The electric form factor G_E of the nucleon is given by the zero-component $F_{\Sigma', \Sigma}^{\mu=0}$, whereas the magnetic form factor G_M can be obtained either from the $F_{\Sigma', \Sigma}^{\mu=1}$ or the $F_{\Sigma', \Sigma}^{\mu=2}$ components in Eq. (18). Due to current conservation, $F_{\Sigma', \Sigma}^{\mu=3}$ must vanish.

2.2 Instant Form

In the instant form the interactions are contained in the three generators of the canonical Lorentz boosts \mathbf{K} and in the zero-component of the four-momentum operator, namely the Hamiltonian H . The spatial components \mathbf{P} of the linear momentum as well as of the angular momentum operator \mathbf{J} remain kinematic. This implies simple addition rules for spins and orbital angular momenta. In contrast to the point form, the boost transformation of observables from one inertial frame to another is complicated due to the interaction-dependence of the boosts.

Again, the interaction is introduced via the Bakamjian-Thomas construction like in Eq. (3). Then the Hamiltonian H and the boost generators \mathbf{K} are given by

$$H = \sqrt{M^2 + \mathbf{P}_{\text{free}}^2} = \sqrt{(M_{\text{free}} + M_{\text{int}})^2 + \mathbf{P}_{\text{free}}^2} \quad (19)$$

$$\mathbf{K} = -\frac{1}{2} \{H, \mathbf{X}_{c, \text{free}}\} - \frac{\mathbf{P}_{\text{free}} \times \mathbf{j}_{c, \text{free}}}{M + H} \quad (20)$$

where $\mathbf{X}_{c, \text{free}}$ and $\mathbf{j}_{c, \text{free}}$ are free auxiliary operators (for details see [13]).

Momentum States In instant form, it is most convenient to use momentum eigenstates (instead of the velocity states in point form). In any arbitrary frame with momentum \mathbf{P} they are given by the Lorentz transformation

$$|\mathbf{P}, \mathbf{k}_i, \mu_i\rangle = \sum_{\sigma_1, \sigma_2, \sigma_3} \prod_{i=1}^3 D_{\sigma_i \mu_i} [R_W(\mathbf{k}_i, B(\mathbf{P}_{\text{free}}/M_{\text{free}}))] |p_i \sigma_i\rangle. \quad (21)$$

Here, the relation between the individual momenta p_i and k_i is given by $p_i = B(\mathbf{P}_{\text{free}}/M_{\text{free}})k_i$, where $M_{\text{free}} = \sum_i \omega_i$ is the eigenvalue of the free mass operator M_{free} with $\omega_i = \sqrt{\mathbf{k}_i^2 + m_i^2}$. Note that in instant form $\mathbf{P} = \mathbf{P}_{\text{free}}$. The momentum states $|\mathbf{P}, \mathbf{k}_i, \mu_i\rangle$ are simultaneous eigenstates of the free four-momentum operator P_{free}^μ and of the free mass operator M_{free} .

Now we write the baryon eigenstates $|\Psi\rangle$ in any arbitrary frame \mathbf{P} as

$$|\Psi\rangle = |\mathbf{P}, J, \Sigma\rangle. \quad (22)$$

Here it is emphasized that they are eigenstates of the four-momentum operator P^μ . Evidently, they are also eigenstates of the mass operator M and the four-velocity operator V^μ ; the latter, however, is no longer the free velocity (as in the point form) but interaction-dependent.

Matrix Elements of Invariant Form Factors Using the notation of the states as in Eq. (22) the invariant form factors in the Breit frame (cf. Eq. (12)) are given by

$$2\sqrt{M'_B M_B} F_{\Sigma', \Sigma}^\mu(Q^2) = \langle P_f, J', \Sigma' | \mathcal{J}^\mu(0) | P_{\text{in}}, J, \Sigma \rangle. \quad (23)$$

where the initial and final momenta P_{in} and P_f are again related by Eq. (11).

IFSA Current For the calculation of the electromagnetic form factors already defined in Eq. (23) we insert the completeness relation for the momentum states to rewrite the current matrix elements in the Breit frame in terms of the elementary degrees of freedom.

Now we make an analogous simplifying assumption about the current as before in the point form in order to arrive at a single-particle operator. In particular, we replace the current operator by $\mathcal{J}_{[1]}^\mu(x)$, meaning that one quark is struck by the virtual photon, whereas the other two are spectators. This is called the instant-form spectator approximation (IFSA). In instant form, however, the spatial components of the momentum transfer \mathbf{q} on the nucleon coincide with the momentum $\tilde{\mathbf{q}}$ transferred to the struck quark

$$\mathbf{q} = \mathbf{P}_f - \mathbf{P}_{\text{in}} = \mathbf{p}'_i - \mathbf{p}_i = \tilde{\mathbf{q}}. \quad (24)$$

This relation, which is evidently different from the one in point form, is a consequence of the fact that in instant form the spatial components of the momentum operator are interaction-free, while the boost operators do contain interactions. Using the fact that for the spectator quarks $i = 2, 3$ the initial and final momenta

are equal, $p_i = p'_i$, one can derive a relation between the internal four-momenta k_i and k'_i before and after the photon interaction

$$k'_i = B(P'_{\text{free}}/M'_{\text{free}})^{-1} B(P_{\text{free}}/M_{\text{free}}) k_i. \quad (25)$$

Assuming pointlike Dirac particles, the single-particle current takes the standard form of Eqs. (16) and (17). Finally, the IFSA expression for the invariant electromagnetic form factors in the Breit frame is

$$\begin{aligned} F_{\Sigma', \Sigma}^{\mu} (Q^2) &= 3 \int dk_1 dk_2 dk_3 dk'_1 dk'_2 dk'_3 \delta(\mathbf{k}_1 + \mathbf{k}_2 + \mathbf{k}_3) \delta(\mathbf{k}'_1 + \mathbf{k}'_2 + \mathbf{k}'_3) \\ &\times \delta^3 \left[k'_2 - B^{-1} \left(\frac{P'_{\text{free}}}{M'_{\text{free}}} \right) B \left(\frac{P_{\text{free}}}{M_{\text{free}}} \right) k_2 \right] \delta^3 \left[k'_3 - B^{-1} \left(\frac{P'_{\text{free}}}{M'_{\text{free}}} \right) B \left(\frac{P_{\text{free}}}{M_{\text{free}}} \right) k_3 \right] \\ &\times \psi_{\Sigma'}^* (k'_1, k'_2, k'_3; \mu'_1, \mu'_2, \mu'_3) \psi_{\Sigma} (k_1, k_2, k_3; \mu_1, \mu_2, \mu_3) \\ &\times \sqrt{\frac{P'_{\text{free}} P_{\text{free}}}{M'_B M_B}} \sqrt{\frac{M_{\text{free}} E'_{\text{free}} (\prod \omega'_i)}{M'_{\text{free}} E_{\text{free}} (\prod \omega_i)}} \frac{1}{2E'_1} D_{\lambda'_1 \mu'_1}^{1/2 *} [R_W(k'_1, B(P'_{\text{free}}/M'_{\text{free}}))] \\ &\times \langle p'_1 \lambda'_1 | j^\mu | p_1 \lambda_1 \rangle D_{\lambda_1 \mu_1}^{1/2} [R_W(k_1, B(P_{\text{free}}/M_{\text{free}}))] \\ &\times D_{\mu'_2 \mu_2}^{1/2} [R_W(k_2, B^{-1}(P'_{\text{free}}/M'_{\text{free}}) B(P_{\text{free}}/M_{\text{free}}))] \\ &\times D_{\mu'_3 \mu_3}^{1/2} [R_W(k_3, B^{-1}(P'_{\text{free}}/M'_{\text{free}}) B(P_{\text{free}}/M_{\text{free}}))] . \end{aligned} \quad (26)$$

Here, $E_{\text{free}} = \sqrt{\mathbf{P}^2 + M_{\text{free}}^2}$ is the free energy. As before, the electric form factor G_E of the nucleon is given by the zero-component $F_{\Sigma', \Sigma}^{\mu=0}$ and the magnetic form factor G_M either by $F_{\Sigma', \Sigma}^{\mu=1}$ or $F_{\Sigma', \Sigma}^{\mu=2}$.

3 Results

In this chapter we present the comparison of the point-form and instant-form calculations of the electromagnetic form factors for a two-body toy model and for a realistic three-body system, namely, the case of the nucleon in the relativistic CQM with GBE hyperfine interactions. Always a single-particle approximation to the full current operator is used, i.e. the results are obtained for the PFSA and IFSA.

3.1 Two-Body System

For the comparison in case of a two-body system we first considered the Wick-Cutkosky model, i.e. a system of two spinless particles interacting via the exchange of a scalar massless boson. The same case has been studied before by A. Amghar et al. [1], and we have essentially recovered the same results. For both the scalar and vector form factors the IFSA and PFSA results are quite similar for low momentum transfers, while they become very distinct at higher momentum transfers.

As a next case we have examined a two-body system with spin. In particular, we have calculated a system of two spin- $\frac{1}{2}$ particles with the same type of mutual

interaction as in the Wick-Cutkosky model (exchange of a scalar massless boson). Here one has four form factors, one for total spin $S = 0$ and three for $S = 1$. In Fig. 3.1 below we only show the electric and magnetic form factors for $S = 1$, $G_E(Q^2)$ and $G_M(Q^2)$, respectively. We demonstrate the behavior of the IFSA and PFSA results and give a comparison to the predictions in nonrelativistic impulse approximation (NRIA) for a certain weak coupling strength characterized by the value $M/m = 1.784$ for the ratio of the total to the constituent mass. It is evident that at low momentum transfers the IFSA and PFSA results are rather similar. The differences grow towards higher momentum transfers. The PFSA results are always lower than the ones of the IFSA; the latter are practically intermediate to the NRIA results. Qualitatively these characteristics are found for all form factors, also the ones not shown here. The discrepancies even grow if the coupling strength is increased.

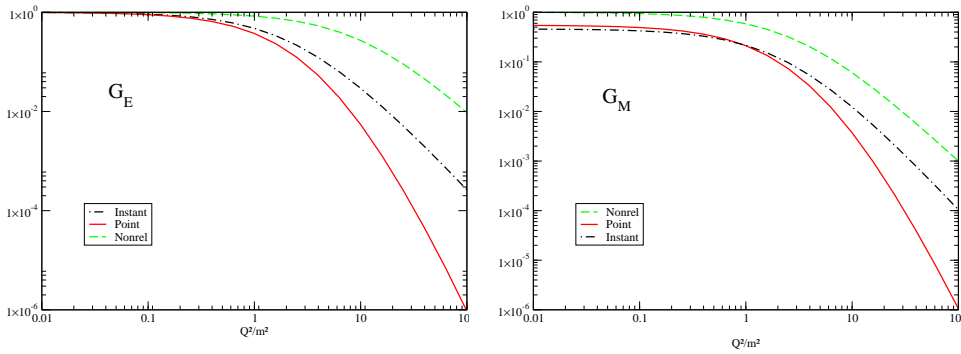


Fig. 1. Electric and magnetic form factors for a two-body system of spin- $\frac{1}{2}$ particles with total spin $S = 1$ calculated in PFSA (solid line), IFSA (dashed-dotted line), and in NRIA (dashed line).

3.2 Three-Body System

Here we consider the same comparison as above but for the case of the nucleon with a realistic wave function and all spins properly included. In Fig. 3.2 we repeat the PFSA results as obtained before with the GBE CQM [17,6,10] and contrast them to the analogous predictions in IFSA and to the NRIA results. It is immediately evident that the IFSA is always very distinct from the PFSA, even at rather small momentum transfers. In IFSA the momentum dependence of the form factors is nowhere matching the one demanded by the experimental data. Not even the electromagnetic observables at $Q^2 = 0$, namely the electric radii and magnetic moments, can be reproduced in a reasonable manner. In fact, the IFSA is quite similar to the NRIA, at least in case of the electric form factors.

In view of the present comparison it appears even the more remarkable that the PFSA results incidentally agree with the experimental data in all aspects investigated so far (electromagnetic and axial nucleon form factors, electric radii

and magnetic moments of the proton, the neutron and other light and strange baryons [17,6,10,4,5]). Note that we are here dealing with direct predictions of the CQM with no additional parameters introduced in the calculation of the form factors. In order to bring the IFSA results closer to the experimental data one would have to include further ingredients like, e.g., quark form factors.

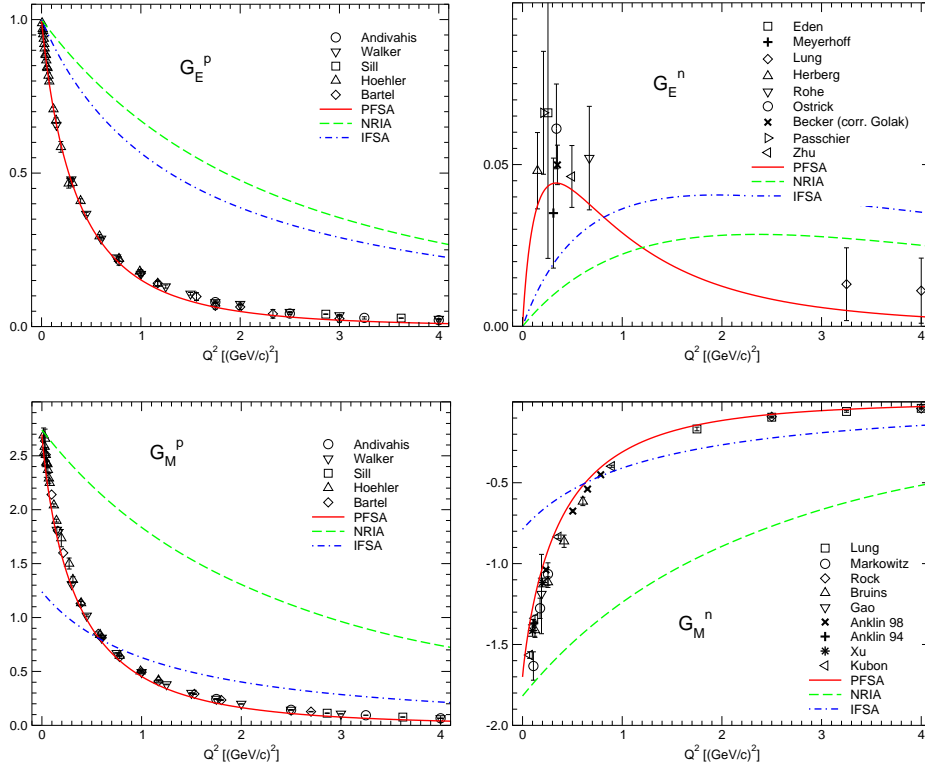


Fig. 2. Electric (upper) and magnetic (lower) form factors of the proton (left) and neutron (right) calculated in PFSA (solid line), IFSA (dashed-dotted line), and in NRIA (dashed line) for the case of the GBE CQM.

4 Conclusion and Outlook

We have made a consistent comparison of the spectator approximation for the electromagnetic current operator in the point and instant forms. The differences of the PFSA and IFSA results for the form factors are demonstrated for two- and three-body bound states of spin- $\frac{1}{2}$ particles. In all cases big discrepancies are found between the PFSA and IFSA results. Regarding the nucleon form factors, the PFSA predictions of the relativistic GBE CQM are remarkably close to the experimental data up to momentum transfers of $Q^2 \sim 1 \text{ GeV}^2$. The analogous IFSA results fail in all respects.

In the context of the present comparison a number of intriguing questions arise. For instance, one must ask what is effectively included (from possible many-body currents) in the spectator approximation in either approach. It is clear that the PFSA current corresponds to a many-body current in instant form and vice versa. Furthermore, each formulation has its own deficiencies. The PFSA current (a-priori) does not strictly fulfill current conservation, even though the violation has been found to be small [16]. Current conservation is also violated in the IFSA. In addition, the IFSA results are frame-dependent – contrary to the PFSA results, which are manifestly covariant. One has to consider this as a serious drawback of the IFSA. One may change the predictions arbitrarily by moving from one frame to another. Specifically, the results are different in the Breit and laboratory frames.

Of course, it is an urgent demand to clarify these problems. Obviously, the adequacy of the spectator approximation can only be estimated in a reliable manner if the contributions of two- and many-body currents are determined. It appears as an ambitious aim to construct these many-body currents in a consistent manner and to complete the relativistic description of electromagnetic form factors.

References

1. A. Amghar, B. Desplanques, and L. Theußl. Nucl. Phys. A **714** (2003) 213.
2. B. Bakamjian and L. H. Thomas. Phys. Rev. **92** (1953) 1300.
3. D. Bartz and F. Stancu. Phys. Rev. C, **60** (1999) 1999.
4. K. Berger, W. Plessas, and R. F. Wagenbrunn. Few-Body Syst., Suppl. **14** (2003) 53.
5. K. Berger, W. Plessas, and R. F. Wagenbrunn. Prog. Part. Nucl. Phys. **50** (2003) 281.
6. S. Boffi, L. Ya. Glozman, W. Klink, W. Plessas, M. Radici, and R. F. Wagenbrunn. Eur. Phys. J. A **14** (2002) 17.
7. P. A. M. Dirac. Rev. Mod. Phys. **21** (1949) 392.
8. L. Ya. Glozman, Z. Papp, W. Plessas, K. Varga, and R. F. Wagenbrunn. Phys. Rev. C **57** (1998) 3406.
9. L. Ya. Glozman, W. Plessas, K. Varga, and R. F. Wagenbrunn. Phys. Rev. D **58** (1998) 094030.
10. L. Ya. Glozman, M. Radici, R. F. Wagenbrunn, S. Boffi, W. Klink, and W. Plessas. Phys. Lett. B **516** (2001) 183.
11. L. Ya. Glozman and D. O. Riska. Phys. Rep. **268** (1996) 263.
12. W. H. Klink. Phys. Rev. C **58** (1998) 3587.
13. A. Krassnigg. Dissertation, University of Graz, 2001. (unpublished).
14. T. Melde, R. F. Wagenbrunn, and W. Plessas. Few-Body Syst., Suppl. **14** (2003) 37.
15. F. Stancu. Phys. Rev. D **58** (1998) 111501.
16. R. F. Wagenbrunn. Contribution to this Workshop, 2003.
17. R. F. Wagenbrunn, S. Boffi, W. Klink, W. Plessas, and M. Radici. Phys. Lett. B **511** (2001) 33.



Light front field theory of quark matter at finite temperature ^{*}

Michael Beyer

Fachbereich Physik, University of Rostock, D-18051 Rostock, Germany

Abstract. A light front field theory for finite temperature and density is currently being developed. It will be used here to describe the transition region from quark matter to nuclear matter relevant in heavy ion collisions and in the early universe. The energy regime addressed is extremely challenging, both theoretically and experimentally. This is because of the confinement of quarks, the appearance of bound states and correlations, special relativity, and nonlinear phenomena that lead to a change of the vacuum structure of quantum chromodynamics. In the region of the phase transition it eventually leads to a change of the relevant degrees of freedom. We aim at describing this transition from quarks to hadronic degrees of freedom in a unified microscopic approach.

1 Introduction

Lattice calculations of quantum chromodynamics (QCD) give firm evidence that nuclear matter undergoes a phase transition to a plasma state at a certain temperature T_c of about 170 to 180 MeV. Calculations have been performed at a chemical potential $\mu = 0$. Recent results are for staggered fermions [1,2] and renormalization group improved Wilson fermions [3]. The low density region reflects, e.g., the scenario during the evolution of the early universe. To achieve information from lattice calculations at small μ several methods have recently been developed, i.e., multiparameter reweighting [4,5], Taylor expansion at $\mu \simeq 0$ [6,7], imaginary μ [8–10]. The region of validity is approximately $\mu \lesssim T$ [11]. Effective approaches to QCD indicate an extremely rich phase diagram also for $\mu > T$ [12]. Experimentally the QCD phase diagram is accessible to heavy ion collisions. In particular relativistic heavy ion collision at SPS/CERN and RHIC/BNL explore the region where hadronic degrees of freedom are expected to be dissolved. Some results of RHIC are now available that give hints of a non-hadronic state of matter [13].

On the other hand light-front quantization of QCD can provide a rigorous alternative to lattice QCD [15]. Although the calculational challenge in real QCD of 3+1 dimension seems large (as does lattice QCD) it starts also from the fundamental QCD. The light-front quantization of QCD has the particular advantage that it is completely formulated in physical degrees of freedom. It has emerged as a promising method for solving problems in the strong coupling regime. Light

^{*} Based also on the invited talk presented at the 310th WE-Heraeus Seminar “Quarks in Hadrons and Nuclei II”, Rothenfels Castle, Oberwölz (Austria) September 15-20, 2003

front quantization makes it possible to investigate quantum field theory in a Hamiltonian formulation [14]. This makes it well suited for its application to systems of finite temperature (and density). The relevant field theory has to be quantized on the light front as well, which is presently being developed [16–27]. I present the light-front field theory at finite temperatures and densities in the next section. For the time being it is applied to the Nambu-Jona-Lasinio model (NJL) model [28,29] that is a powerful tool to investigate the non-perturbative region of QCD as it exhibits spontaneous breaking of chiral symmetry and the appearance of Goldstone bosons in a transparent way. Finally, going a step further I shall give the general in-medium light cone time ordered Green functions that allow us to treat quark correlations that lead to hadronization.

2 Light front thermal field theory

The four-momentum operator P^μ on the light-front is given by (notation of Ref. [15])

$$P^\mu = \int d\omega_+ T^{+\mu}(x), \quad (1)$$

where $T^{\mu\nu}(x)$ denotes the energy momentum tensor defined through the Lagrangian of the system and S_μ is the quantization surface. The Hamiltonian is given by P^- . To investigate a grand canonical ensemble we need the number operator,

$$N = \int d\omega_+ j^+(x), \quad (2)$$

where $j^\nu(x)$ is the conserved current. These are the necessary ingredients to generalize the covariant partition operator at finite temperature [30–32] to the light-front. The grand canonical partition operator on the light-front is given by

$$Z_G = \exp \left\{ \int d\omega_+ [-\beta_\nu T^{+\nu}(x) + \alpha J^+(x)] \right\}, \quad (3)$$

where $\alpha = \mu/T$, with the Lorentz scalars temperature T and chemical potential μ . The velocity of the medium is given by the time-like vector $u_\nu u^\nu = 1$ [30], and $\beta_\nu = u_\nu/T$. We choose the medium to be at rest, $u^\nu = (u^-, u^+, \mathbf{u}^\perp) = (1, 1, 0, 0)$. The grand partition operator then becomes

$$Z_G = e^{-K/T}, \quad K \equiv \frac{1}{2}(P^- + P^+) - \mu N \quad (4)$$

with P^\pm and N defined in (1) and (2). The density operator for a grand canonical ensemble [33,34] in equilibrium follows

$$\rho_G = (\text{Tr } e^{-K/T})^{-1} e^{-K/T}. \quad (5)$$

The corresponding Fermi distribution functions of particles $f^+ \equiv f$ and antiparticles f^- are given by

$$f^\pm(k^+, \mathbf{k}_\perp) = \left[\exp \left\{ \frac{1}{T} \left(\frac{1}{2} k_{\text{on}}^- + \frac{1}{2} k^+ \mp \mu \right) \right\} + 1 \right]^{-1} \quad (6)$$

and $k_{\text{on}}^- = (k_{\perp}^2 + m^2)/k^+$. This fermionic distribution function (for particles) on the light-front has first been given in [16]. The fermi function for the canonical ensemble can be achieved by simply setting $\mu = 0$. This then coincides with the distribution function given recently in Ref. [21] (up to different metric conventions).

The light-front time-ordered Green function for fermions is

$$i\mathcal{G}_{\alpha\beta}(x-y) = \theta(x^+ - y^+) \langle \Psi_{\alpha}(x)\Psi_{\beta}(y) \rangle - \theta(y^+ - x^+) \langle \bar{\Psi}_{\beta}(y)\Psi_{\alpha}(x) \rangle. \quad (7)$$

We note here that the light-cone time-ordered Green function differs from the Feynman propagator S_F in the front form by a contact term $\gamma^+/2k^+$ and therefore coincides with the light-front propagator given previously in Ref. [35]. To evaluate the ensemble average $\langle \dots \rangle = \text{Tr}(\rho_G \dots)$ of (7), we utilize the imaginary time formalism [33,34]. We rotate the light-front time of the Green function to imaginary value. Hence the k^- -integral is replaced by a sum of light-front Matsubara frequencies ω_n according to [16],

$$\frac{1}{2}k^- \rightarrow i\omega_n - \frac{1}{2}k^+ + \mu \equiv \frac{1}{2}k_n^- \rightarrow \frac{1}{2}z, \quad (8)$$

where $\omega_n = \pi\lambda T$, $\lambda = 2n + 1$ for fermions [$\lambda = 2n$ for bosons]. In the last step we have performed an analytic continuation to the complex plane. For noninteracting Dirac fields the (analytically continued) imaginary time Green function becomes

$$\begin{aligned} G(z, \bar{k}) &= \frac{\gamma k_{\text{on}} + m}{z - k_{\text{on}}^- + i\varepsilon} \frac{\theta(k^+)}{k^+} (1 - f^+(\bar{k})) + \frac{\gamma k_{\text{on}} + m}{z - k_{\text{on}}^- - i\varepsilon} \frac{\theta(k^+)}{k^+} f^+(\bar{k}) \\ &+ \frac{\gamma k_{\text{on}} + m}{z - k_{\text{on}}^- + i\varepsilon} \frac{\theta(-k^+)}{k^+} f^-(-\bar{k}) + \frac{\gamma k_{\text{on}} + m}{z - k_{\text{on}}^- - i\varepsilon} \frac{\theta(-k^+)}{k^+} (1 - f^-(-\bar{k})), \end{aligned} \quad (9)$$

where $\bar{k} = (k^+, k_{\perp})$. For equilibrium the imaginary time formalism and the real time formalism are linked by the spectral function [33,34,26]. For $\mu = 0$ this propagator coincides with that of [26], but differs from that of [21,25].

3 Spontaneous symmetry breaking and restoration

3.1 NJL model on the light-front

The Nambu-Jona-Lasinio (NJL) originally suggested in [28,29] has been reviewed in Ref. [36] as a model of quantum chromo dynamics (QCD), where also a generalization to finite temperature and finite chemical potential has been discussed. Its generalization to the light-front including a proper description of spontaneous symmetry breaking, which is not trivial, has been done in Ref. [37], which we use here. The Lagrangian is given by

$$\mathcal{L} = \bar{\psi}(i\gamma\partial - m_0)\psi + G((\bar{\psi}\psi)^2 + (\bar{\psi}i\gamma_5\tau\psi)^2). \quad (10)$$

In mean field approximation the gap equation is

$$m = m_0 - 2G\langle\bar{\psi}\psi\rangle = m_0 + 2iG\lambda \int \frac{d^4k}{(2\pi)^4} \text{Tr}S_F(k), \quad (11)$$

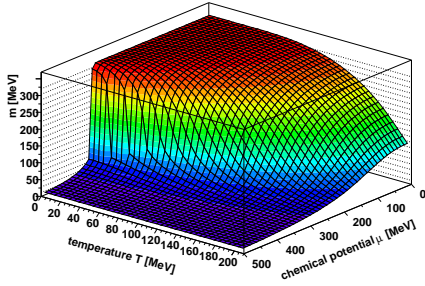


Fig. 1. Effective quark mass as a function of temperature and chemical potential. The fall-off is related to the vanishing condensate $\langle \bar{u}u \rangle$, which shows the onset of chiral symmetry restoration. Critical temperature at $\mu = 0$ is $T_c \simeq 190$ MeV.

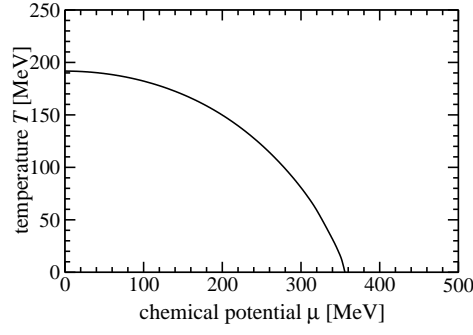


Fig. 2. Chiral phase transition as defined in [38]. The lower part is the chiral broken phase, whereas the upper part reflects the restored phase.

where $\lambda = N_f N_c$ in Hartree and $\lambda = N_f N_c + \frac{1}{2}$ in Hartree-Fock approximation, N_c (N_f) is the number of colors (flavors). For the isolated case $S_F(k)$ is the Feynman propagator. Taking only the lowest order in $1/N_c$ expansion of the 1-body or 2-body operators the light front gap equation can be achieved by a k^- integration, where in addition $m_0 \rightarrow \tilde{m}_0$ and $G \rightarrow \tilde{G}$ have to be renormalized to accommodate the expansion. For details see [37]. The propagator to be used in (11) is given in (9). The gap equation becomes

$$m(T, \mu) = \tilde{m}_0 + 2\tilde{G}\lambda \int \frac{dk^+ d^2k_\perp}{2k^+(2\pi)^3} 4m(T, \mu)(1 - f^+(k^+, \mathbf{k}_\perp) - f^-(k^+, \mathbf{k}_\perp)). \quad (12)$$

To regularize (12) we require $k_{\text{on}}^- + k^+ < 2\Omega$. As a consequence $k_1^+ < k^+ < k_2^+$ and

$$k_\perp^2 < 2\Omega k^+ - (k^+)^2 - m^2, \quad (13)$$

$$k_{1,2}^+ = \Omega \mp \sqrt{\Omega^2 - m^2}. \quad (14)$$

For the isolated case this regularization is fully equivalent to the Lepage-Brodsky one and the three-momentum cut-off. For the in medium case this Ω regularization leads to analytically the same expressions as given in [36] for the instantaneous case [27]. The calculation of the pion mass m_π , the pion decay constant f_π , and the condensate value are also available on the light-front [37].

3.2 Results

The model parameters are adjusted to the isolated system. We use the Hartree approximation, i.e. $\lambda = N_c N_f = 6$. Parameter values are chosen to reproduce the pion mass $m_\pi = 140$ MeV, the decay constant $f_\pi = 93$ MeV, and to give a constituent quark mass of $m = 336$ MeV, i.e. $\tilde{G} = 5.51 \times 10^{-6}$ MeV, $\tilde{m}_0 = 5.67$ MeV, and $\Omega = 714$ MeV. The parameters are reasonably close to the cases

used in the review Ref. [36]. The difference between the bare mass \tilde{m}_0 and the constituent mass is due to the finite condensate, which is $\langle \bar{u}u \rangle^{1/3} = -247$ MeV.

In hot and dense quark matter the surrounding medium leads to a change of the constituent quark mass due to the quasiparticle nature of the quark. The constituent mass as solution of (12) is plotted in Fig. 1 as a function of temperature and chemical potential. The fall-off is related to chiral symmetry restoration, which would be complete for $m_0 = 0$. It is related to the QCD phase transition. For $T \lesssim 60$ MeV the phase transition is first order, which is reflected by the steep change of the constituent mass. To keep close contact with the 3M results we have chosen for the Ω in-medium regulator mass $\Omega^2(T, \mu) = \Lambda_{3M}^2 + m^2(T, \mu)$ with $\Lambda_{3M} = 630$ MeV fixed for all T and μ .

We define the phase transition to occur at a temperature at which $m(T, \mu)$ is half of the isolated constituent quark mass [38]. The phase diagram is shown in Fig. 2. The line indicates the phase boundary separating the hadronic phase from the quark gluon plasma phase. Results presented in this section are based on an effective interaction in the $q\bar{q}$ channel. They have to be supplemented by the medium dependence of f_π and m_π that are currently underway.

4 Few-particle correlations

We are now interested in the qq channel. Since we are going up to the three-particle system, we presently approximate the spin structure. To solve the full three-fermion problem on the light front even for the isolated case is quite a challenge. The spin structure is already rather complex, see e.g. [39]. Therefore the elementary spins are averaged $\text{Tr} \gamma = 0$ (in the medium) and hence, for the time being, we are only dealing with bose type particles however subject to Fermi-Dirac statistics. Our main focus here is to see how such a three-particle system is dynamically influenced by a medium of finite temperature and density; ultimately, how nucleons are formed in the hot and dense environment of a plasma of quarks and gluons as the temperature and the density becomes smaller and how the relevant degrees of freedom in the Fermi function change as the many-particle system undergoes a change to hadronic degrees of freedom. To this end we need to formulate suitable few-body equations that describe clusters of quarks in a medium. In addition, because of the drastic mass change, see Fig. 1, these equations have to be relativistic ones. The equations derived here are based on a systematic quantum statistical framework formulated on the light front using a cluster expansion for the Green functions. The formalism has been given elsewhere [16]. We repeat here the basics to make a connection to the previous sections. The light-front time ordered cluster Green function is defined by

$$i\mathcal{G}_{\alpha\beta}(x-y) = \theta(x^+ - y^+) \langle A_\alpha(x) \bar{A}_\beta(y) \rangle \mp \theta(y^+ - x^+) \langle \bar{A}_\beta(y) A_\alpha(x) \rangle. \quad (15)$$

where all particles $A_\alpha(x) \equiv A_\alpha(x^+, \underline{x}) = \Psi_{\alpha_1}(x^+, \underline{x}_1) \Psi_{\alpha_2}(x^+, \underline{x}_2) \Psi_{\alpha_3}(x^+, \underline{x}_3) \dots$ are all taken at the same light front time x^+ and $\underline{x} = (x_+, \underline{x}_\perp)$. The upper (lower) sign stands for fermion (boson) type clusters. Because of the global light-cone time introduced, the dynamical equation for a cluster is equivalent to a Dyson

equation with a complicated mass operator that contains an instantaneous part and a memory (or retardation) part. For the time being we neglect the memory term. This is equivalent to a mean field approximation for clusters leading to Faddeev-type three-body equations.

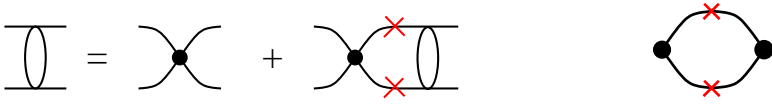


Fig. 3. Equation for the two-body t-matrix with zero range interaction. The crosses refer to the Pauli-blocking factor. **Fig. 4.** Loop diagram corresponding to the kernel of the integral equation (16).

For a simple zero range interaction the t matrix, Fig. 3, separates and is given by the propagator $t(M_2)$, i.e.

$$t(M_2) = (i\lambda^{-1} - B(M_2))^{-1}. \quad (16)$$

The expression for $B(M_2)$ is represented by the loop diagram of Fig. 4 and, in the rest system of the two-body system $P^\mu = (M_2, M_2, \mathbf{0}_\perp)$, given by

$$B(M_2) = -\frac{i}{(2\pi)^3} \int \frac{dx d^2k_\perp}{x(1-x)} \frac{1 - f(x, \mathbf{k}_\perp^2) - f(1-x, \mathbf{k}_\perp^2)}{M_2^2 - M_{20}^2}, \quad (17)$$

where $M_{20}^2 = (\mathbf{k}_\perp^2 + m^2)/x(1-x)$ and $f \equiv f^-$ given in (6) with $x = k^+/P_2^+$ where $\bar{P}_2 = \bar{k}_1 + \bar{k}_2$. For a fermi system there are two important effects occurring due to the blocking factors of (17). One is the dissociation limit (Mott effect) where $M_2(T_d, \mu_d) = 2m(T_d, \mu_d)$. Above a certain temperature and density no bound states can be formed. The second effect is related to the appearance of a bose pole in the t matrix. This happens for $M_2(T_c, \mu_c) = 2\mu_c$ and defines the critical temperature below which the system becomes unstable and forms a new vacuum consisting of Cooper pairs or a condensate. This is related to superconductivity or superfluidity. In this case for $M_2^2 \rightarrow M_{02}^2$, we get

$$f(x, \mathbf{k}_\perp^2) \Big|_{M_{02}^2 \rightarrow M_2^2 = 4\mu^2} = f(1-x, \mathbf{k}_\perp^2) \Big|_{M_{02}^2 \rightarrow M_2^2 = 4\mu^2} = \frac{1}{2}, \quad (18)$$

i.e. both nominator and denominator of (17) are zero.

The three-particle case is driven by the Fadeev-type in medium equation

$$\Gamma(y, \mathbf{q}_\perp) = \frac{i}{(2\pi)^3} t(M_2) \int \frac{dx d^2k_\perp}{x(1-y-x)} \frac{1 - f(x, \mathbf{k}_\perp^2) - f(1-x-y, (\mathbf{k} + \mathbf{q})_\perp^2)}{M_3^2 - M_{03}^2} \Gamma(x, \mathbf{k}_\perp), \quad (19)$$

where we have introduced vertex functions Γ and $t(M_2)$ given before, and an invariant cut-off $M_{30}^2 < \Lambda^2$. Here the mass of the virtual three-particle state (in the rest system $P^\mu = (M_3, M_3, \mathbf{0}_\perp)$) is

$$M_{03}^2 = \frac{\mathbf{k}_\perp^2 + m^2}{x} + \frac{\mathbf{q}_\perp^2 + m^2}{y} + \frac{(\mathbf{k} + \mathbf{q})_\perp^2 + m^2}{1-x-y}, \quad (20)$$

which is the sum of the on-shell minus-components of the three particles. The nucleon scale is introduced by setting $M_3 = 938$ MeV. The isolated quark mass used in these calculations is $m = 386$ MeV.

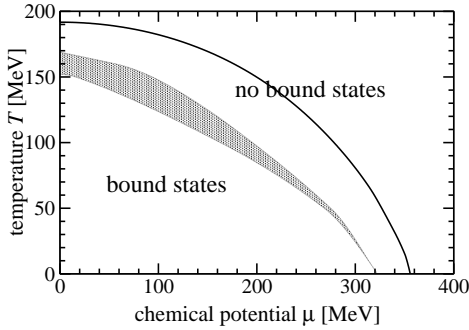


Fig. 5. Nucleon dissociation region (shaded area due to different cut-offs). Solid line chiral phase transition of Fig. 2.

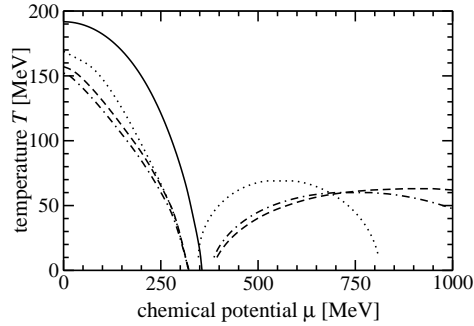


Fig. 6. Phase diagram supplemented with critical temperature for color superconductivity. Different cut-offs: $\Lambda = 4m$ (dot), $\Lambda = 6m$ (dash), $\Lambda = 8m$ (dash-dot).

Fig. 5 shows a shaded area that reflects the region where the transition from baryons to quarks (or quark diquarks) occur. The area is defined by use of different regularization masses. The chiral phase transition given before is indicated by the solid line. Fig. 6 shows the possible transition of quark matter to a superconducting phase.

5 Conclusion and Outlook

We have given a relativistic formulation of field theory at finite temperature and densities utilizing the light front form. The proper partition operator (and the statistical operator) have been given for the grand canonical ensemble. The special case of a canonical ensemble is given for $\mu = 0$. The resulting Fermi function depends on transverse and also on the k^+ momentum components. The k^+ components emerge in a natural way in a covariant approach. As an application we have revisited the NJL low energy model of QCD. We reproduce the phenomenology of the NJL model, in particular the gap-equation and the chiral phase transition. We have further given consistent relativistic three-quark equations valid in a dense medium of finite temperature. We find that the dissociation transition and the critical temperature for the color superconductivity agree qualitatively with results expected from other sources. However, the latter results are by no means final. We have shown that it is possible to write down meaningful consistent equations to solve the relativistic in-medium problem on the light front. The next steps would be to use the NJL model all through to give a consistent picture for the $q\bar{q}$ and the qq channel. Further insight into this just emerging possibilities of treating relativistic many-particle systems on the light front might be provided by other theories, like 1+1 QCD, the Yukawa model, and finally real QCD.

Acknowledgment: I gratefully acknowledge the fruitful collaboration with S. Mattiello, T. Frederico, and H.J. Weber, who have substantially contributed to the work I had the pleasure to present in this talk. I also thank S. Brodsky for his interest and discussion on this new approach. In particular, I would like to thank the organizers of the workshop for a fruitful and well organized meeting. Work supported by Deutsche Forschungsgemeinschaft, grant BE 1092/10.

References

1. C. Bernard *et al.* [MILC Collaboration], arXiv:hep-lat/0309118 and refs. therein
2. F. Karsch, E. Laermann and A. Peikert, Nucl. Phys. B **605** (2001) 579.
3. A. Ali Khan *et al.* [CP-PACS collaboration], Phys. Rev. D **64** (2001) 074510.
4. Z. Fodor and S. D. Katz, Phys. Lett. B **534**, 87 (2002).
5. Z. Fodor, S. D. Katz and K. K. Szabo, Phys. Lett. B **568**, 73 (2003).
6. C. R. Allton *et al.*, Phys. Rev. D **66**, 074507 (2002).
7. C. R. Allton *et al.*, Phys. Rev. D **68**, 014507 (2003).
8. P. de Forcrand and O. Philipsen, Nucl. Phys. B **642**, 290 (2002).
9. M. D'Elia and M. P. Lombardo, Phys. Rev. D **67**, 014505 (2003).
10. P. de Forcrand and O. Philipsen, arXiv:hep-lat/0307020.
11. S. D. Katz, arXiv:hep-lat/0310051.
12. M. G. Alford, Nucl. Phys. Proc. Suppl. **117** (2003) 65.
13. U. W. Heinz, Nucl. Phys. A **721** (2003) 30.
14. P. A. Dirac, Rev. Mod. Phys. **21**, 392 (1949).
15. S. J. Brodsky, H. C. Pauli and S. S. Pinsky, Phys. Rept. **301**, 299 (1998), and refs. therein.
16. M. Beyer, S. Mattiello, T. Frederico and H. J. Weber, Phys. Lett. B **521**, 33 (2001).
17. S. Mattiello, M. Beyer, T. Frederico and H. J. Weber, Few Body Syst. **31**, 159 (2002).
18. S. J. Brodsky, Acta Phys. Polon. B **32**, 4013 (2001).
19. S. J. Brodsky, Fortsch. Phys. **50**, 503 (2002).
20. S.J. Brodsky, Nucl. Phys. Proc. Suppl. **108**, 327 (2002).
21. V. S. Alves, A. Das and S. Perez, Phys. Rev. D **66**, 125008 (2002).
22. S. Mattiello, M. Beyer, T. Frederico and H. J. Weber, Few Body Syst. Suppl. **14**, 379 (2003)
23. H. A. Weldon, Phys. Rev. D **67**, 085027 (2003).
24. H. A. Weldon, Phys. Rev. D **67**, 128701 (2003).
25. A. Das and X. x. Zhou, arXiv:hep-th/0305097.
26. A. N. Kvinikhidze and B. Blankleider, arXiv:hep-th/0305115.
27. M. Beyer, S. Mattiello, T. Frederico and H. J. Weber, arXiv:hep-ph/0310222.
28. Y. Nambu and G. Jona-Lasinio, Phys. Rev. **122**, 345 (1961).
29. Y. Nambu and G. Jona-Lasinio, Phys. Rev. **124**, 246 (1961).
30. W. Israel, Annals Phys. **100**, 310 (1976).
31. W. Israel, Physics **106A**, 204 (1981).
32. H. A. Weldon, Phys. Rev. D **26**, 1394 (1982).
33. L.P.Kadanov and G. Baym, *Quantum Statistical Mechanics* (Mc Graw-Hill, New York 1962).
34. A.L. Fetter, J.D. Walecka, *Quantum Theory of Many-Particle Systems* (McGraw-Hill, New York 1971) and Dover reprints 2003.
35. S.-J. Chang, R.G. Root, and T.-M. Yan, Phys. Rev. **D7**, 1133 (1973); S.J. Chang and T.-M. Yan, Phys. Rev. **D7**, 1147 (1973).
36. S.P. Klevansky, Rev. Mod. Phys. **64**, 649 (1992).
37. W. Bentz, T. Hama, T. Matsuki and K. Yazaki, Nucl. Phys. A **651**, 143 (1999).
38. M. Asakawa and K. Yazaki, Nucl. Phys. **A504**, 668 (1989).
39. M. Beyer, C. Kuhrt and H. J. Weber, Annals Phys. **269**, 129 (1998).



Scalar mesons in the Gaussian approximation to the linear Σ model

V. Dmitrašinović

Vinča Institute (Lab 010), P.O.Box 522, 11001 Belgrade

Abstract. I report on recent progress in our understanding of the bosonic sector of the linear sigma model in the nonperturbative Gaussian wave functional approximation, accomplished in collaboration with I. Nakamura. We have proven a number of chiral Ward-Takahashi identities, such as the Nambu-Goldstone theorem and axial current conservation in the Gaussian approximation to these models. The particle content of the models is elucidated with particular emphasis on the question of multiple states in the scalar channel.

1 Introduction

One of the most persistent problems in hadron spectroscopy is that of the low-lying scalar mesons: there are too many of them and they do not fit into the flavour singlet + octet pattern. It is clear from the P-wave meson LS splitting that the lightest scalars ($f_0(980)$ and $a_0(980)$) are too light to be $q\bar{q}$ states. The only plausible alternative is that they are $(q\bar{q})^2$ states, either as (a) resonances/bound states of two ordinary $q\bar{q}$ (pseudoscalar) mesons, or (b) related to “hidden-colour” $(q\bar{q})^2$ states embedded in the ordinary two-meson continuum.

In this talk we concentrate on class (a) models. Even within this class a large number of different strategies and models have been used, some of them non-relativistic and nonchiral. As the masses of scalar mesons are at least twice those of their “constituent” pseudoscalars, we believe that relativity and chiral symmetry are indispensable in this problem. Moreover, unitarity, causality and non-perturbative nature of the approximation all seem to be a must in this problem (similarity to the “bootstrap” program is not accidental).

Within the class of relativistic chiral models there are (at least) two options: (i) linear, and (ii) nonlinear realization models. [There is also the older calculation of Törnqvist [1] that does not specify a Lagrangian.] In either approach it is important to have a clear criterion for the differentiation between the underlying (“bare”) $q\bar{q}$ states and the (“composite”) $(q\bar{q})^2$ states with identical quantum numbers, even if it is defined in some perhaps unusual limit. Models of type (ii) have recently been constructed, most notably by the Syracuse, N.Y. and two Spanish groups [2–4]. These calculations display many interesting features, but suffer from all the usual difficulties of nonlinear models, and a few that are specific to the nonperturbative nature of their approximation.

We shall take the route (i). As the scalar fields are the chiral partners of the pseudoscalar mesons in a linearly realized chiral symmetry, it has long been suspected that the scalar meson problem is related to linear realization of chiral symmetry. The open question is: how does one implement a consistent Lorentz invariant, unitary, causal and chirally symmetric approximation to such models that can also describe bound states? The very existence of such an approximation, let alone its technical details, was not known until recently. A solution to this problem that has all the required properties was found in a little known variational approach to QFT, called the Gaussian wave functional approximation, which also happens to be an answer to the old meson “bootstrap” problem, albeit within field theory. This solution “dresses” the underlying (“fundamental”) mesons with “meson cloud”, which in turn changes their properties to such an extent that they cannot be recognized as the original Nambu-Goldstone [NG] particles any more. The NG particles become two-body bound states of the dressed mesons.

In the following we give a short introduction to this method and discuss its implementation in the two-flavour linear sigma model of Gell-Mann—Levy [5]. This model has been derived (“bosonized”) [6] from the NJL chiral quark model which includes the QCD instanton-induced ‘t Hooft quark (self)interaction [7], with all the free parameters/coupling constants determined. Thus the boson fields correspond to (bare) $q\bar{q}$ bound states.

2 Basics of the Gaussian variational method

This variational method is based on the minimization of the ground state’s [g.s.] energy density $\mathcal{E}_0 = \mathcal{E}_0(m_i, \phi_i)$ (for infinite homogeneous systems) with respect to the variational parameters m_i, ϕ_i . The g.s. energy is evaluated with a Gaussian Ansatz [8,9] for the g.s. wave functional $|\Psi_0\rangle$, which, in a theory with N scalar fields like the sigma model, is a function of $2N$ variational parameters (the fields’ masses and v.e.v.s) $(m_i, \phi_i), i \in (1, \dots, N)$, i.e., $|\Psi_0\rangle = |\Psi_0(m_i, \phi_i)\rangle$,

$$E_0(m_i, \phi_i) = \langle \Psi_0 | H | \Psi_0 \rangle \langle \Psi_0 | \Psi_0 \rangle^{-1},$$

in the Schroedinger representation of QFT. Similarly one can construct one-, two-, ..., n -body states and minimize their energies. Of course, only few-body states are amenable to practical applications. The $2N$ vacuum energy minimization/stationarity equations

$$\left(\frac{\partial \mathcal{E}_0(m_i, \langle \phi_i \rangle)}{\partial \langle \phi_i \rangle} \right)_{\min} = 0 = \left(\frac{\partial \mathcal{E}_0(m_i, \langle \phi_i \rangle)}{\partial m_i} \right)_{\min}; \quad i = 0, \dots, 3;$$

turn out to have a Feynman diagrammatic interpretation as (truncated) Schwinger-Dyson [SD] equations for the one- and two-point Green functions [10], i.e. for the equations determining the vacuum and single particle properties. (The truncation in question is a consequence of the approximate nature of the Gaussian Ansatz, and it implies elimination of the two-loop $O(\hbar^2)$ diagrams from their respective SD equations.) This should not have been a surprise as the minimized “vacuum”

energy density $\mathcal{E}_0(m_i, \phi_i)_{\min}$ is (up to an additive constant) also the Gaussian approximation effective potential

$$V_{\text{eff}}(\phi_i) = \mathcal{E}_0(m_i, \phi_i)_{\min} - \mathcal{E}_0(m_i, \phi_i = 0)$$

with all its usual properties, in particular its being the generating function of the one-particle irreducible Green functions at vanishing external momenta. This means that derivatives of the effective potential yield higher order Green functions [11], the “only” problem being a positive identification of SD eqs., i.e., of Feynman diagrams from the corresponding analytic expressions. In other words, there should be no ambiguity as to which Feynman diagrams enter the GA equations of motion. The practical significance of this fact will become clear only when the GA is applied to linear sigma models.

3 Application to the linear Σ model

The linear sigma model of Gell-Mann and Levy is the simplest one so we shall consider it first. It is an $O(4)$ symmetric ϕ^4 (pseudo)scalar field theory with the Lagrangian

$$\mathcal{L} = \frac{1}{2} (\partial_\mu \phi)^2 - V(\phi^2), \quad (1)$$

where

$$\phi = (\phi_0, \phi_1, \phi_2, \phi_3) = (\sigma, \pi),$$

is meson quartet consisting of an isoscalar scalar σ and a pseudoscalar isotriplet of pions π and V is the characteristic “Mexican hat” potential

$$V(\phi^2) = -\frac{1}{2}\mu_0^2\phi^2 + \frac{\lambda_0}{4}(\phi^2)^2.$$

We assume here that λ_0 and μ_0^2 are not only positive, but such that spontaneous symmetry breakdown (SSB) occurs in the mean-field approximation [MFA] to be introduced later. That leads to spontaneous breaking of the internal $O(4)$ (chiral) symmetry, and in the last parentheses we have written the explicit symmetry breaking term. As the chiral symmetry breaking (χ SB) term in the Lagrangian we take

$$\mathcal{L}_{\chi\text{SB}} = -\mathcal{H}_{\chi\text{SB}} = \varepsilon\sigma. \quad (2)$$

In the first perturbative (“Born”) approximation we have $m_\pi = 0$ in the chiral limit $\varepsilon = 0$, i.e., the Nambu-Goldstone (NG) theorem holds. The Born approximation σ meson mass is not constrained by chiral symmetry, but rather its square is proportional to the coupling constant λ_0 . It remains to be seen what happens to this mass in higher approximations. We shall see that the nonperturbative Gaussian approximation particle content of this model can differ from the one in perturbation theory, viz. from the simple $O(4)$ multiplet, depending on the strength of the coupling λ_0 . The GA equations in the linear sigma model of Gell-Mann—Levy are shown in Figs. 1 and 2.

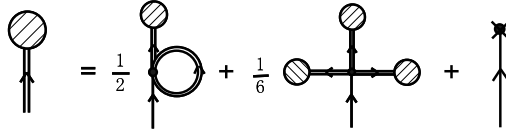


Fig. 1. Zero-particle, or “vacuum” (one-point) Green function Schwinger-Dyson equation.

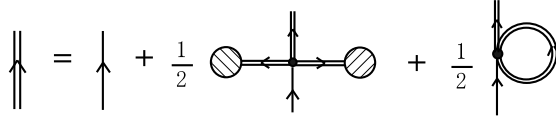


Fig. 2. One-particle, or “gap” (two-point) Green function Schwinger-Dyson equation.

Note their (self-)consistency: the solution to one SD equation enters the definition of the other, and *vice versa*. This is also an expected property of so-called “bootstrap” solutions to field theory. Figures 1 and 2 lead to two coupled nonlinear equations in two unknowns:

$$M^2 = \frac{\varepsilon}{v} + 2\lambda_0 v^2 \quad (3)$$

$$\mu^2 = \frac{\varepsilon}{v} + 2\lambda_0 \hbar [I_0(\mu) - I_0(M)] , \quad (4)$$

where

$$I_0(m_i) = i \int \frac{d^4 k}{(2\pi)^4} \frac{1}{[k^2 - m_i^2 + i\varepsilon]} \quad (5)$$

depending implicitly on the cutoff Λ , which is necessary for the regularization of infinities in the integrals $I_0(m_i)$, and the bare coupling constant λ_0 . Due to the relation between M^2 and $\lambda_0 f_\pi^2$, Eq. 3, M is proportional to $\sqrt{\lambda_0}$, meaning that a change in M corresponds to a change in λ_0 at fixed $v = f_\pi = 93\text{MeV}$.

The solutions M, μ do not have the (naively) expected properties viz. the (NG) pion field is not massless ($\mu \neq 0$), even in the chiral limit, as first noted by Kamefuchi and Umezawa in 1964 [12]. (We show the nonchiral solutions with fixed pion decay constant in Fig. 3. Note that the boson loops tend to restore the broken symmetry, unlike the fermion ones.)

This fact presented a serious problem for the GA for the following 30 years. The solution to this problem, first proposed in 1994 [13], consists in constructing two-body states which mix with the corresponding “elementary” one-body (or Castillejo-Dalitz-Dyson, or CDD) states, and observing their properties, thus finding a massless state among them with all the right NG boson properties, validity of the chiral Ward identities being just one of them. In other words, there are massless bound states of two massive mesons in the GA, a provocative idea at the time.

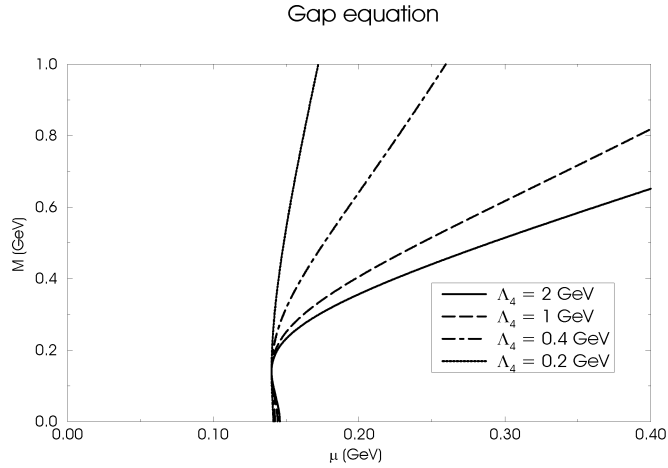


Fig. 3. Solutions to the gap equation in the GML model: M , and μ .

3.1 Chiral symmetry and the Gaussian approximation

Originally the Nambu-Goldstone boson problem was solved by direct construction of the Gaussian approximation two-body (SD) equation, a.k.a. the Bethe-Salpeter (BS) equation (The same result, only at vanishing external momenta, can be obtained by differentiating the effective potential.). In Ref. [13] we have shown that the Nambu-Goldstone particles appear as poles in the *two-particle propagator* i.e. they are bound states of the two distinct massive elementary excitations in the theory. We specify the two-body dynamics in the theory in terms of the four-point SD equation or, equivalently, of the Bethe-Salpeter equation, see Figs. 4 and 5. The appearance of massless NG bound states of two massive single-particle

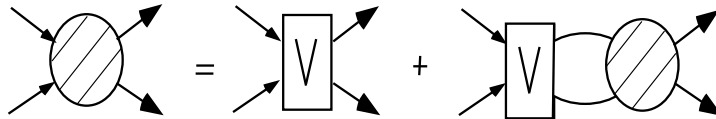


Fig. 4. Four-point Green function Schwinger-Dyson, or Bethe-Salpeter equation. The square “box” represents the potential, whereas the round “blob” is the BS amplitude itself. All lines are meant as dressed fields, i.e. as double lines in Figs. 1 and 2.

states produced a certain amount of surprise and confusion, as it seems to imply a doubling of states with identical (“flavour”) quantum numbers: in each flavour channel, beside the massive one-body CDD state there is also a lighter two-body state. At first sight this “bootstrap” mechanism would appear to explain the “supernumerary” scalar states ($f_0(980)$, $a_0(980)$), but on second inspection one can see that it produces new problems in that it also implies particle doubling in channels other than the scalar ones where supernumerary states have not been found.

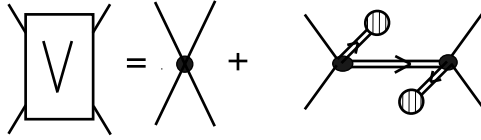


Fig. 5. The potential (square “box”) entering the Bethe-Salpeter equation, as defined in the RPA.

3.2 Real and fake particle doubling

The problem of (naive) supernumerary states (CDD poles) was resolved in Ref. [11,14] by way of spectral analysis: the Kallen-Lehmann functions were calculated from the solutions to the BS equation in the GA and it was found that the single-particle (CDD) poles disappear altogether from the spectra:

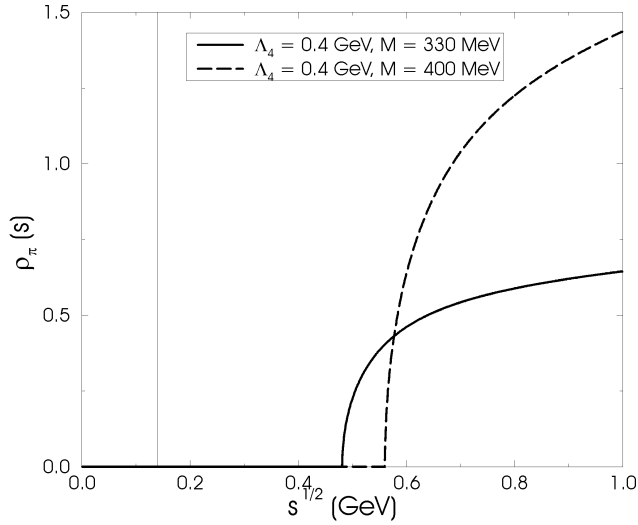


Fig. 6. Pion channel Kallen-Lehmann spectral function for various values of M .

The remaining delta function in the π spectrum, Fig. 6, corresponds to the dynamical state (solution to the BS equation) with the (pion) mass squared fixed by the Dashen relation at ε/v , which is always below the single-particle (CDD) mass μ . Similarly the peak in the σ channel spectral function, Fig. 7, corresponds to the dynamical state mass, which lies below the corresponding single particle mass M , Ref. [10].

So, one may say that the influence of the two-particle continuum has pushed the masses of the dynamical states below their single-particle values and below the two-particle threshold, see Fig. 8, where the exact solutions to the BS equation are shown together with the two-body thresholds. Note however, that there are other solutions to the BS equation, see Fig. 9, at higher masses, which do not show up in the spectral functions due to their even larger imaginary parts.

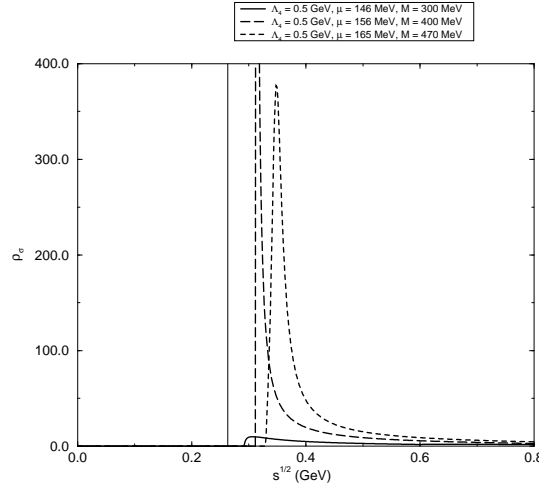


Fig. 7. Sigma channel Kallen-Lehmann spectral function for various values of M , μ .

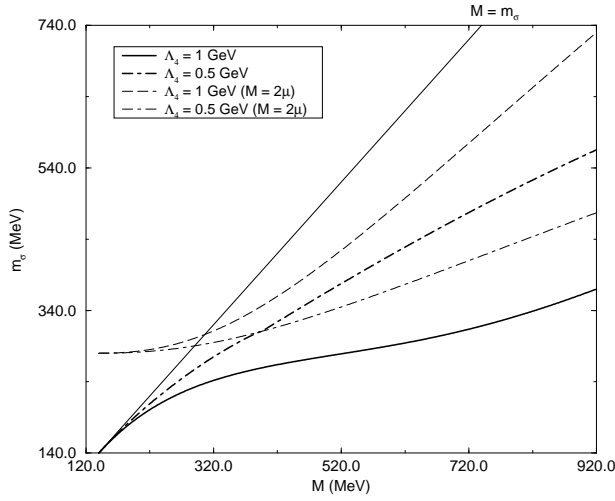


Fig. 8. Sigma mass as a function of M , and the position of the lowest threshold ($M = 2\mu$).

These solutions owe their existence to the large nonlinearities in the BS equation at very large masses/couplings. Yet, we must keep the possibility of such solutions in mind, in case they move to lower masses for a different model Lagrangian.

Moreover, we have proven in Ref. [11] the identity of the Gaussian BS and the N/D equations in the S-matrix theory, which fact immediately implies unitarity and causality of their solutions. This translates into analytic properties of the scattering amplitude which tell us what branch of the equations to solve and

the solution's physical interpretation. The solutions to the N/D equations are not unique in general, however, the arbitrariness showing up in the form of so-called Castillejo-Dalitz-Dyson (CDD) poles. The position of a CDD pole, and the coefficient multiplying it are arbitrary in the usual S-matrix, or N/D approach, but in our approach they are completely determined by the Gaussian approximation to the underlying σ model.

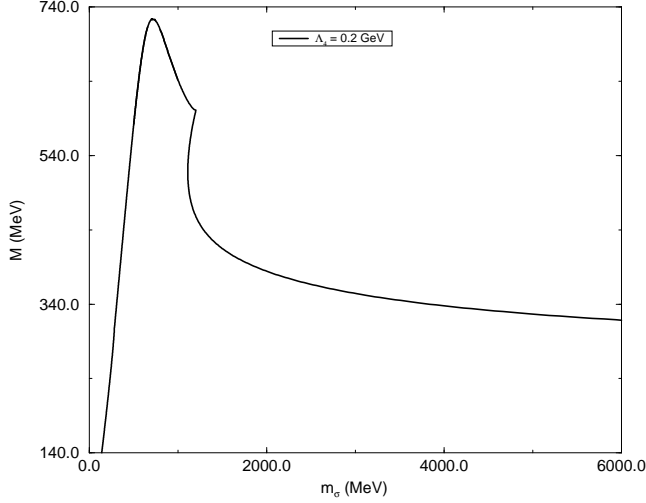


Fig. 9. Sigma mass as a function of M .

4 Conclusions

We have shown that the Gaussian Approximation is: (a) Lorentz and chirally invariant, (b) causal and unitary, and (c) selfconsistent and nonperturbative, i.e., it may describe mesons as bound states of other mesons. These are precisely the properties demanded of a relativistic quantum theory in the so-called “bootstrap” approach to hadronic particle physics of the 1960’s, but with several profound differences, viz. (1) a Lagrangian starting point based on a chiral quark model, therefore with a definite number of CDD poles with well defined properties (the bare Lagrangian free parameters are fixed by the quark model); (2) no arbitrariness at all: the “subtraction constants”, in S-matrix language, i.e., “infinite parts” of Feynman diagrams are known due to the renormalizability of the GA.

These results open new questions: for certain Lagrangians, such as the ‘t Hooft and the SU(3) linear sigma models, the number of flavour channels (greatly) exceeds the number of fields, i.e., there is no one-to-one correspondence between the Lagrangian fields and the available flavour channels, thus opening the possibility of light bound states in channels without CDD poles (almost inevitably these are exotic channels). We shall return to these issues in the future.

References

1. N.A. Törnqvist, *Z. Phys.* **C 68**, 647 (1995).
2. D. Black, A. H. Fariborz, F. Sannino, J. Schechter, *Phys.Rev.* **D 59**: 074026 (1999).
3. J.A. Oller, E. Oset, J.R. Pelaez, *Phys.Rev.* **D 59**: 074001, (1999).
4. J. Nieves, E. Ruiz Arriola, *Nucl. Phys.* **A 679**, 57, (2000).
5. G. 't Hooft, *Phys. Rep.* **142**, 357 (1986).
6. V. Dmitrašinović, *Phys. Rev.* **C 53**, 1383 (1996).
7. G. 't Hooft, *Phys. Rev.* **D 14**, 3432 (1976), (E) *ibid.* **D 18**, 2199 (1978).
8. T. Barnes and G.I. Ghandour, *Phys.Rev.* **D22**, 924 (1980); see also eds. L. Polley and D.E.L. Pottinger, *Variational Calculations in Quantum Field Theory*, World Scientific, Singapore (1987).
9. R.J. Rivers, *Path Integral Methods in Quantum Field Theory*, Cambridge University Press, Cambridge (1987); and B. Hatfield, *Quantum Field Theory of Point Particles and Strings*, Addison-Wesley, Reading (1992).
10. Issei Nakamura and V. Dmitrašinović, *Prog. Theor. Phys.* **106**, 1195 (2001).
11. Issei Nakamura and V. Dmitrašinović, *Nucl. Phys.* **A 713**, 133 (2003).
12. S. Kamefuchi, and H. Umezawa, *Nuov. Cim.* **31**, 429 (1964).
13. V. Dmitrašinović, J. A. McNeil and J. Shepard, *Z. Phys.* **C 69**, 359 (1996).
14. V. Dmitrašinović, *Phys. Lett.* **B 433**, 362 (1998).
15. V. Dmitrašinović and Issei Nakamura, *J. Math. Phys.* **44**, 2839 (2003).



Quark-meson model in a Tamm-Dancoff inspired approximation ^{*}

D. Horvat^a, D. Horvatić^b, and D. Tadić^b

^aPhysics Department, Faculty of Electrical Engineering, University of Zagreb, Unska 3, 10000 Zagreb, Croatia

^bPhysics Department, University of Zagreb, Bijenička c. 32, 10000 Zagreb, Croatia

Abstract. The nonlinear chiral quark meson $U(3) \times U(3)$ model is solved using the Tamm-Dancoff inspired approximation (TDIA) which is described in our earlier paper [1]. The resulting system of 15 coupled nonlinear differential equations self-consistently determines all quark-meson coupling constants. Obtained solutions for quark and meson fields are stable and physically acceptable. These approximate Heisenberg fields resulted from dynamics in which u , d and s quarks were treated on the same footing. They were used to calculate $SU(3)$ baryon octet magnetic moments and axial vector coupling constants. The baryon state vectors containing valence quarks were used. The results strongly indicate that simple state vectors and currents cannot adequately describe physical baryons.

1 Introduction

The Tamm-Dancoff inspired approximation (TDIA) [1] was applied some time ago to the chiral quark meson model based on the $SU(2)$ linear σ -model [2,3]. The results seemed to be comparable to those obtained using the hedgehog Ansätze [4–7]. That is to some extent understandable as both methods lead to similarly looking sets of equations for meson solitons (fields). All details of the TDIA are described in ref. [1]. It is well known that the Tamm-Dancoff method [8] is a better approximation than the perturbation theory. That feature it has in common with the hedgehog based meson field solutions [5–7].

In ref. [1] the linear σ -model was used as a transparent example for the application of TDIA. However since 1996. evidence has been found for the existence of the σ meson [9–11]. It has been stated [10,11] that the linear σ -model with three flavors works much better than what was generally believed. In the linear σ -model one can treat both scalar and pseudoscalar nonets simultaneously. The scalars are the chiral partners of π , η , etc. and the analysis strongly suggests that they, like the pseudoscalars, are $\bar{q}q$ states [10,11]. Such theoretical conclusions made TDIA approach quite attractive as in that approximation mesons (solitons)

^{*} Talk delivered by D. Horvatić

naturally appear, in the lowest order as $\bar{q}q$ states. In TDIA one works in the Heisenberg picture [12], expands field operators in the free field creation and annihilation operators and then truncates the expansion. That leads automatically, after truncations, to meson fields (soliton phases) which depend on bilinear combinations of quark/antiquark operators, i.e. to $\bar{q}q$ structures.

The chiral quark/meson $U(3)\times U(3)$ model under consideration has the familiar form which was used previously when the $SU(2)$ model [5,6] was enlarged by cranking involving intrinsic flavor space [7]. The system of nonlinear differential equations obtained here bears some similarity to the systems obtained by using hedgehog ansätze [5–7]. It has been argued that the linear σ -model [10,11] and its close relative the quark-meson model [7] might capture the essential features of QCD in the low energy region, while being easier to handle than the complex exact quark-gluon theory. The TDIA treatment of the $U(3)\times U(3)$ quark-gluon model thus might give some physical insights in the baryon structure.

Even with the bag formalism for quarks retained [1,13], thus using the static spherical cavity approximation and with the modest symmetry breaking, the lowest order TDIA leads to the coupled system of 15 nonlinear differential equations and 21 boundary conditions. That problem is completely solvable, as it will be outlined below. The strengths of quark-meson couplings are self consistently determined by the system. In principle the spherical cavity approximation for quarks can be dropped. That would lead to somewhat larger system of equations.

The structure of this model [1] is very transparent and all of its features are always discernible. One can see directly how the approximate baryon states, made of valence quarks only [14,15], perform. In order to do that one calculates the matrix elements of the (approximate) Heisenberg operators. As in TDIA the isospin (and hypercharge) and spin are separably conserved, the solutions can be used to calculate magnetic moments and axial-vector coupling constants for the baryon octet. The results indicate the need for richer structure ($s\bar{s}$ pairs etc.) of baryon state vectors [16] and for the inclusion of exchange current corrections [17]. The inclusion of quark triplet in the dynamical scheme does not seem to be sufficient by itself alone.

2 Model formalism

TDIA has been already described in some detail elsewhere [1]. Here we give some particulars concerning the quark linear σ -model and TDIA approximation. The Lagrangian in which the linear σ -model is embedded in the bag environment has the well known form [1,6,18]

$$\mathcal{L} = \mathcal{L}_\psi \Theta + \mathcal{L}_{\text{int}} \delta_S + [\mathcal{L}_\chi + U(\chi)] \bar{\Theta}. \quad (2.1)$$

Here all pieces but the symmetry-breaking one (\mathcal{L}_{SB}), are $U(3)\times U(3)$ invariant [3,7,11] i.e.

$$\begin{aligned}
 \mathcal{L}_\psi &= \frac{i}{2} (\bar{\Psi} \gamma^\mu \partial_\mu \psi - \partial_\mu \bar{\Psi} \gamma^\mu \psi) \\
 \mathcal{L}_{\text{int}} &= \frac{g}{2} \bar{\Psi} (\sigma_a + i\pi_a \gamma_5) \lambda^a \psi \\
 \mathcal{L}_\chi &= \frac{1}{2} (\partial^\mu \sigma_a \partial_\mu \sigma_a + \partial^\mu \pi_a \partial_\mu \pi_a) \\
 U(\chi) &= -\frac{1}{2} \mu^2 (\sigma_a^2 + \pi_a^2) - \frac{1}{4} \lambda^2 (\sigma_a^2 + \pi_a^2)^2 + \mathcal{L}_{\text{SB}}.
 \end{aligned} \tag{2.2}$$

Here $(\sigma^a, \pi^a, a=0,1,\dots,8)$ are (scalar, pseudoscalar) U(3) nonets. The symmetry is broken in a minimal way by the vacuum expectation values of U(3) scalars σ and ζ

$$\begin{aligned}
 \mathcal{L}_{\text{SB}} &= m_\pi^2 f_\pi \sigma + \frac{(2m_K^2 f_K - m_\pi^2 f_\pi)}{\sqrt{2}} \zeta \\
 \sigma_{\text{vac}} &= f_\pi \Rightarrow \sigma \rightarrow \sigma - f_\pi \\
 \zeta_{\text{vac}} &= \frac{(2f_K - f_\pi)}{\sqrt{2}} \Rightarrow \zeta \rightarrow \zeta - \zeta_{\text{vac}}.
 \end{aligned} \tag{2.3}$$

That leaves pseudoscalar (scalar) masses in the corresponding U(3) nonets degenerate.

The standard variational procedure leads to the coupled system which contains equations of motion, linear boundary and derivative boundary conditions involving quantum fields. However as system retains lot of symmetry in TDIA this gets reduced to a smaller set of c-equations. Here we sketch TDIA procedure and list nonlinear system of c-equations which will be solved numerically.

The "driving" Ansätze are the ones for the quark fields. For the massless u and d fields one uses:

$$\begin{aligned}
 \psi_f^c &= \frac{N_0}{\sqrt{4\pi}} \left[\begin{pmatrix} f_0 \\ i(\boldsymbol{\sigma}\hat{r})g_0 \end{pmatrix} \chi_\mu^f b_{\mu,f}^c + \begin{pmatrix} (\boldsymbol{\sigma}\hat{r})g_0 \\ if_0 \end{pmatrix} \chi_\mu^{f\dagger} d_{\mu,f}^{c\dagger} \right] \\
 f_0 &= j_0 \left(\frac{\omega_0 r}{R} \right), \quad g_0 = j_1 \left(\frac{\omega_0 r}{R} \right) \\
 N_0^2(\omega_0) &= \frac{1}{R^3} \left[j_0^2(\omega_0) + j_1^2(\omega_0) - \frac{2j_0(\omega_0)j_1(\omega_0)}{\omega_0} \right]^{-1}.
 \end{aligned} \tag{2.4}$$

The SU(3)-flavor symmetry is explicitly broken by assuming that s-quark has a mass $m_s \neq 0$, with corresponding Ansatz

$$\begin{aligned}
 \psi_f^c &= \frac{N_m}{\sqrt{4\pi}} \left[\begin{pmatrix} f_m \\ i(\boldsymbol{\sigma}\hat{r})g_m \end{pmatrix} \chi_\mu^f b_{\mu,f}^c + \begin{pmatrix} (\boldsymbol{\sigma}\hat{r})g_m \\ if_m \end{pmatrix} \chi_\mu^{f\dagger} d_{\mu,f}^{c\dagger} \right] \\
 f_m &= \sqrt{\frac{E+m_s}{E}} j_0 \left(\frac{\omega_m r}{R} \right), \quad g_m = \sqrt{\frac{E-m_s}{E}} j_1 \left(\frac{\omega_m r}{R} \right) \\
 E(m, R) &= \frac{1}{R} \sqrt{\omega^2 + (m_s R)^2}
 \end{aligned}$$

$$N_m^2(\omega_m) = \frac{N_0^2(\omega_m)}{1 + N_0^2(\omega_m)N_R}, \quad N_R = \frac{m_s j_0(\omega_m) j_1(\omega_m) R^3}{E\omega_m}. \quad (2.5)$$

Here the indices c, f and μ denote color, flavor and spin respectively.

Boundary conditions involving quark fields determine (by use of Ansätze (2.4) and (2.5)), the Ansätze for the meson fields. This matching then automatically produces mesons "made out of quark pairs", as suggested in the σ -model analysis [9–11]. One needs for pseudoscalar fields, for example:

$$\begin{aligned} \pi^+ = & \pi_s^+(r) (b_{m,d}^{c\dagger} d_{m',\bar{u}}^{c\dagger} + d_{m,\bar{d}}^c b_{m',u}^c) \chi_m^\dagger \chi_{m'} + \\ & + \pi_p^+(r) (b_{m,d}^{c\dagger} b_{m',u}^c - d_{m',\bar{u}}^{c\dagger} d_{m,\bar{d}}^c) \chi_m^\dagger (\sigma\hat{r}) \chi_{m'} \end{aligned} \quad (2.6)$$

Both scalar (π_s, K_s, η_s) and pseudoscalar ($\pi_p, \sigma\hat{r}, \eta_p, \sigma\hat{r}$ etc.) components of the pseudoscalar mesons are induced by the boundary conditions. The scalar parts formally correspond to physical "mesons" while the pseudoscalar ones are connected with the solitons. The solitons contribute to the baryonic current matrix elements. All that are just $U(3) \times U(3)$ generalizations of our earlier $U(2)$ based results [1]. For scalar fields, scalar and pseudoscalar contributions are reversed. Everything is again driven by boundary conditions, which require the following

The system of q-equations is in TDIA transformed in a system of differential c-equations. The operator equalities are expressed through Ansätze (2.4)-(2.6). They are then sandwiched between suitable states. An example for that can be found in ref. [1], equation (2.16).

One ends with the profile function and with some Pauli matrices and spinors. In that way all the creation (annihilation) operators from Ansätze can be contracted and one ends with the system of 20 equations of motion, 8 linear boundary conditions and 18 derivative boundary conditions.

3 The numerical procedure

The numerical procedure is analogous to the one used by ref. [1]. It relies on the code COLSYS, the collocation system solver developed by Ascher, Christiansen and Russel [19]. However, one should keep in mind that here one deals with much larger system, which contains many novel features, and which stretches COLSYS to its upper bounds.

The parameters assume the following values

$$\begin{aligned} m_\pi = 140 \text{ MeV}, & \quad f_\pi = 92.6 \text{ MeV} \\ m_K = 494 \text{ MeV}, & \quad f_K = 113 \text{ MeV} \\ m_s = 125 \text{ MeV}, & \quad R = 5 \text{ GeV}^{-1}. \end{aligned} \quad (3.1)$$

The parameters μ and λ from $U(\chi)$ (2.2) were selected by the requirement that all the profile functions appearing in (3.1), vanish at the infinity.

Using that requirement we have:

$$\mu^2 = -1.29525 \cdot 10^{-2} \text{ GeV}^2, \quad \lambda = 9.95484.$$

The coupling constants g_M ($M=\eta, \pi, \dots$) in (2.2) are connected with the linear boundary conditions. This cannot be satisfied by an universal coupling constant g which figures in (2.2) and one encounters, as it was found before [1], some dynamical symmetry breaking. The $U(3) \times U(3)$ model determines all coupling constants g_M leading to the values, shown in Table 3.1.

Table 3.1. The quark-meson dimensionless coupling constants.

g_M	g_σ	g_π	g_κ	g_η	$g_{\eta'}$	g_{a_0}	g_ζ	g_ζ
10.7	4.0	7.8	4.0	3.1	1.5	3.9	10.5	

The model g_π value is, interestingly, close to the estimated value in ref. [17]. The corresponding ω values are

$$\omega_0 = 2.0; \quad \omega_m = 2.28 \quad (3.2)$$

In Fig. 3.1 the radial dependencies of $r^2 \phi^2(r)$ ($\phi=\pi_p, K_p, \sigma_s, a_{0,s}$) are plotted. The function corresponding to scalar fields ($r^2 \sigma_s^2, r^2 a_{0,s}^2$) are much smaller than the contributions associated with pseudoscalars (π_p and K_p).

As one has solved the complex coupled system, which contains both non-strange and strange profile functions, one can say that u, d, π etc. profile functions "feel" the presence of the s -quark dynamics.

4 Results and Conclusions

Our model formalism in TDIA is used for the evaluation of the magnetic moments and the axial vector coupling constants of the nonstrange and strange baryons.

The baryon magnetic moments are determined by quark $\mu^{(Q)}$ and meson $\mu^{(M)}$ pieces. As the flavor $SU(3)$ is broken only by $m_s \neq 0$, the quark piece has the contribution coming from the u, d quarks $\mu_0^{(Q)}$ and the contribution coming from the s quark $\mu_s^{(Q)}$. The meson pieces depend on the pion soliton $\mu_\pi^{(M)}$ and the kaon soliton $\mu_K^{(M)}$. Their values are:

$$\mu_0^{(Q)} = 1.886, \quad \mu_s^{(Q)} = 1.695 \quad (4.1)$$

$$\mu_\pi^{(M)} = \frac{8\pi}{3} \int_{R_{\text{bag}}}^{\infty} r^2 dr \pi_p^2(r) = 0.027, \quad (4.2)$$

$$\mu_K^{(M)} = \frac{8\pi}{3} \int_{R_{\text{bag}}}^{\infty} r^2 dr K_p^2(r) = 0.020. \quad (4.3)$$

In Table 4.1 the model values are compared with experimental results.

Table 4.1. Baryon magnetic moments.

Baryon	μ_Q	μ_M	μ	μ_{exp}	$\Delta\mu$ %
p	1.886	0.027	1.913	2.793	46
n	-1.257	-0.026	-1.284	-1.913	49
Λ	-0.564	-0.020	-0.584	-0.613	8
Σ^0	0.607	0.010	0.617	-	-
$\Sigma^0 \rightarrow \Lambda$	1.089	0.021	1.110	1.610	45
Σ^-	-0.650	0.000	-0.650	-1.160	78
Σ^+	1.864	0.020	1.884	2.458	31
Ξ^0	-1.172	-0.020	-1.191	-1.250	5
Ξ^-	-0.543	0.000	-0.543	-0.651	20

Both quark Q and meson M phases were calculated in a model which includes s quarks. However the simplest "valence" proton state vectors were used. The same "valence" approximation [14,15] was used for the other baryon state vectors.

The s-quark admixture in the nonstrange baryon state vectors would pick up additional contributions from quark and meson fields calculated in TDIA. That would change both the theoretical expressions for the magnetic moments and for the axial vector coupling constants. However, from the point of view of the present work, that would require a substantial addition to the model.

A very similar conclusion follows from the investigation of the axial vector coupling constants.

Table 4.2. Diagonal axial vector constants.

Constant	$g_A^{(Q)}$	$g_A^{(M)}$	g_A	Experiment	Δg in %
g_A^3	1.110	0.184	1.294	1.267	2
g_A^0	0.666	0.111	0.777	0.280	178
g_A^8	0.666	0.111	0.777	0.579	34

It seems reasonable to assume that the discrepancies are again caused by the too poor structure of the proton state vectors. It is usually stated [16] that s-quark admixture in the proton state vector must be important. However the prediction for the isovector axial vector coupling constant g_A^3 is very good. This seems to be some general characteristic of the chiral models which are constructed to satisfactorily reproduce $g_A^{I=1}$. Moreover the present nonlinear, nonperturbative approach seems to work somewhat better than some simple expansions which might lead to too large $g_A^{I=1}$.

As shown in Table 4.3 the calculated g_A 's, for the semileptonic decays, seem reasonable in two cases. All signs are correctly predicted, absolute magnitude of the Λ -decay constant is 14% too large, Σ -decay constant is 53% too small and the Ξ^- -decay constant is 13% too large.

Table 4.3. g_A in semileptonic decays.

Decay	$(g_A)_Q$	$(g_A)_M$	g_A	exp. Δg in %
$\Lambda \rightarrow p + e^- + \bar{\nu}_e$	-0.758	-0.059	-0.817	-0.718 14
$\Sigma^- \rightarrow n + e^- + \bar{\nu}_e$	0.206	0.016	0.222	0.340 53
$\Xi^- \rightarrow \Lambda + e^- + \bar{\nu}_e$	-0.253	-0.029	-0.282	-0.250 13

Here, as in Tables 4.1-4.2 the meson phase contribution is noticeably smaller than the quark phase contributions. This might look as a support for the simple quark models [14,15]. However our model which contains the spherical cavity as an essential ingredient, might be biased in that direction. Thus in the future one should attempt to solve a model in which a quark bound state does not need a bag.

In its present form this nonlinear self consistent model shows interesting features. For example π and K contributions are considerably larger than the σ and a_0 contribution. One is tempted to conclude that this reflects the fact that in baryonic processes the presence of scalars was hard to detect. Generally speaking the model offers the stable and physically acceptable [9–11] solutions.

In this model the complete problem with u , d and s quarks and two meson nonets has been solved in TDIA. Quite complicated nonlinear operator dynamics has been reduced to the highly nontrivial, but solvable, nonlinear system.

All model dependent quantities, Tables 4.1-4.3 have acceptable orders of magnitude. All relative signs for μ and g_A are correctly predicted. The discrepancies with the experimental magnitudes reflect the exploratory character of the present TDIA solution. They might be connectable to the too simple description of the baryon state vectors [16] and to the absence of the exchange current corrections [17]. A future development of TDIA based solution might lead to better predictions.

References

1. D. Horvat, B. Podobnik and D. Tadić, Phys. Rev. **D 58**, 034003-1 (1998).
2. J. Schwinger, Ann. Phys. **2**, 407 (1957); M. Geel-Mann and M. Lévi, Nuovo Cimento **16**, 705 (1960); B. W. Lee, Nucl. Phys. **B 9**, 649 (1969); S. Gasiorowicz and D.A. Geffen Rev. Mod. Phys. **41**, 531 (1969); J. Schechter and Y. Ueda, Phys. Rev. **D 3**, 2874 (1971); H. Pagels, Phys. Rep. **C 16**, 218 (1975).
3. M. Lévi, Nuovo Cimento **52 A**, 23 (1967).
4. T.H.R. Skyrme, Proc. Roy. Soc. London, **260**, 127 (1961); **262**, 237 (1961); Nucl. Phys. **31**, 550 (1962); G.S. Adkins, C.R. Nappi and E. Witten, Nucl. Phys. **B 228**, 552 (1983), **B 233** 109 (1984); I. Zahed and G.E. Brown, Phys. Rep. **142**, 1 (1986).
5. A. Chodos and B.C.Thorn, Phys. Rev **D 12**, 2733 (1975).
6. M.C. Birse and M.K. Banerjee, Phys. Lett. **136B**, 284 (1984) ; Phys. Rev. **D 31**, 118 (1985); M.C. Birse, Phys. Rev **D 33**, 1934 (1986).
7. J.A. McGovern and M.C. Birse, Phys Lett. **B 200**, 401 (1987); J.A. McGovern and M.C. Birse, Nucl. Phys. **A 506**, 367 (1990); *ibid.* **A 506**, 393 (1990); J.A. McGovern and M.C. Birse, Fizika **19**, Suppl. 2, 56 (1987).
8. I. Tamm, J. Phys. (Moscow) **9**, 449 (1945); S.M. Dancoff, Phys. Rev. **78**, 382 (1950).

9. N.A. Törnqvist, Phys. Rev. Lett. **49**, 624 (1982); Z. Phys. **C 68**, 647 (1995).
10. N.A. Törnqvist, Phys. Rev. Lett. **76**, 1575 (1996).
11. N.A. Törnqvist, Phys. Lett. B **426**, 105 (1998); hep-ph/9905282 (1999); hep-ph/9910443 (1999).
12. G. Källén, *Quantum Electrodynamics*, (Springer-Verlag, New York-Heidelberg-Berlin, 1972)
13. A. W. Thomas, Adv. Nucl. Physics **13**, 1, ed. J. W. Negele and E. Vogt, (Plenum, New York, 1984), Vol. 13, p. 1; G. E. Brown and M. Rho, Phys. Lett. B **82**, 177 (1979); G. E. Brown, M. Rho and V. Vento, Phys. Lett. B **84**, 383 (1979); H. Hogaasen and F. Myhrer, Z. Phys. C **73** **21** (1983); Xue-Qian Li and Zhen Qi, Commun. Theor. Phys. **213** **18** (1992); G. E. Brown and M. Rho, Comments on Nucl. Part. Phys. **1** **18** (1988); F. Myhrer, in *Quarks and Nuclei, Vol. 1. of International Review of Nuclear Physics*, edited by W. Weise, (World Scientific, Singapore, 1984); A. Hosaka and H. Toki, Phys. Rep. **65** **277** (1996).
14. U. Mosel: "Fields, Symmetries and Quarks", McGraw-Hill, Hamburg (1988).
15. J.F. Donoghue, E. Golowich, B.R. Holstein: "Dynamics of the Standard Model". Cambridge University Press, Cambridge 1992.
16. J.F. Donoghue, E. Golowich, Phys. Lett. **B 69**, 4337 (1977); *ibid* , Phys. Rev. **D 15**, 3421 (1977); V. Sanjose and V. Vento, FTUV/88-29,IFIC/88-12, (1988); C. H. Chang, J. G. Hu, C. S. Huang and X. Q. Li, AS-ITP-90-25, (1991); H. W. Hammer, D. Drechsel and T. Mart, nucl-th/9701008 (1997); H. J. Lee, D. P. Min, B. Y. Park, M. Rho and V. Vento, Nucl. Phys. A **657**, 75 (1999); B. Q. Ma, I. Schmidt and J. J. Yang, Eur. Phys. J. A **12**, 353 (2001); S. D. Bass, hep-ph/0210214 (2002).
17. L.Ya. Glozman, D.O. Riska, Phys. Rept. **268** 263 (1996); K. Tsushima, D.O. Riska and P.G. Blunden, Nucl. Phys. A **559**, 543 (1993); C. Helminen, K. Dannbom, D. O. Riska and L. Y. Glozman, Nucl. Phys. A **616**, 555 (1997); D. O. Riska, Few Body Syst. Suppl. **10**, 415 (1999); L. Hannelius, D. O. Riska and L. Y. Glozman, Nucl. Phys. A **665**, 353 (2000); L. Hannelius and D. O. Riska, Phys. Rev. C **62**, 045204 (2000).
18. M. Fiolhais, J.N. Urbano and K. Goeke, Phys. Lett. **B 150**, 253 (1985); K. Goeke, M. Fiolhais, J.N. Urbano and M. Harvey, *ibid.* **B 164**, 249 (1985); E. Ruiz Arriola, P. Alberto, J.N. Urbano and K. Goeke, Z. Phys. A **333**, 203 (1989); T. Nauber, M. Fiolhais, K. Goeke, and J.N. Urbano, Nucl. Phys. A **560**, 909 (1993).
19. U. Ascher, J. Christiansen and R. D. Russel, Math. Comp. **33** 659 (1979); ACM Trans. Math. Software **7** 209 (1981); SIAM (Soc. Ind. Appl. Math.) Rev. **23** 238 (1981).
20. D. Horvat, D. Horvatić, B. Podobnik and D. Tadić, Fizika **B 9**, 181, (2000).



Autoclustering in baryon spectra

M. Kirchbach

Instituto de Física, Universidad Autónoma de San Luis Potosí,
Av. Manuel Nava 6, San Luis Potosí, S.L.P. 78240, México

Abstract. A nearest-neighbor analysis of baryon mass spectra reveals a striking autoclustering of resonances to swarms of increasing sizes. Each cluster contains K binomials of opposite parities whose spins range from $1/2$ to $K - 1/2$ and a mono-parity state of the highest spin $K + 1/2$ in the swarm. The clusters with $K = 1, 3,$ and 5 are observed in both the nucleon and the Δ excitations (up to the two nucleon states $F_{17}, H_{1,11}$ with respective masses around 1700 MeV and 2200 MeV, and the three Δ states $P_{31}, P_{33},$ and D_{33} with masses around 2500 MeV). Clusters with K even and non-zero are unoccupied so far. We trace back above regularity pattern to internal nucleon and Δ structures dominated by a quark-di-quark configuration and its respective rotational-vibrational excitations. Clusters of the above type are appealing because upon boosting they transform (up to form factors) as a Lorentz tensor of rank- K with Dirac components, i.e. as $\psi_{\mu_1 \dots \mu_K}$, and thus allow for a covariant description of resonances in flight.

1 Order in excited light-quark baryons

The structure of the nucleon spectrum is far from being settled despite its long history. This situation relates to the fact that the first facility that measured nucleon levels, the Los Alamos Meson Physics Facility (LAMPF) failed to find all the states that were possible as excitations of three quarks. Later on, the Thomas Jefferson National Accelerator Facility (TJNAF) was designed to search (among others) for those “missing resonances”. At present, all data have been collected and are awaiting evaluation [1].

In a series of papers [2] I performed a near neighbour analysis of data on mass distribution of nucleon resonances reported in Ref. [3] and drew attention to the not overlookable (by the unbiased eye) increase of state densities in a few narrow mass bands and its exact replica in the $\Delta(1232)$ spectrum (see Fig. 1).

The first group of nearly degenerate resonances consists of two equal spin- $\frac{1}{2}$ of opposite parities (one parity binomial) and a mono-parity spin- $\frac{3}{2}^-$ state. The second group starts with three parity binomials with spins ranging from $\frac{1}{2}^\pm$ to $\frac{5}{2}^\pm$, and terminates with a mono-parity spin- $\frac{7}{2}^+$ resonance. Finally, the third group begins with five parity binomials with spins ranging from $\frac{1}{2}^\pm$ to $\frac{9}{2}^\pm$, and terminates by a mono-parity spin $\frac{11}{2}^+$ resonance (see Ref. [6] for the complete N and $\Delta(1232)$ spectra). A comparison between the N and $\Delta(1232)$ spectra shows that they are identical up to two unoccupied resonances on the nucleon side (these are the counterparts of the F_{37} and $H_{3,11}$ states of the Δ excitations) and

up to three unoccupied states on the Δ side (these are the counterparts of the nucleon P_{11} , P_{13} , and D_{13} states from the third group). The $\Delta(1600)$ resonance which is most probably and independent hybrid state, is the only state that at present seems to drop out of our systematics.

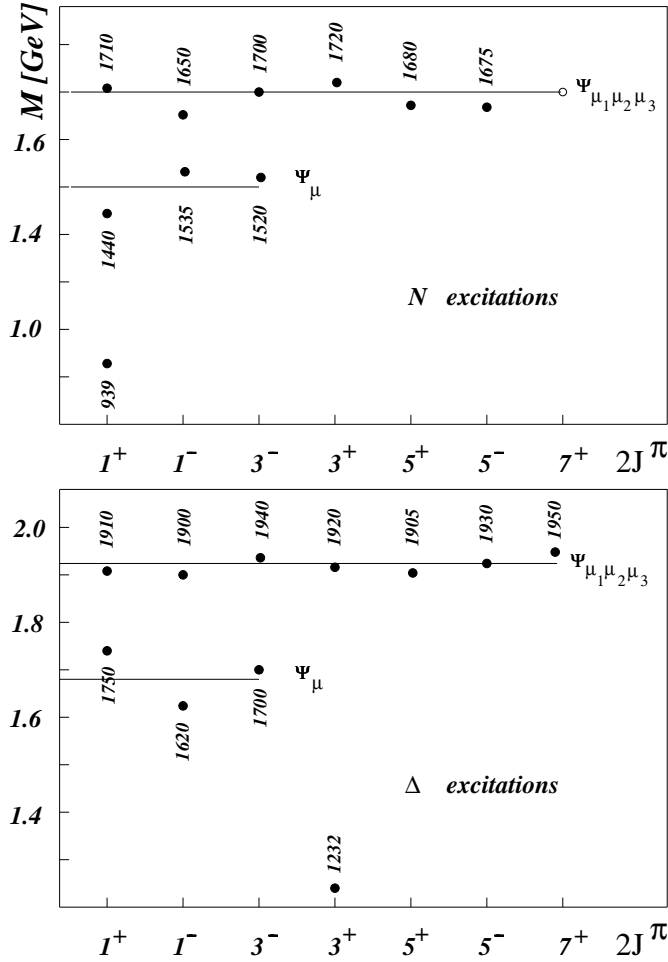


Fig. 1. Summary of the data on the nucleon and the Δ resonances. The breaking of the mass degeneracy for each of the clusters at about 5% may in fact be an artifact of the data analysis, as has been suggested by Höhler [4]. The filled circles represent known resonances, while the sole empty circle corresponds to a prediction. Figure taken from [5].

The existence of identical nucleon- and Δ crops of resonances raises the question as to what extent are we facing here a new type of symmetry which was not anticipated by any model or theory before. The next section devotes itself to answering this question.

2 Spectroscopy of autoclustering

2.1 Relevance of the quark–di-quark configuration

To the extent QCD prescribes baryons to be constituted of three quarks in a color singlet state, one may feel encouraged to exploit for the description of baryonic systems algebraic models developed for the purposes of triatomic molecules, a path pursued by Refs. [7].

In the dynamical limit $U(7) \longrightarrow U(3) \times U(4)$ of the three quark system, two of the quarks act as an independent entity, a di-quark (Dq), while the third quark (q) acts as a spectator. The di-quark approximation [8] turned out to be rather convenient in particular in describing various properties of the ground state baryons [9], [10].

The necessity for having a quark–di-quark configuration within the nucleon is independently supported by arguments related to spin in QCD. In Refs. [11], and [12] the notion of spin in QCD was re-visited in connection with the proton spin puzzle. As it is well known, the spins of the valence quarks are by themselves not sufficient to explain the spin- $\frac{1}{2}$ of the nucleon. Rather, one needs to account for the orbital angular momentum of the quarks (here denoted by L_{QCD}) and the angular momentum carried by the gluons (so called field angular momentum, G_{QCD}):

$$\begin{aligned} \frac{1}{2} &= \frac{1}{2} \Delta \Sigma + L_{\text{QCD}} + G_{\text{QCD}} \\ &= \int d^3x \left[\frac{1}{2} \bar{\psi} \gamma \gamma_5 \psi + \psi^\dagger (\mathbf{x} \times (-\mathbf{D})) \psi + \mathbf{x} \times (\mathbf{E}^a \times \mathbf{B}^a) \right]. \end{aligned}$$

In so doing one encounters the problem that neither L_{QCD} , nor G_{QCD} satisfy the spin $su(2)$ algebra. If at least $(L_{\text{QCD}} + G_{\text{QCD}})$ is to do so,

$$\left[(L_{\text{QCD}}^i + G_{\text{QCD}}^i), (L_{\text{QCD}}^j + G_{\text{QCD}}^j) \right] = i \epsilon^{ijk} (L_{\text{QCD}}^k + G_{\text{QCD}}^k), \quad (1)$$

then $\mathbf{E}^{i;a}$ has to be *restricted* to a chromo-electric charge, while $\mathbf{B}^{i;a}$ has to be a chromo-magnetic dipole according to,

$$\mathbf{E}^{i;a} = \frac{g \chi'^i}{r'^3} \mathbf{T}^a, \quad \mathbf{B}^{i;a} = \left(\frac{3 \chi^i \chi^l m^l}{r^5} - \frac{m^i}{r^3} \right) \mathbf{T}^a, \quad (2)$$

where $\chi'^i = \chi^i - R^i$. The above color fields are the perturbative one-gluon approximation typical for a di-quark-quark structure. The di-quark and the quark are in turn the sources of the color Coulomb field, and the color magnetic dipole field. In terms of color and flavor degrees of freedom, the nucleon wave function indeed has the required quark–di-quark form $|p_\uparrow\rangle = \frac{\epsilon_{ijk}}{\sqrt{18}} [u_{i\downarrow}^+ d_{j\uparrow}^+ - u_{i\uparrow}^+ d_{j\downarrow}^+] u_{k\uparrow}^+ |0\rangle$. A similar situation appears when looking for covariant QCD solutions in form of a membrane with the three open ends being associated with the valence quarks. When such a membrane stretches to a string, so that a linear action (so called gonihedric string) can be used, one again encounters that very K-cluster degeneracies in the excitations spectra of the baryons, this time as a part of an infinite

tower of states. The result was reported by Savvidy in Ref. [13]. Thus the covariant spin-description provides an independent argument in favor of a dominant quark-di-quark configuration in the structure of the nucleon, while search for covariant resonant QCD solutions leads once again to infinite K-cluster towers. Within the context of the quark–di-quark (q-Dq) model, the ideas of the rovibron model, known from the spectroscopy of diatomic molecules [14] acquires importance as a tool for the description of the rotational-vibrational (rovibron) excitations of the q–Dq system.

2.2 The quark rovibron

In the rovibron model (RVM) the relative q–Dq motion is described by means of four types of boson creation operators s^+ , p_1^+ , p_0^+ , and p_{-1}^+ . The operators s^+ and p_m^+ in turn transform as rank-0, and rank-1 spherical tensors, i.e. the magnetic quantum number m takes in turn the values $m = 1, 0$, and -1 . In order to construct boson-annihilation operators that also transform as spherical tensors, one introduces the four operators $\tilde{s} = s$, and $\tilde{p}_m = (-1)^m p_{-m}$. Constructing rank- k tensor product of any rank- k_1 and rank- k_2 tensors, say, $A_{m_1}^{k_1}$ and $A_{m_2}^{k_2}$, is standard and given by

$$[A^{k_1} \otimes A^{k_2}]_m^k = \sum_{m_1, m_2} (k_1 m_1 k_2 m_2 | km) A_{m_1}^{k_1} A_{m_2}^{k_2}. \quad (3)$$

Here, $(k_1 m_1 k_2 m_2 | km)$ are the standard $O(3)$ Clebsch-Gordan coefficients.

Now, the lowest states of the two-body system are identified with N boson states and are characterized by the ket-vectors $|n_s n_p l m\rangle$ (or, a linear combination of them) within a properly defined Fock space. The constant $N = n_s + n_p$ stands for the total number of s - and p bosons and plays the rôle of a parameter of the theory. In molecular physics, the parameter N is usually associated with the number of molecular bound states. The group symmetry of the rovibron model is well known to be $U(4)$. The fifteen generators of the associated $su(4)$ algebra are determined as the following set of bilinears

$$\begin{aligned} A_{00} &= s^+ \tilde{s}, & A_{0m} &= s^+ \tilde{p}_m, \\ A_{m0} &= p_m^+ \tilde{s}, & A_{mm'} &= p_m^+ \tilde{p}_{m'}. \end{aligned} \quad (4)$$

The $u(4)$ algebra is then recovered by the following commutation relations

$$[A_{\alpha\beta}, A_{\gamma\delta}]_- = \delta_{\beta\gamma} A_{\alpha\delta} - \delta_{\alpha\delta} A_{\gamma\beta}. \quad (5)$$

The operators associated with physical observables can then be expressed as combinations of the $u(4)$ generators. To be specific, the three-dimensional angular momentum takes the form

$$L_m = \sqrt{2} [p^+ \otimes \tilde{p}]_m^1. \quad (6)$$

Further operators are $(D_m)_-$ and (D'_m) defined as

$$D_m = [p^+ \otimes \tilde{s} + s^+ \otimes \tilde{p}]_m^1, \quad (7)$$

$$D'_m = i[p^+ \otimes \tilde{s} - s^+ \otimes \tilde{p}]_m^1, \quad (8)$$

respectively. Here, \mathbf{D} plays the rôle of the electric dipole operator.

Finally, a quadrupole operator Q_m can be constructed as

$$Q_m = [p^+ \otimes \tilde{p}]_m^2, \quad \text{with } m = -2, \dots, +2. \quad (9)$$

The $u(4)$ algebra has the two algebras $su(3)$, and $so(4)$, as respective sub-algebras. The $so(4)$ sub-algebra of interest here, is constituted by the three components of the angular momentum operator L_m , on the one side, and the three components of the operator D'_m , on the other side. The chain of reducing $U(4)$ down to $O(3)$

$$U(4) \supset O(4) \supset O(3), \quad (10)$$

corresponds to an exactly soluble RVM limit. The Hamiltonian of the RVM in this case is constructed as a properly chosen function of the Casimir operators of the algebras of the subgroups entering the chain. For example, in case one approaches $O(3)$ via $O(4)$, the Hamiltonian of a dynamical $SO(4)$ symmetry can be cast into the form [15]:

$$H_{RVM} = H_0 - f_1 (4\mathcal{C}_2(so(4)) + 1)^{-1} + f_2 \mathcal{C}_2(so(4)). \quad (11)$$

The Casimir operator $\mathcal{C}_2(so(4))$ is defined accordingly as

$$\mathcal{C}_2(so(4)) = \frac{1}{4} (\mathbf{L}^2 + \mathbf{D}'^2) \quad (12)$$

and has an eigenvalue of $\frac{K}{2} (\frac{K}{2} + 1)$. Here, the parameter set has been chosen as

$$H_0 = M_{N/\Delta} + f_1, \quad f_1 = 600 \text{ MeV}, \quad f_2^N = 70 \text{ MeV}, \quad f_2^\Delta = 40 \text{ MeV}. \quad (13)$$

Thus, the $SO(4)$ dynamical symmetry limit of the RVM picture of baryon structure motivates existence of quasi-degenerate resonances gathering to crops in both the nucleon- and Δ baryon spectra. The Hamiltonian that will fit masses of the reported cluster states is exactly the one in Eq. (11).

In order to demonstrate how the RVM applies to baryon spectroscopy, let us consider the case of q - D_q states associated with $N = 5$ and for the case of a $SO(4)$ dynamical symmetry. It is of common knowledge that the totally symmetric irreps of the $u(4)$ algebra with the Young scheme $[N]$ contain the $SO(4)$ irreps $(\frac{K}{2}, \frac{K}{2})$ (here K plays the role of the four-dimensional angular momentum) with

$$K = N, N - 2, \dots, 1 \quad \text{or} \quad 0. \quad (14)$$

Each one of the K - irreps contains $SO(3)$ multiplets with three dimensional angular momentum

$$l = K, K - 1, K - 2, \dots, 1, 0. \quad (15)$$

In applying the branching rules in Eqs. (14), (15) to the case $N = 5$, one encounters the series of levels

$$\begin{aligned} K = 1: & \quad l = 0, 1; \\ K = 3: & \quad l = 0, 1, 2, 3; \\ K = 5: & \quad l = 0, 1, 2, 3, 4, 5. \end{aligned} \quad (16)$$

The parity carried by these levels is $\eta(-1)^l$ where η is the parity of the relevant vacuum. In coupling now the angular momentum in Eq. (16) to the spin- $\frac{1}{2}$ of the three quarks in the nucleon, the following sequence of states is obtained:

$$\begin{aligned} K = 1: \quad \eta J^\pi &= \frac{1^+}{2}, \frac{1^-}{2}, \frac{3^-}{2}; \\ K = 3: \quad \eta J^\pi &= \frac{1^+}{2}, \frac{1^-}{2}, \frac{3^-}{2}, \frac{3^+}{2}, \frac{5^+}{2}, \frac{5^-}{2}, \frac{7^-}{2}; \\ K = 5: \quad \eta J^\pi &= \frac{1^+}{2}, \frac{1^-}{2}, \frac{3^-}{2}, \frac{3^+}{2}, \frac{5^+}{2}, \frac{5^-}{2}, \frac{7^-}{2}, \frac{7^+}{2}, \frac{9^-}{2}, \frac{11^-}{2}. \end{aligned} \quad (17)$$

Therefore, rovibron states of half-integer spin transform according to $(\frac{K}{2}, \frac{K}{2}) \otimes [(\frac{1}{2}, 0) \oplus (0, \frac{1}{2})]$ representations of $SO(4)$. The isospin structure is accounted for pragmatically through attaching to the K -clusters an isospin spinor χ^I with I taking the values $I = \frac{1}{2}$ and $I = \frac{3}{2}$ for the nucleon, and the Δ states, respectively. As illustrated by Fig. 1, the above quantum numbers cover both the nucleon and the Δ excitations.

The states in Eq. (17) are degenerate and the dynamical symmetry is $O(4)$. The above considerations apply to the rest frame. In order to describe clusters in flight one needs to subject the $O(4)$ degenerate resonance states to a Lorentz boost.

The most efficient way to achieve this task is not to boost the spin by spin but rather the K multiplet as a whole, which takes one (up to form factors) to the K Lorentz tensors with Dirac spinor components, $\psi_{\mu_1 \dots \mu_K}$.

2.3 Observed and unoccupied clusters within the rovibron model

The comparison of the states in Eq. (17) with the reported ones in Fig. 1 shows that the predicted sets are in agreement with the characteristics of the non-strange baryon excitations with masses below ~ 2500 MeV, provided, the parity η of the vacuum changes from scalar ($\eta = 1$) for the $K = 1$, to pseudoscalar ($\eta = -1$) for the $K = 3, 5$ clusters. A pseudoscalar ‘‘vacuum’’ can be modeled in terms of an excited composite di-quark carrying an internal angular momentum $L = 1^-$ and maximal spin $S = 1$. In one of the possibilities the total spin of such a system can be $|L - S| = 0^-$. To explain the properties of the ground state, one has to consider separately even N values, such as, say, $N' = 4$. In that case another branch of excitations, with $K = 4, 2$, and 0 will emerge. The $K = 0$ value characterizes the ground state, $K = 2$ corresponds to $(1, 1) \otimes [(\frac{1}{2}, 0) \oplus (0, \frac{1}{2})]$, while $K = 4$ corresponds to $(2, 2) \otimes [(\frac{1}{2}, 0) \oplus (0, \frac{1}{2})]$. These are the multiplets that we will associate with the ‘‘missing’’ resonances predicted by the rovibron model. In this manner, reported and ‘‘missing’’ resonances fall apart and populate distinct $U(4)$ - and $SO(4)$ representations. In making observed and ‘‘missing’’ resonances distinguishable, reasons for their absence or, presence in the spectra are easier to be searched for. In accordance with Ref. [16] we here will treat the $N = 4$ states to be all of natural parities and identify them with the nucleon ($K = 0$), the natural parity $K = 2$, and the natural parity $K = 4$ -clusters. We shall refer to the latter as ‘‘missing’’ rovibron clusters. In Table I we list the masses of the K -clusters concluded from Eqs. (11), and (13).

Table 1. Predicted mass distribution of observed (obs), and missing (miss) ro vibron clusters (in MeV) according to Eqs. (9,11). The sign of η in Eq. (15) determines natural- ($\eta = +1$), or, unnatural ($\eta = -1$) parity states. The experimental mass averages of the resonances from a given K-cluster have been labeled by “exp”.

K	sign η	N^{obs}	N^{exp}	Δ^{obs}	Δ^{exp}	N^{miss}	Δ^{miss}
0	+	939	939	1232	1232		
1	+	1441	1498	1712	1690		
2	+					1612	1846
3	-	1764	1689	1944	1922		
4	+					1935	2048
5	-	2135	2102	2165	2276		

In Ref. [15] we presented the four dimensional Racah algebra that allows to calculate transition probabilities for electromagnetic de-excitations of the ro vibron levels. The interested reader is invited to consult the quoted article for details. Here I restrict myself to reporting the following two results: (i) All resonances from a K- mode have same widths. (ii) As compared to the natural parity $K = 1$ states, the electromagnetic de-excitations of the unnatural parity $K = 3$ and $K = 5$ ro vibron states appear strongly suppressed. To illustrate our predictions I compiled in Table 2 below data on experimentally observed total widths of resonances belonging to $K = 3$, and $K = 5$. The suppression of the electromagnetic

Table 2. Reported widths of resonance clusters

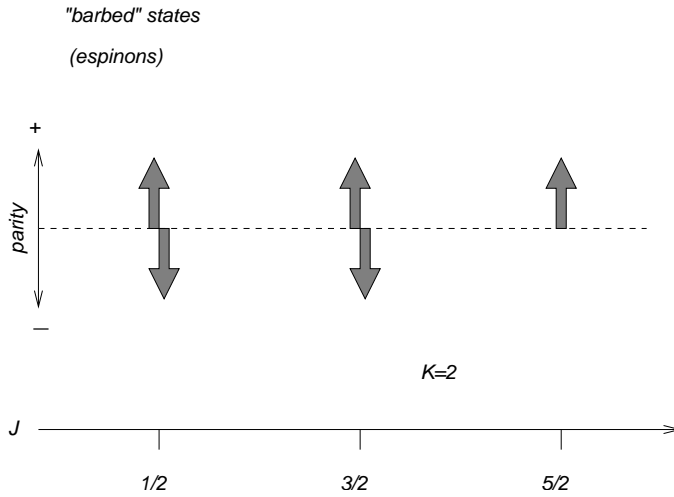
K	Resonance	width [in GeV]
3	$N \left(\frac{1}{2}^-; 1650 \right)$	0.15
3	$N \left(\frac{1}{2}^+; 1710 \right)$	0.10
3	$N \left(\frac{3}{2}^+; 1720 \right)$	0.15
3	$N \left(\frac{3}{2}^-; 1700 \right)$	0.15
3	$N \left(\frac{5}{2}^-; 1675 \right)$	0.15
3	$N \left(\frac{5}{2}^+; 1680 \right)$	0.13
5	$N \left(\frac{3}{2}^+; 1900 \right)$	0.50
5	$N \left(\frac{5}{2}^+; 2000 \right)$	0.49

de-excitation modes of unnatural parity states to the nucleon (of natural parity) is shown in Table 3. It is due to the vanishing overlap between the scalar di-quark in the latter case, and the pseudo-scalar one, in the former. Non-vanishing widths can signal small admixtures from natural parity states of same spins belonging to even K number states from the “missing” resonances. For example, the significant

Table 3. Reported helicity amplitudes of resonances.

K	parity of the spin-0 di-quark	Resonance	$A_{\frac{1}{2}}^p$	$A_{\frac{3}{2}}^2$	$[10^{-3}\text{GeV}^{-\frac{1}{2}}]$
3	—	$N\left(\frac{1}{2}^+; 1710\right)$	9 ± 22		
3	—	$N\left(\frac{3}{2}^+; 1720\right)$	18 ± 30	-19 ± 20	
3	—	$N\left(\frac{3}{2}^-; 1700\right)$	-18 ± 30	-2 ± 24	
3	—	$N\left(\frac{5}{2}^-; 1675\right)$	19 ± 8	15 ± 9	
3	—	$N\left(\frac{5}{2}^+; 1680\right)$	-15 ± 6	133 ± 12	
1	+	$N\left(\frac{3}{2}^-; 1520\right)$	-24 ± 9	166 ± 5	

value of $A_{\frac{3}{2}}^p$ for $N\left(\frac{5}{2}^+; 1680\right)$ from $K = 3$ may appear as an effect of mixing with the $N\left(\frac{5}{2}^+; 1612\right)$ state from the natural parity “missing” cluster with $K = 2$. This gives one the idea to use helicity amplitudes to extract “missing” states.

**Fig. 2.** K-excitation mode of a quark-diquark string: *barbed* states (*espinons*).

The above considerations show that a K-mode of an excited quark-di-quark string (be the diquark scalar, or, pseudoscalar) represents an independent entity (particle?) in its own rights which deserves its own name. To me the different spin facets of the K-cluster pointing into different “parity directions” as displayed in Fig. 2 look like barbs. That’s why I suggest to refer to the K-clusters as *barbed* states to emphasize the aspect of alternating parity. Barbs could also be associated with thorns (Spanish, *espinos*), and *espinons* could be another sound name for K-clusters.

3 Conclusions

Beyond pointing onto the phenomenon of an evident autoclustering in the spectra of the light quark baryons, it was argued that the swarms of resonances can be (i) explained as a consequence of rotational-vibrational modes of an excited quark-di-quark configuration, be the di-quark scalar, or, pseudoscalar, when at rest, and (ii) described covariantly in terms of $\psi_{\mu_1 \dots \mu_K}$, when in flight.

Acknowledgments

The quark-di-quark dynamics behind the resonance clusters was revealed by the help of Marcos Moshinsky and Yuri Smirnov.

Thanks to Mitja Rosina, Bojan Golli, and Simon Širca for having managed such an unforgettable event. Especially the vibrant discussions with Mitja Rosina helped throwing more light on various cluster facets.

Work supported by Consejo Nacional de Ciencia y Tecnología (CONACyT, Mexico) under grant number C01-39820.

References

1. V. Burkert, Eur. Phys. J. **A17**, 303 (2003).
2. M. Kirchbach, Mod. Phys. Lett. **A12**, 2373-2386 (1997); Few Body Syst. Suppl. **11**, 47-52 (1999).
3. Particle Data Group, Eur. Phys. J. **C15**, 1 (2000).
4. G. Höhler, in *Pion-Nucleon Scattering* (Springer Publishers, Heidelberg, 1983), Landolt-Börnstein Vol. I/9b2, Ed. H. Schopper.
5. M. Kirchbach, D. V. Ahluwalia, Phys. Lett. **B529**, 124-131 (2002).
6. M. Kirchbach, Nucl. Phys. **A689**, 157c-166c (2001).
7. R. Bijker, F. Iachello, and A. Leviatan, Phys. Rev. **C54**, 1935-1953 (1996);
R. Bijker, F. Iachello, and A. Leviatan, Ann. of Phys. **236**, 69-116 (1994).
8. Proc. Int. Conf. *Diquarks 3*, Torino, Oct. 28-30 (1996), eds. M. Anselmino and E. Predazzi, (World Scientific).
9. M. Oettel, R. Alkofer, and L. von Smekal Eur. Phys. J. **A8**, 553-566 (2000).
10. K. Kusaka, G. Piller, A. W. Thomas, and A. G. Williams, Phys. Rev. **D55**, 5299-5308 (1997).
11. D. Singleton, Phys. Lett. **B427**, 155-160 (1998).
12. X. Ji, Phys. Rev. Lett. **78**, 610-613 (1997);
X. Ji, Phys. Rev. Lett. **79**, 1255-1228 (1997).
13. G. Savvidy, Phys. Lett. **B438**, 69-79 (1998).
14. F. Iachello, and R. D. Levin, *Algebraic Theory of Molecules* (Oxford Univ. Press, N.Y.) 1992.
15. M. Kirchbach, M. Moshinsky, and Yu. F. Smirnov, Phys. Rev. **D64**, 114005 (2001).
16. M. Kirchbach, Int. J. Mod. Phys. **A15**, 1435-1451 (2000).



$\langle A^2 \rangle$ -condensate and Dyson-Schwinger approach to mesons ^{*}

Dubravko Klabučar^a and Dalibor Kekez^b

^a Department of Physics, Faculty of Science, Zagreb University, Bijenička c. 32, 10000 Zagreb, Croatia

^b Rudjer Bošković Institute, P.O.B. 180, 10002 Zagreb, Croatia

Abstract. The dimension 2 gluon condensate $\langle A_{\mu}^a A^{a\mu} \rangle \equiv \langle A^2 \rangle$ may have a significant effect on quark-gluon interactions. Enhancement of these interactions at intermediate ($Q^2 \sim 0.5 \text{ GeV}^2$) spacelike transferred momenta is needed in phenomenological Dyson-Schwinger studies, but until recently has not been explained in terms of possible QCD condensates. We have recently proposed that taking into account the dimension 2 gluon condensate $\langle A^2 \rangle$ leads to a phenomenologically successful enhancement of the quark-gluon interaction.

1 Introduction

Dyson-Schwinger (DS) equations provide a prominent approach to physics of strong interactions. To reproduce the hadronic phenomenology well, the Dyson-Schwinger approach in the rainbow-ladder approximation must employ an effective interaction between quarks which is fairly strong at intermediate ($-p^2 = Q^2 \sim 0.5 \text{ GeV}^2$) spacelike transferred momenta p . We have recently proposed [1] that such an interaction may originate from the dimension 2 gluon condensate $\langle A^2 \rangle$ which has recently attracted much attention [2–6] among theorists and lattice QCD. We also showed [1] that the resulting effective running coupling leads to the sufficiently strong dynamical chiral symmetry breaking and successful phenomenology at least in the light sector of pseudoscalar mesons. In the present paper, we give a more detailed presentation of the parameter dependence of these results.

2 DS approach and its effective interaction

DS approach to hadrons and their quark-gluon substructure [7–9] has strong and clear connections with QCD. Besides being covariant, this approach is chirally well-behaved and nonperturbative. This has been crucial, especially in the light-quark sector of QCD, for successful descriptions of bound states achieved by phenomenological DS studies (e.g., see recent reviews [8,9] and references therein), where one can treat soundly [10] even the processes influenced by axial anomaly

^{*} Talk delivered by Dubravko Klabučar

which is really remarkable for a bound-state approach. In the process of solving DS equations, one in essence derives a constituent quark model which turns out to be successful over a very wide range of masses. Its chief virtue is that it incorporates the correct chiral symmetry behavior through the gap equation for the full, dynamically dressed quark propagator S_q and the Bethe-Salpeter (BS) equation for the bound states of the dynamically dressed quarks (and antiquarks). That is, the constituent quarks arise through dressing resulting from dynamical chiral symmetry breaking (D χ SB) in the (“gap”) DS equation for the full quark propagators, while the *light* $q\bar{q}$ pseudoscalar solutions of the BS equation (in a *consistent* approximation) are (*almost* massless) *quasi*-Goldstone bosons of D χ SB. Generation of D χ SB is well-understood [7,8,11–13] in the rainbow-ladder approximation (RLA). Thus, phenomenological DS studies have mostly been relying on RLA and using *Ansätze* of the form

$$K(k) = i4\pi\alpha_{\text{eff}}(-k^2) D_{\mu\nu}^{\text{ab}}(k)_0 \frac{\lambda^{\text{a}}}{2} \gamma^\mu \otimes \frac{\lambda^{\text{b}}}{2} \gamma^\nu \quad (1)$$

for interactions between quarks. In this equation, $D_{\mu\nu}^{\text{ab}}(k)_0$ is the *free* gluon propagator, while $\alpha_{\text{eff}}(Q^2)$ is an effective running coupling which may incorporate (if only by parametrization) various effects, such as the dressing of the full gluon propagator or the dressing of the full quark-gluon vertex.

What is important to get a successful hadronic phenomenology, especially in the light-quark sector ($q = u, d, s$), is that D χ SB is sufficiently strong. This means that the gap DS equation should yield dressed quark propagator solutions resulting in the dressed-quark mass function $M_q(p^2)$ whose values *at low* $-p^2$ are of the order of typical constituent mass values, namely several hundred MeV, even in the chiral limit.

Indeed, the issue of the origin of the interaction (1), or, equivalently, $\alpha_{\text{eff}}(Q^2)$ which would enable successful phenomenology is crucial for the DS studies. The form of α_{eff} is only partially known from the fact that at large spacelike momenta it must reduce to $\alpha_{\text{pert}}(Q^2)$, the well-known running coupling of perturbative QCD. However, for momenta $Q^2 \lesssim 1 \text{ GeV}^2$, where non-perturbative QCD applies, the interactions are still not known; therefore, in phenomenological DS studies, $\alpha_{\text{eff}}(Q^2)$ must be modeled for $Q^2 \lesssim 1 \text{ GeV}^2$ - e.g., see Refs. [14,11–13,7–9]. There, one can see that phenomenologically most successful of those modeled interactions have a rather large bump at the intermediate momenta, around $Q^2 \sim 0.5 \text{ GeV}^2$. For example, in Fig. 1 compare $\alpha_{\text{eff}}(Q^2)$ used by Jain and Munczek (JM) [11] and by Maris, Roberts and Tandy (MRT) [12,13,8,9]. In any case, successful DS phenomenology requires that this modeled part of the interaction (1) be fairly strong. That is, regardless of details of the interaction, its *integrated strength* in the infrared must be fairly high to achieve acceptable description of hadrons, notably mass spectra and D χ SB [8,9].

Theoretical explanations on what could be the origin of so strong nonperturbative part of the phenomenologically required interaction are obviously very much needed, either from the *ab initio* studies of sets of DS equations for Green’s functions of QCD (see, e.g., the recent review [7]) or from somewhere outside DS approach. The particularly important result of the *ab initio* DS studies is that, in

the Landau gauge, the effects of ghosts are absolutely crucial for the intermediate-momenta enhancement of the effective quark-gluon interaction [7,15–17]. This is obvious in the expression for the strong running coupling $\alpha_s(Q^2)$ in these Landau-gauge studies [7,15–17],

$$\alpha_s(Q^2) = \alpha_s(\mu^2) Z(Q^2) G(Q^2)^2, \quad (2)$$

where $\alpha_s(\mu^2) = g^2/4\pi$ and $Z(\mu^2)G(\mu^2)^2 = 1$ at the renormalization point $Q^2 = \mu^2$. In the Landau gauge, the gluon renormalization function $Z(-k^2)$ defines the full gluon propagator $D_{\mu\nu}^{ab}(k) = Z(-k^2)D_{\mu\nu}^{ab}(k)_0$. Similarly, $G(-k^2)$ is the ghost renormalization function which defines the full ghost propagator $D_G^{ab}(k) = \delta^{ab}G(-k^2)/k^2$.

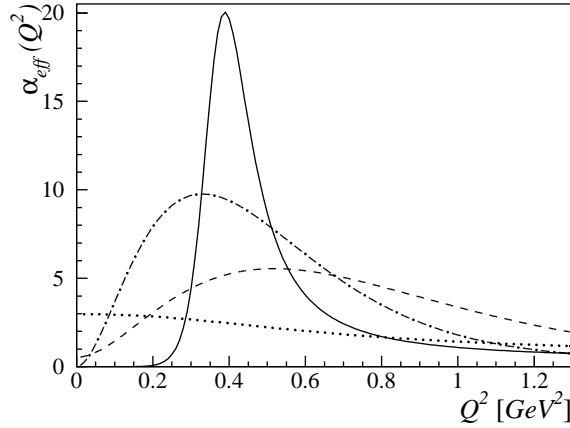


Fig. 1. The momentum dependence of various strong running couplings mentioned in the text. JM [11] and MRT [13,8] $\alpha_{\text{eff}}(Q^2)$ are depicted by, respectively, dashed and dash-dotted curves. The effective coupling (3) proposed and analyzed in the present paper is depicted by the solid curve, and $\alpha_s(Q^2)$ (2) of Fischer and Alkofer [16] (their fit A) by the dotted curve.

While the *ab initio* DS studies [7,15–17] do find significant enhancement of $\alpha_s(Q^2)$, Eq. (2), until recently this seemed still not enough to yield a sufficiently strong $D\chi\text{SB}$ (e.g., see Sec. 5.3 in Ref. [7]) and a successful phenomenology. However, for carefully constructed dressed quark-gluon vertex *Ansätze*, Fischer and Alkofer [16] have recently managed to obtain good results for dynamically generated constituent quark masses and pion decay constant f_{π} , although not simultaneously also for the chiral quark-antiquark $\langle \bar{q}q \rangle$ condensate, which then came out somewhat larger than the phenomenological value. Thus, the overall situation is that there is progress in this direction [15–18], but that further investigation and elucidation of the origin of phenomenologically successful effective interaction kernels remains one of primary challenges in contemporary DS studies [8,9]. This provided the motivation for our paper [1], where we pointed out that such an interaction kernel for DS studies in the Landau gauge resulted from

cross-fertilization of the DS ideas on the running coupling of the form (2) [7,15–17] and the ideas on the possible relevance of the dimension 2 gluon condensate $\langle A_\mu^\alpha A^{\alpha\mu} \rangle \equiv \langle A^2 \rangle$ [2–6,19–22].

In Ref. [1], we gave arguments that the $\langle A^2 \rangle$ -contributions to the OPE-improved gluon (A) and ghost (G) polarization functions (found a long time ago by Refs. [19–22] and more recently confirmed by Kondo [5]) lead to an effective coupling $\alpha_{\text{eff}}(Q^2)$ given by

$$\alpha_{\text{eff}}(Q^2) = \alpha_{\text{pert}}(Q^2) Z^{\text{Npert}}(Q^2) G^{\text{Npert}}(Q^2)^2, \quad (3)$$

where $\alpha_{\text{pert}}(Q^2)$ is the (Landau-pole-regularized) running coupling of perturbative QCD, and

$$Z^{\text{Npert}}(Q^2) = \frac{1}{1 + \frac{m_A^2}{Q^2} + \frac{C_A}{Q^4}}, \quad (4)$$

$$G^{\text{Npert}}(Q^2) = \frac{1}{1 - \frac{m_G^2}{Q^2} + \frac{C_G}{Q^4}}. \quad (5)$$

The functions $Z^{\text{Npert}}(Q^2)$ and $G^{\text{Npert}}(Q^2)$ are the nonperturbative (N_{pert}) parts of the, respectively, gluon and ghost renormalization functions $Z(Q^2)$ and $G(Q^2)$. They crucially depend on the quantity m_A which can be interpreted as a dynamically generated effective gluon mass, and which is proportional to the dimension 2 gluon condensate $\langle A^2 \rangle$. Concretely, for the Landau gauge (to which we stick throughout this paper), the number of QCD colors $N_c = 3$ and the number of space-time dimensions $D = 4$,

$$m_A^2 = \frac{3}{32} g^2 \langle A^2 \rangle = -m_G^2, \quad (6)$$

where m_G is a dynamically generated effective ghost mass.

For $g^2 \langle A^2 \rangle$, the Landau-gauge lattice studies of Boucaud *et al.* [2] yield the value 2.76 GeV². This is compatible with the bound resulting from the discussions of Gubarev *et al.* [3,4] on the physical meaning of $\langle A^2 \rangle$ (although it is gauge-variant) and its possible importance for confinement. We thus use this value in Eq. (6) and obtain

$$m_A = 0.845 \text{ GeV}. \quad (7)$$

In our considerations below, this value will turn out to be a remarkably good initial estimate for the dynamical masses m_A and m_G .

The coefficients C_A and C_G appearing in $Z^{\text{Npert}}(Q^2)$ (4) and $G^{\text{Npert}}(Q^2)$ (5), can, in principle, be related to various other condensates [20–22], but some of them are completely unknown at present. Therefore, both C_A and C_G should at this point be treated as free parameters to be fixed by phenomenology. Fortunately, Ref. [1] managed to make the estimate $C_A = (0.640 \text{ GeV})^4$. This estimate [1] is based on the role of only one condensate [23], the well-known gauge-invariant dimension 4 condensate $\langle F^2 \rangle$ [24], and thus misses some (unknown) three- and four-gluon contributions [21,22]. Therefore, and since the true value of $\langle F^2 \rangle$ is still rather uncertain [25], we do not attach too much importance to the above precise value of C_A but just use it as an inspired initial estimate.

There is no similar estimate for C_G , but one may suppose that it would not differ from C_A by orders of magnitude. We thus try

$$C_G = C_A = (0.640 \text{ GeV})^4 \quad (8)$$

as an initial guess. It turns out *a posteriori* that this value of C_G leads to a very good fit to phenomenology.

Our $\alpha_{\text{eff}}(Q^2)$ (3) exhibits such an enhancement centered around $Q^2 \approx m_A^2/2$, as shown by the solid curve representing it in Fig. 1. This enhancement is readily understood when one notices that Eq. (3) has four poles in the complex Q^2 plane, given by

$$(Q^2)_{1,2} = \frac{1}{2} \left(m_A^2 \mp i\sqrt{4C_G - m_A^4} \right) \quad [\text{poles of } G^{\text{Npert}}(Q^2)] , \quad (9)$$

$$(Q^2)_{3,4} = \frac{1}{2} \left(-m_A^2 \mp i\sqrt{4C_A - m_A^4} \right) \quad [\text{poles of } Z^{\text{Npert}}(Q^2)] . \quad (10)$$

For $\min\{C_G, C_A\} > m_A^4/4$ there is no pole on the real axis, but a saddle point in the middle of two complex conjugated poles. For the DS studies, which are almost exclusively carried out in Euclidean space, spacelike k^2 (i.e., $Q^2 > 0$ in our convention) is the relevant domain and is thus pictured in Fig. 1. There, the maximum of $\alpha_{\text{eff}}(Q^2)$ (3) at the real axis is at $Q^2 \approx m_A^2/2$, i.e., the real part of its *double* poles $(Q^2)_{1,2}$. The height and the width of the peak is influenced by both C_G and m_A . The enhancement of $\alpha_{\text{eff}}(Q^2)$ (3) is thus crucially determined by the $\langle A^2 \rangle$ condensate through Eq. (6), and by the manner this condensate contributes to the ghost renormalization function, which enters squared into the effective coupling (3).

3 Light pseudoscalars with the condensate-enhanced coupling

We solved the gap DS equations for quark propagators and BS equations for pseudoscalar $q\bar{q}$ ($q = u, d, s$) bound states in the same way as in our previous phenomenological DS studies [26–29]. This essentially means as in the JM approach [11], except that instead of JM’s $\alpha_{\text{eff}}(Q^2)$, Eq. (3) is employed in the RLA interaction (1). We can thus immediately present the results because we can refer to Refs. [26–29] for all calculational details, such as procedures for solving DS and BS equations, all model details, and explicit expressions for calculated quantities, e.g., for f_π .

DS approach to hadrons is chirally well-behaved and exhibits the correct behavior in the chiral limit, such as appearance of Goldstone bosons which are simultaneously massless pseudoscalar $q\bar{q}$ bound states, and satisfying the Gell-Mann-Oakes-Renner (GMOR) relation, at the level of a couple of percent. In this limit the bare (and current) quark masses vanish and the only parameters are those defining our $\alpha_{\text{eff}}(Q^2)$ (3), namely m_A , C_A and C_G . It turns out that the initial estimates (7) and (8), motivated above, need only a slight modification to provide a very good description of the light pseudoscalar sector: it is enough to

increase the estimate $m_A = 0.845$ GeV by just 5%, as the parameter set

$$C_A = (0.640 \text{ GeV})^4 = C_G \quad , \quad m_A = 0.884 \text{ GeV} \quad (11)$$

leads to the constituent quark masses $[M_q(p^2 \sim 0)]$ in the right ballpark $[M_q(p^2 \sim 0) \sim M_{\text{nucleon}}/3 \sim M_\rho/2]$, as well as the good chiral limit values of the pion decay constant ($f_\pi \approx 88$ MeV) and the $\bar{q}q$ condensate $[\langle \bar{q}q \rangle \approx (-214 \text{ GeV})^3]$ [1].

Our results are very sensitive to C_G and m_A . This is understandable, since from Eqs. (9) it is clear that C_G , in combination with m_A , influences the height and width of the peak of $\alpha_{\text{eff}}(Q^2)$ (3) for spacelike momenta. In spite of this sensitivity, we were able to find other combinations of parameter values which also lead to good or even better results, for example the values

$$C_A = (0.6060 \text{ GeV})^4 = C_G \quad , \quad m_A = 0.8402 \text{ GeV} . \quad (12)$$

This indicates that there may be an interesting interplay between m_A and C_G and motivates us to find how the phenomenologically favorable values of m_A and C_G are related. However, we will do it below in the more realistic, massive case, away from the chiral limit. There, the quark bare masses (and the related current masses) deviate from zero so that empirical masses of pseudoscalar mesons can be obtained.

Table 1. The masses and decay constants of pions and kaons, and the $\pi^0 \rightarrow \gamma\gamma$ decay amplitude $\Gamma_{\pi^0}^{\gamma\gamma}$, obtained in DS approach with our $\alpha_{\text{eff}}(Q^2)$ (3). The first two lines result from the initial parameters $m_A, C_{A,G}$ (11) and the quark bare mass parameters (13) fixed already by the broad JM phenomenological fit [11]. These masses (13) with another ($m_A, C_{A,G}$) parameter set (12) give the third and the fourth line. Similarly, the fifth and the sixth line result from $\alpha_{\text{eff}}(Q^2)$ with $m_A, C_{A,G}$ given by Eq. (12), and the slightly altered bare masses (14). The last two lines are the corresponding experimental values.

$\alpha_{\text{eff}}, C_G, C_A,$ $m_A, \tilde{m}_u, \tilde{m}_s$	H	M_H [MeV]	f_H [MeV]	$\Gamma_{\pi^0}^{\gamma\gamma}$ [MeV $^{-1}$]
Eqs. (3),(11) and (13)	π K^+	136.70 520.72	91.2 112.1	0.272×10^{-3}
Eqs. (3),(12) and (13)	π K^+	136.17 516.28	93.0 112.5	0.256×10^{-3}
Eqs. (3),(12) and (14)	π K^+	134.96 494.92	92.9 111.5	0.256×10^{-3}
experimental values	π^0 K^+	134.9766 ± 0.0006 493.677 ± 0.016	91.9 ± 3.5 112.8 ± 1.0	$(0.274 \pm 0.010) \times 10^{-3}$

It turns out that both Eqs. (11) and (12) gives a good fit also away from the chiral limit. As the first shot, we adopt without any change the explicit breaking of chiral symmetry from JM, that is, the bare mass parameters (\tilde{m}_q) of light quarks ($q = u, d, s$) leading to the broad phenomenological fit with *their* α_{eff} [11], namely

$$\tilde{m}_u = \tilde{m}_d = 3.1 \cdot 10^{-3} \text{ GeV} \quad , \quad \tilde{m}_s = 73 \cdot 10^{-3} \text{ GeV} . \quad (13)$$

These values of $\tilde{m}_{u,d}$ lead to an excellent description of the pion as a quasi-Goldstone boson of $D\chi$ SB also in conjunction with our α_{eff} (3) and Eq. (11), as witnessed by the first line in Table 1, where we predict pion mass, weak decay constant, and $\pi^0 \rightarrow \gamma\gamma$ amplitude very close to their empirical values (in the seventh line of Table 1). For the same reason as in the chiral limit, the results are again quite sensitive to changes of C_G but not to C_A . It turns out that one can increase or decrease C_A by a factor of two, and the results change little.

The second line of Table 1 reveals that the parameter set (11)&(13) works somewhat less well in the strange sector, as the kaon mass is 5% too high. However, a deviation of this size is not worrisome in the present circumstances where we know that the model interaction anyway misses some aspects (such as the $Q^2 \rightarrow 0$ behavior and non-ladder contributions), and where we just want to point out that the $\langle A^2 \rangle$ condensate is a possible source of the needed enhancement of $\alpha_{\text{eff}}(Q^2)$. In fact, the empirical success in the strange sector is reasonable considering that we used the standard JM mass parameters [11], (as we did also in [26–29]) and no refitting was performed there (although $\alpha_{\text{eff}}(Q^2)$ was different).

Nevertheless, it is interesting to see what changes are brought by refitting. If one for example tries the values of m_A , C_G and C_A given by Eq. (12) instead of Eq. (11), one gets the third and the fourth line in Table 1 instead of, respectively, the first and second line. Thus, the improvement achieved thereby is not significant, indicating that we should try changes of the bare quark masses \tilde{m}_q . It turns out that slight changes of the values (13) are sufficient to achieve agreement with experiment in the both non-strange and strange sectors. For example, the parameter set which gives the fifth and sixth lines of Table 1, thus reproducing the empirical mass of both π^0 and K^+ together with good results for their decay constants and $\pi^0 \rightarrow \gamma\gamma$ amplitude $T_{\pi^0}^{\gamma\gamma}$, is given by m_A , C_G and C_A from Eq. (12) and by the bare quark masses

$$\tilde{m}_u = \tilde{m}_d = 3.046 \cdot 10^{-3} \text{ GeV} \quad , \quad \tilde{m}_s = 67.70 \cdot 10^{-3} \text{ GeV} . \quad (14)$$

The parameter set (12)&(14) also gives us a good description of the η - η' complex, along the lines of our Refs. [27,30]. Although it means employing just a minimal extension of the DS approach, we must relegate this to another paper [31].

The preferred parameter set (12)&(14) is a result of a systematic examination of refitting possibilities performed by studying the dependence on the input parameters $\chi = (\tilde{m}_u, \tilde{m}_s, m_A, C_G, C_A)$ of the function

$$F[\chi] = \sum_y \left(\frac{y_{\text{exp}} - y_{\text{th}}}{y_{\text{exp}}} \right)^2 \times 100\% , \quad (15)$$

namely the sum of squared differences of the four experimentally measured (y_{exp}) and presently theoretically calculated (y_{th}) quantities $y \in \{M_{\pi^0}, f_{\pi^\pm}, M_{K^0}, f_{K^\pm}\}$. We kept choosing $C_A = C_G$ for simplicity, since we find that moderate variations of C_A do not affect our results much anyway, as already stressed above.

Minimization of Eq. (15) shows different respective characters of the α_{eff} parameters (m_A, C_G, C_A) and the mass parameters (\tilde{m}_u, \tilde{m}_s). The point (14) in the parameter subspace (\tilde{m}_u, \tilde{m}_s) is the location of a non-degenerate minimum of

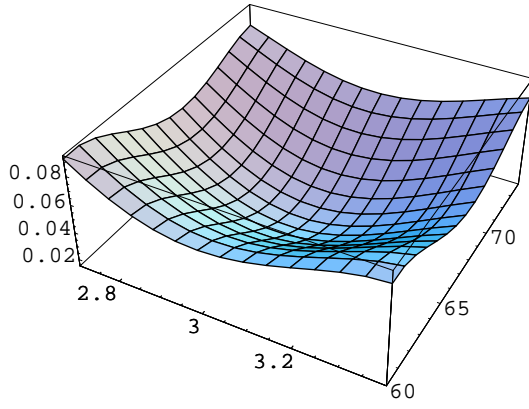


Fig. 2. The dependence of F (15) on the masses $(\tilde{m}_u, \tilde{m}_s)$, for the α_{eff} -parameters fixed at Eq. (12). The simple, non-degenerate minimum is at the bare quark mass values (14).

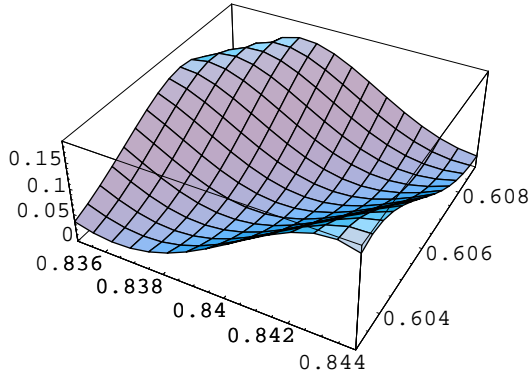


Fig. 3. F vs. $(m_A, C_G^{1/4})$ three-dimensional plot. The degenerate minimum (the bottom of the “valley”) is given by Eq. (16) and corresponds to $F \sim 1.5\%$.

F (15). Thus, the possible values of the bare quark masses $(\tilde{m}_u, \tilde{m}_s)$ can be precisely restricted by demanding that the function (15) be below certain value. The three-dimensional plot of F vs. $(\tilde{m}_u, \tilde{m}_s)$ is given on Fig. 2. At the minimum, for $(\tilde{m}_u, \tilde{m}_s)$ values (14), we obtain $F \approx 1.5\%$.

In contrast to the bare quark masses $(\tilde{m}_u, \tilde{m}_s)$, the parameters defining α_{eff} cannot be determined so unambiguously. By this we do not mean just the aforementioned weak sensitivity to C_A . They also cannot be fixed by minimization of F (15) in the same sense as the bare quark masses even though the results are very sensitive to m_A and C_G . The point is that F has no simple minimum in the $(m_A, C_G^{1/4})$ -plane as it has in $(\tilde{m}_u, \tilde{m}_s)$ plane: Fig. 3 reveals a minimum in the form of a “valley” described very well by a linear relation between m_A and $C_G^{1/4}$.

Thus, in spite of high sensitivity to m_A and C_G , there are many pairs of these quantities which give a fit comparable (within few percent) to that resulting from the values (12), as long as they approximately satisfy the linear relation

$$(C_G)^{1/4} = 0.7742 m_A - 0.0444 \text{ GeV} . \quad (16)$$

That is, the function (15) measuring the difference between the calculated and experimental values of $M_{\pi^0}, f_{\pi^\pm}, M_{K^0}, f_{K^\pm}$ has a degenerate minimum in the shape of a narrow valley. It is bounded by the values $(C_G)_{\min} \approx (0.6 \text{ GeV})^4$ and $(C_G)_{\max} \approx (0.9 \text{ GeV})^4$ in the sense that between these values we managed to find solutions providing excellent fits (F of the order 1.5%) to the empirical values.

4 Conclusion

The dimension 2 gluon condensate $\langle A^2 \rangle$ enabled the derivation [1] of a suitably enhanced $\alpha_{\text{eff}}(Q^2)$. This effective interaction leads to the sufficiently strong $D\chi\text{SB}$ and successful phenomenology at least in the light sector of pseudoscalar mesons. This opens the possibility that instead of modeling $\alpha_{\text{eff}}(Q^2)$, its enhancement at intermediate Q^2 may be understood in terms of gluon condensates, which seem to provide an important mechanism proposed and studied for the first time in our recent Ref. [1]. The systematic examination of various fitting possibilities set forth in the present paper, allows us to conclude that this scenario is compatible with reasonable values of both $\langle A^2 \rangle$ -condensate and the gauge-invariant dimension 4 gluon condensate $\langle F^2 \rangle$ [24]. In the relevant momentum region, $\alpha_{\text{eff}}(Q^2)$ (and thus also the solutions of DS and BS equations and results for calculated measurable quantities) depend only very weakly on C_A , which parametrizes contributions of dimension 4 condensates to the gluon propagator. The essential parameters C_G and m_A , on which the dependence is very strong, are not independent. Thus, due to the relation (16), Eq. (3) is an essentially one-parameter model for α_{eff} , albeit on a relatively small interval of C_G . This can be interpreted as another instance that what counts is the integrated strength of the interaction. Over the possible range, we have a continuous set of parameter pairs (m_A, C_G) ; their values are such that they give higher peaks at smaller squared momenta, resulting in similar integrated strengths. We find that the phenomenologically allowed range of values of the dynamically generated gluon mass m_A is in agreement with the lattice results [2] on $\langle A^2 \rangle$ in the Landau gauge. Also, phenomenologically allowed values of C_G , which parametrizes contributions of dimension 4 condensates to the ghost propagator, are such that they might be a sign that C_G is indeed mostly determined by the dimension 4 gluon condensate $\langle F^2 \rangle$ [24].

References

1. D. Kekez and D. Klabučar, arXiv:hep-ph/0307110.
2. P. Boucaud, A. Le Yaouanc, J. P. Leroy, J. Micheli, O. Pene and J. Rodriguez-Quintero, Phys. Lett. B **493**, 315 (2000).
3. F. V. Gubarev, L. Stodolsky and V. I. Zakharov, Phys. Rev. Lett. **86**, 2220 (2001).

4. F. V. Gubarev and V. I. Zakharov, Phys. Lett. B **501**, 28 (2001).
5. K. I. Kondo, Phys. Lett. B **514**, 335 (2001).
6. K. I. Kondo, T. Murakami, T. Shinohara and T. Imai, Phys. Rev. D **65**, 085034 (2002).
7. R. Alkofer and L. von Smekal, Phys. Rept. **353**, 281 (2001).
8. P. Maris and C. D. Roberts, Int. J. Mod. Phys. E **12**, 297 (2003).
9. C. D. Roberts, arXiv:nucl-th/0304050.
10. See, e.g., Refs. [32,33] for the $\pi^0 \rightarrow \gamma\gamma$ transition amplitude $T_{\pi^0}^{\gamma\gamma}$, and Refs. [34–37] for the related transition $\gamma \rightarrow \pi^+\pi^0\pi^-$.
11. P. Jain and H. J. Munczek, Phys. Rev. D **48**, 5403 (1993).
12. P. Maris and C. D. Roberts, Phys. Rev. C **56**, 3369 (1997).
13. P. Maris and P. C. Tandy, Phys. Rev. C **60**, 055214 (1999).
14. H. J. Munczek and A. M. Nemirovsky, Phys. Rev. D **28**, 181 (1983).
15. R. Alkofer, C. S. Fischer and L. von Smekal, Acta Phys. Slov. **52**, 191 (2002).
16. C. S. Fischer and R. Alkofer, Phys. Rev. D **67**, 094020 (2003).
17. R. Alkofer, C. S. Fischer and L. von Smekal, Prog. Part. Nucl. Phys. **50**, 317 (2003).
18. P. Maris, A. Raya, C. D. Roberts and S. M. Schmidt, arXiv:nucl-th/0208071.
19. M. J. Lavelle and M. Schaden, Phys. Lett. B **208**, 297 (1988).
20. M. Lavelle and M. Schaden, Phys. Lett. B **246**, 487 (1990).
21. J. Ahlback, M. Lavelle, M. Schaden and A. Streibl, Phys. Lett. B **275**, 124 (1992).
22. M. Lavelle and M. Oleszczuk, Mod. Phys. Lett. A **7**, 3617 (1992).
23. M. Lavelle, Phys. Rev. D **44**, 26 (1991).
24. M. A. Shifman, A. I. Vainshtein and V. I. Zakharov, Nucl. Phys. B **147**, 385 (1979); *ibid.* **448** (1979).
25. B. L. Ioffe and K. N. Zyablyuk, Eur. Phys. J. C **27**, 229 (2003).
26. D. Kekez and D. Klabučar, Phys. Lett. B **387**, 14 (1996).
27. D. Klabučar and D. Kekez, Phys. Rev. D **58**, 096003 (1998).
28. D. Kekez, B. Bistrotić and D. Klabučar, Int. J. Mod. Phys. A **14**, 161 (1999).
29. D. Kekez and D. Klabučar, Phys. Lett. B **457**, 359 (1999).
30. D. Kekez, D. Klabučar and M. D. Scadron, J. Phys. G **26**, 1335 (2000).
31. D. Kekez and D. Klabučar, in preparation.
32. P. Maris and C. D. Roberts, Phys. Rev. C **58**, 3659 (1998).
33. C. D. Roberts, Nucl. Phys. A **605**, 475 (1996).
34. R. Alkofer and C. D. Roberts, Phys. Lett. B **369**, 101 (1996).
35. B. Bistrotić and D. Klabučar, Phys. Rev. D **61**, 033006 (2000).
36. B. Bistrotić and D. Klabučar, Phys. Lett. B **478**, 127 (2000).
37. S. R. Cotanch and P. Maris, Phys. Rev. D **68**, 036006 (2003).



Relativistic Constituent Quark Models: Theory and Applications

W. Plessas

Institute for Theoretical Physics, University of Graz, Universitätsplatz 5, A-8010 Graz, Austria

Abstract. A short critical survey of the present status of constituent quark models for low-energy hadronic physics is given.

Constituent quark models (CQMs) have proven to be a reasonable concept for low-energy quantum chromodynamics (QCD). Especially over the past years a considerable amount of new insight has been gained in the foundation/justification, the construction, and the application of CQMs. As a result, one is presently able to describe a number of aspects of hadronic physics within CQMs. Not only are CQMs successful in their primary domain of hadron spectroscopy but gradually also in hadronic reactions, especially if hadron ground states are involved (such as hadron elastic form factors, electric radii, magnetic moments etc.).

The notion of constituent quarks (Q) as effective degrees of freedom of low-energy QCD has by now become rather well manifested from several sources. For instance, also several studies of lattice QCD have recently found the generation of quasiparticles with an increasing dynamical mass in the low-energy limit. Thus it appears as a reasonable approach to consider hadrons as bound states and resonances of $\{QQ\}$ and $\{QQQ\}$ systems. One can describe such systems as two- and three-body systems of confined constituent quarks. The corresponding confinement interaction can be modelled directly from results of QCD (e.g., the string tension and/or lattice measurements). There is, however, a lot of discussion about the proper hyperfine interaction. Several models are still competing in the attempt to produce the most convincing dynamical concept (see, for instance, the proceedings of the most recent N^* Workshop [1]).

There should be no question about using a relativistic framework for treating few-quark systems. Many reasons have by now been found why nonrelativistic CQMs are inadequate, are bound to fail, and should no longer be pursued. At the same time convincing evidence has been gained why relativistic CQMs are reasonable, successful, and promising. In fact, the usage of various CQMs that have been formulated in a relativistic context has much advanced the quality of results obtained in low-energy hadronic physics and has provided valuable insight for the understanding of the underlying physics. Therefore the symmetries implied

by relativistic covariance must be included in the construction of a CQM, in addition to the symmetries (or symmetry breakings) characterizing low-energy QCD.

The main dynamical concepts for the hyperfine interaction of constituent quarks have by now been formulated along *relativistic* CQMs. For instance, the assumption of the one-gluon-exchange (OGE) mechanism is realized in the CQM by Capstick and Isgur [2], the instanton-induced (II) forces are implemented in the CQM by the Bonn group [3], and the Goldstone-boson-exchange (GBE) is considered in the CQM by the Graz group [4,5]. While the II CQM is calculated with the Bethe-Salpeter equation, the OGE and the GBE CQMs are treated along relativistic (i.e. Poincaré-invariant) quantum mechanics; in the latter cases one solves the eigenvalue problem of a relativistic mass operator, which constitutes an approach quite distinct from a field-theoretical one.

A quantitative comparison of these three types of CQMs in the relevant sectors of baryon spectroscopy was given in ref. [6]. It is evident that a considerable amount of flavor-dependent interactions (as prevailing in the GBE CQM) is needed in order to produce a reasonable level scheme in agreement with phenomenological data. The pertinent reasons have been studied in much detail by B. Sengl [7], and we may refer to her contribution in these proceedings [8].

Obviously, CQMs have to prove successful also in hadron reactions. Only then they can be accepted as effective models for hadronic physics at low energies. An immediate first test beyond spectroscopy consists in calculating ground-state form factors using the wave functions that each CQM produces. By now we know the covariant predictions for nucleon electroweak form factors of the CQMs pertaining to the OGE, II, and GBE dynamics. A comparison of the OGE and the GBE CQMs is given in ref. [9]. It should be further compared with the results obtained for the II CQM by the Bonn group along the Bethe-Salpeter-equation approach [10]. The striking observation from all of these results is that the direct relativistic predictions are all very similar, irrespective of the fact whether a field-theoretical approach (Bethe-Salpeter equation) or a relativistic quantum-mechanical method is chosen. Once the constraints of relativistic covariance are implemented, the results of the present calculations (which are still deficient in some aspects) are furthermore close to the experimental data in the regime of low-momentum transfers. For a more detailed discussion, including also the results for electric radii and magnetic moments of the octet and decuplet baryon ground states, we may refer to the contribution of K. Berger [11].

A most recent application of a relativistic CQM concerns the calculation of baryon resonance decays. The Graz group has followed the point-form approach to producing the predictions of the OGE and GBE CQMs for the widths of pionic decay modes of N and Δ resonances. The corresponding results have been reported already in ref. [12], and a comparison is presented in ref. [9]. While a considerable improvement over earlier nonrelativistic studies has been achieved, the situation is not yet satisfactory with regard to describing the decay widths. Several reasons may be responsible for the deficiencies still existing. A more realistic form of the resonance wave functions (instead of excited-state wave functions with zero widths) might be an immediate demand. Further questions concern the decay mechanism itself.

In summary we are facing an exciting development of CQMs for low-energy hadronic physics. Future studies will have to address interesting problems whose exploration has become possible along with the recent technical advances. Most importantly the CQMs will have to be improved with respect to the description of the resonances (as states with finite widths) in a relativistic framework. This will open the access to treating a wealth of hadron reaction phenomena in a more realistic manner. We may be confident to gain valuable new insights from these investigations.

References

1. S.A. Dytman and E.S. Swanson (Eds.), *NSTAR2002, Proceedings of the Workshop on the Physics of Excited Nucleons*, (World Scientific, Singapore, 2003); see especially the articles by S. Capstick (p. 142), W. Plessas (p. 147), B. Metsch (p. 152), and E. Swanson (p. 157).
2. S. Capstick and N. Isgur, *Phys. Rev. D* **34**, 2809 (1986).
3. U. Löring, B.C. Metsch, and H.R. Petry, *Eur. Phys. J.* **A10**, 395 (2001); *ibid.* **A10**, 447 (2001).
4. L. Ya. Glozman, W. Plessas, K. Varga, and R.F. Wagenbrunn, *Phys. Rev. D* **58**, 094030 (1998).
5. L.Ya. Glozman, W. Plessas, K. Varga, and R.F. Wagenbrunn, *Phys. Rev. C* **57**, 3406 (1998).
6. W. Plessas, *Few-Body Suppl.* **14**, 13 (2003).
7. B. Sengl, Diploma Thesis, University of Graz, 2003, (unpublished).
8. B. Sengl, contribution in these proceedings.
9. W. Plessas, *Few-Body Suppl.* **15**, 139 (2003).
10. D. Merten, U. Löring, K. Kretzschmar, B. Metsch, and H. R. Petry, *Eur. Phys. J.* **A14**, 477 (2002).
11. K. Berger, contribution in these proceedings.
12. T. Melde, R.F. Wagenbrunn, and W. Plessas, *Few-Body Syst. Suppl.* **14**, 37 (2003).



Effective Quark-Quark Interaction in Baryons

B. Sengl

Institute for Theoretical Physics, University of Graz, Universitätsplatz 5, A-8010 Graz,
Austria

1 Introduction

In the low-energy regime of QCD, where the fundamental theory is not accurately solvable, one is interested in the effective degrees of freedom that govern the properties of hadrons at this scale. A promising approach to low-energy hadrons consists in constituent-quark models (CQMs). In this context one of the central problems is to find the proper effective interaction between constituent quarks. Traditional CQMs - originally constructed in a non-relativistic framework - adopted one-gluon exchange (OGE) [1] as the hyperfine interaction between constituent quarks (Q). Over the years it has become quite evident that a CQM relying only on OGE Q-Q interactions is not able to describe, e.g., the light and strange baryon spectra. A hyperfine interaction based on OGE leads to the wrong level orderings of positive- and negative-parity excitations specifically in the N and Δ spectra. Furthermore, due to the missing flavor dependence it is not possible to reproduce the N and Λ spectra at the same time. In addition, the OGE interaction produces strong spin-orbit splittings that can hardly be found in the empirical data. Several attempts have been made in order to solve this problem, i.e., one supplemented the color-magnetic interaction by other types of forces, e.g., one introduced an additional meson exchange. These so-called hybrid models, however, did not lead to satisfactory results either [2].

In addition, also other types of CQMs with a different kind of hyperfine interaction have been constructed, such as the ones based on instanton-induced (II) forces [3] or on Goldstone-boson-exchange (GBE) dynamics [4]. Whereas the II CQM is left with the wrong level orderings of the first positive- and negative-parity excitations above the nucleon ground state as well, the GBE CQM is able to reproduce these states in the right places, in accordance with experiment. In this contribution we will mainly be concerned with the extended GBE CQM recently developed by the Graz group.

A considerable number of theoretical and experimental results indicate that QCD at low energies is mainly driven by the mechanism of the spontaneous breaking of chiral symmetry ($SB\chi S$). Once we accept this, the original degrees of freedom governing the light-flavor sector of the baryons, namely current quarks and gluons, have to be replaced by effective ones. On the one hand, $SB\chi S$ leads to constituent quarks with a dynamically generated mass much larger than that of the current quarks. On the other hand, $SB\chi S$ is at the same time also responsible

for the appearance of Goldstone bosons which can be associated with a residual $SU(3)_V$ symmetry. This leads automatically to an effective Lagrangian for the hyperfine interaction in CQMs, which is based on constituent-quark and Goldstone-boson degrees of freedom [5].

The version of the GBE CQM of Ref. [4] relies only on the spin-spin component of the pseudoscalar GBE for the hyperfine interaction of the constituent quarks. This is expected to be the most relevant interaction part with respect to the baryon spectra. Nevertheless, for completeness one must also consider the other possible potential components, i.e., one may also expect multiple Goldstone-boson exchange [6], which brings about even further forces. The extended GBE CQM considers also vector and scalar exchanges and thus contains not only spin-spin but also central, tensor, and spin-orbit forces. In the following we briefly review the extension of the GBE CQM and discuss how the different potential parts of the hyperfine interaction contribute to the total energy of the various light and strange baryon states.

2 Extended GBE CQM

In the extended version of the GBE CQM [7,8] one employs a semi-relativistic Hamiltonian of the form

$$H = \sum_{i=1}^3 \sqrt{\mathbf{p}_i^2 + m_i^2} + \sum_{i<j} [V_{\text{conf}}(i,j) + V_\chi(i,j)]. \quad (1)$$

Here the first term is the relativistic kinetic energy of the constituent quarks and V_{conf} is the linear confinement, which has a strength comparable to the string-tension of QCD. The term V_χ represents the hyperfine interaction (motivated from the $SB\chi S$) and contains pseudoscalar (ps), vector (v), and scalar (s) meson exchanges

$$\begin{aligned} V_\chi(i,j) &= V^{\text{ps}}(i,j) + V^{\text{v}}(i,j) + V^{\text{s}}(i,j) \\ &= \sum_{\alpha=1}^3 [V_\pi(i,j) + V_\rho(i,j) + V_{a_0}(i,j)] \lambda_i^\alpha \lambda_j^\alpha \\ &\quad + \sum_{\alpha=4}^7 [V_K(i,j) + V_{K^*}(i,j) + V_\kappa(i,j)] \lambda_i^\alpha \lambda_j^\alpha \\ &\quad + [V_\eta(i,j) + V_{\omega_8}(i,j) + V_{f_0}(i,j)] \lambda_i^8 \lambda_j^8 + \frac{2}{3} [V_{\eta'}(i,j) + V_{\omega_0}(i,j) + V_\sigma(i,j)], \end{aligned} \quad (2)$$

where λ_i denote the Gell-Mann flavor matrices of the individual quarks. The explicit expressions of the individual meson-exchange potentials are for pseudoscalar mesons ($\gamma = \pi, K, \eta, \eta'$)

$$V_\gamma(i,j) = V_\gamma^{\text{SS}}(\mathbf{r}_{ij}) \boldsymbol{\sigma}_i \cdot \boldsymbol{\sigma}_j + V_\gamma^{\text{T}}(\mathbf{r}_{ij}) [3(\hat{\mathbf{r}}_{ij} \cdot \boldsymbol{\sigma}_i)(\hat{\mathbf{r}}_{ij} \cdot \boldsymbol{\sigma}_j) - \boldsymbol{\sigma}_i \cdot \boldsymbol{\sigma}_j], \quad (3)$$

for vector mesons ($\gamma = \rho, K^*, \omega_8, \omega_0$)

$$\begin{aligned} V_\gamma(i,j) &= V_\gamma^{\text{C}}(\mathbf{r}_{ij}) + V_\gamma^{\text{SS}}(\mathbf{r}_{ij}) \boldsymbol{\sigma}_i \cdot \boldsymbol{\sigma}_j \\ &\quad + V_\gamma^{\text{T}}(\mathbf{r}_{ij}) [3(\hat{\mathbf{r}}_{ij} \cdot \boldsymbol{\sigma}_i)(\hat{\mathbf{r}}_{ij} \cdot \boldsymbol{\sigma}_j) - \boldsymbol{\sigma}_i \cdot \boldsymbol{\sigma}_j] + V_\gamma^{\text{LS}}(\mathbf{r}_{ij}) \mathbf{L}_{ij} \cdot \mathbf{S}_{ij}, \end{aligned} \quad (4)$$

and for scalar mesons ($\gamma = a_0, \kappa, f_0, \sigma$)

$$V_\gamma(i, j) = V_\gamma^C(\mathbf{r}_{ij}) + V_\gamma^{LS}(\mathbf{r}_{ij}) \mathbf{L}_{ij} \cdot \mathbf{S}_{ij}, \quad (5)$$

where σ_i are the Pauli spin matrices. The terms V^{SS} , V^T , V^C , and V^{LS} represent the radial potential parts of the spin-spin, tensor, central, and spin-orbit forces, respectively. In case of the vector mesons the real mesons ω and ϕ , being strong mixings of flavor octet and singlet states, are replaced by fictitious pure octet and singlet states ω_8 and ω_0 . Similarly, we assume that the scalar mesons f_0 and σ are pure octet and singlet states, respectively, and introduce a light kaonic scalar meson κ to complete the nonet.

The formulae for the radial dependences of the individual potential parts are given explicitly in Refs. [7,8]. They contain a number of parameters which are either fixed or obtained by a fit to the phenomenological baryon spectra. Here we deal with the version of the extended GBE CQM whose parameters have been determined specifically in Ref. [8]; they are quoted in Table 1. The masses of the constituent quarks m_u, m_d, m_s have been fixed a-priori to some standard values known from the literature. For the meson masses μ_γ , which govern the long-range parts of the meson-exchange potentials, one has employed the experimental values. The coupling constants g_γ have been derived from meson-nucleon phenomenology assuming $SU(3)_F$ symmetry; they determine the strengths of all potential parts. In the version of the extended GBE CQM of Ref. [8], however, the spin-orbit forces have been treated as an exception and have been given a different strength g^{LS} determined by a fit to the spectra. Among the free parameters, the cut-offs Λ_γ have been introduced in order to regularize the short-range parts of the meson-exchange potentials. The parameter C represents the strength of the linear confinement and V_0 is needed to fix the lowest eigenvalue to the nucleon mass. Altogether the extended GBE CQM comprises eight free parameters, while all other ingredients can be considered as predetermined.

Table 1. Parameters of the extended version of the CQM based on GBE as given in Ref. [8].

Fixed Parameters		
$m_u = m_d = 340$ MeV	$m_s = 507$ MeV	$\mu_\pi = 139$ MeV
$\mu_K = 493.6$ MeV	$\mu_\eta = 547$ MeV	$\mu_{\eta'} = 958$ MeV
$\mu_\rho = 770$ MeV	$\mu_{K^*} = 892$ MeV	$\mu_{\omega_8} = 869$ MeV
$\mu_{\omega_0} = 947$ MeV	$\mu_\sigma = 680$ MeV	$\mu_{sc} = 980$ MeV
$g_8^2/4\pi = 0.67$	$(g_0/g_8)^2 = 1$	$(g_8^V)^2/4\pi = 0.55$
$(g_8^T)^2/4\pi = 0.16$	$(g_0^V)^2/4\pi = 1.107$	$(g_0^T)^2/4\pi = 0.0058$
$g_s^2/4\pi = 0.67$		
Free Parameters		
$C = 1.935$ fm ⁻²	$V_0 = -334$ MeV	$(g^{LS})^2/4\pi = 0.8$
$\Lambda_\gamma = \Lambda_0 + \mu_\gamma$	$\Lambda_K = 1420$ MeV	$\Lambda_{\eta'} = 1400$ MeV
$\Lambda_0^{ps} = 695$ MeV	$\Lambda_0^v = 375$ MeV	$\Lambda_0^s = 833$ MeV

Among the main achievements of the original (pseudoscalar-exchange) version of the GBE CQM [4] has been the appropriate level ordering of states with

positive and negative parities. This typical behaviour is maintained also in the extended model. In our investigations we considered two versions of the extended GBE CQM, namely, the ones with and without spin-orbit forces [8].

In Fig. 1 we demonstrate the effect of the GBE hyperfine interaction in case of the extended version without spin-orbit forces. Starting out from the case with confinement only, the inversion of the lowest positive- and negative-parity states in the N spectrum is gradually achieved when the coupling is increased. At the same time the level crossing of the analogous states in the Λ spectrum is avoided, just as demanded by phenomenology. If spin-orbit forces are included, the same behaviour of the level shifts persists.

In the next section we shall provide evidence how the different potential parts influence the energy levels. Such type of investigations lead to a better understanding of the dynamics stemming from GBE.

3 Influences of Different Force Components

In Ref. [9] we performed a detailed study of the influence of different force components on the light and strange baryon spectra. Here we are going to discuss the most important results, which provide valuable insight into the behaviour of the potential components derived from GBE dynamics.

From phenomenology we observe that the tensor force effects must be minor, as the splittings within LS multiplets (like, e.g., N(1535)-N(1520)) are rather small. Without any tensor and spin-orbit forces the levels within LS multiplets are degenerate. This is evident from Fig. 2a where at the starting point of the plot only spin-spin and central components of the potential act. When the tensor force (of the pseudoscalar exchange) is gradually turned on, there occur rather large splittings in the lowest-lying multiplets of $\frac{1}{2}^-$ - $\frac{3}{2}^-$ - $\frac{5}{2}^-$ nucleon resonances, namely, of N(1535)-N(1520) and N(1650)-N(1700)-N(1675). Such a behaviour is not seen in the phenomenological spectra. The situation can be remedied by including also the tensor force from vector-meson exchanges, as is done in the extended GBE CQM. They have an effect opposite to the pseudoscalar tensor force [10]. As a result the level splittings within the LS-multiplets get much reduced after the addition of vector-meson exchange (see Fig. 2b), where the action of the vector-meson exchange tensor force is demonstrated as a function of increasing strength. A similar behaviour is found in the splittings of other multiplets, e.g., in the Λ spectrum.

The vector- and scalar-meson exchanges also give rise to spin-orbit forces between the constituent quarks. Their effects on the spectra have been discussed extensively in Refs. [8,9] and they are shown in Fig. 3. The spin-orbit forces allow to improve the description of the practically degenerate $J = \frac{5}{2}^-$ and $J = \frac{5}{2}^+$ nucleon excitations (which are known to a rather good accuracy from experiment). The same is true for the corresponding states in the Λ spectrum. For this purpose, however, one had to use a phenomenological strength g^{LS} in the model of Ref. [8]. Otherwise the spin-orbit forces do not bring much improvement but slightly worsen the description in some cases.

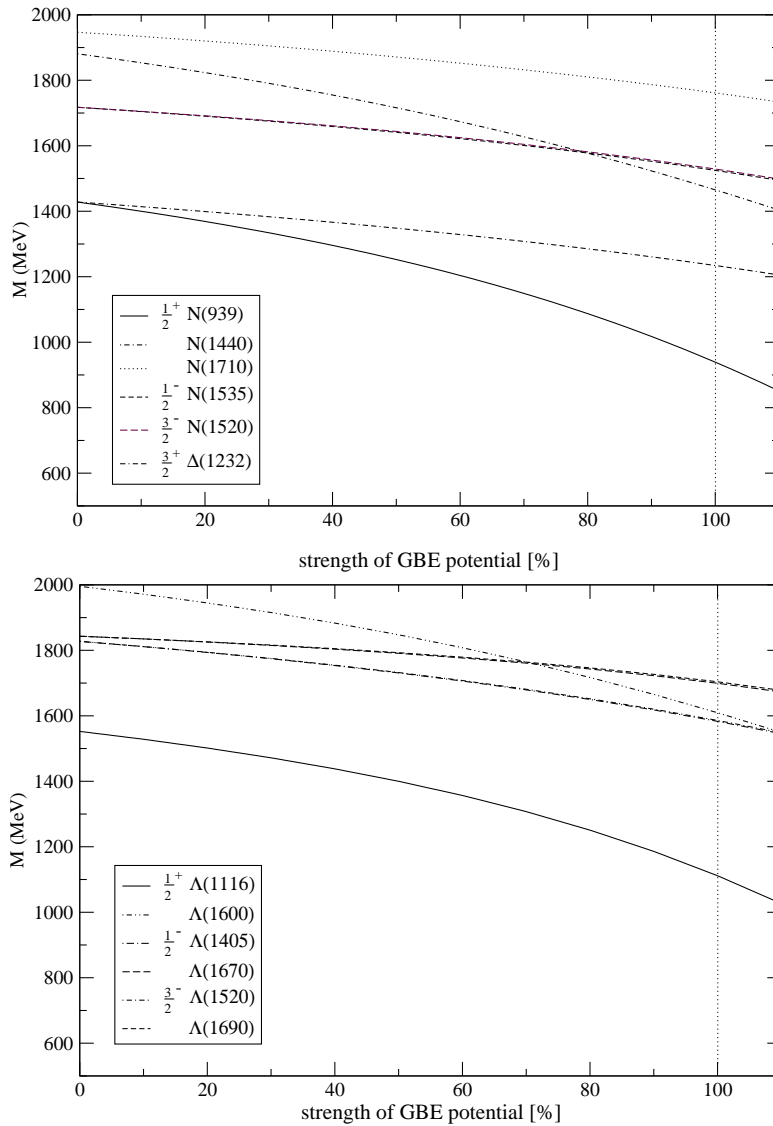


Fig. 1. Level shifts of the nucleon, Δ , and Λ due to the hyperfine interaction in case of the extended GBE CQM (without spin-orbit forces). The full strength of the potential is recovered at 100%.

In summary, in order to reach a good description of the baryon spectra in close agreement with phenomenology (generally small splittings in LS multiplets) one must take into account at least both the pseudoscalar and vector exchanges. For completeness (of the inclusion of multiple GBE) one has also foreseen scalar-meson exchange. However, it plays only a minor role in the level splittings, at least for the moderate magnitude of its coupling deduced from meson-nucleon phenomenology. It has been shown in Ref. [11] that the scalar-meson

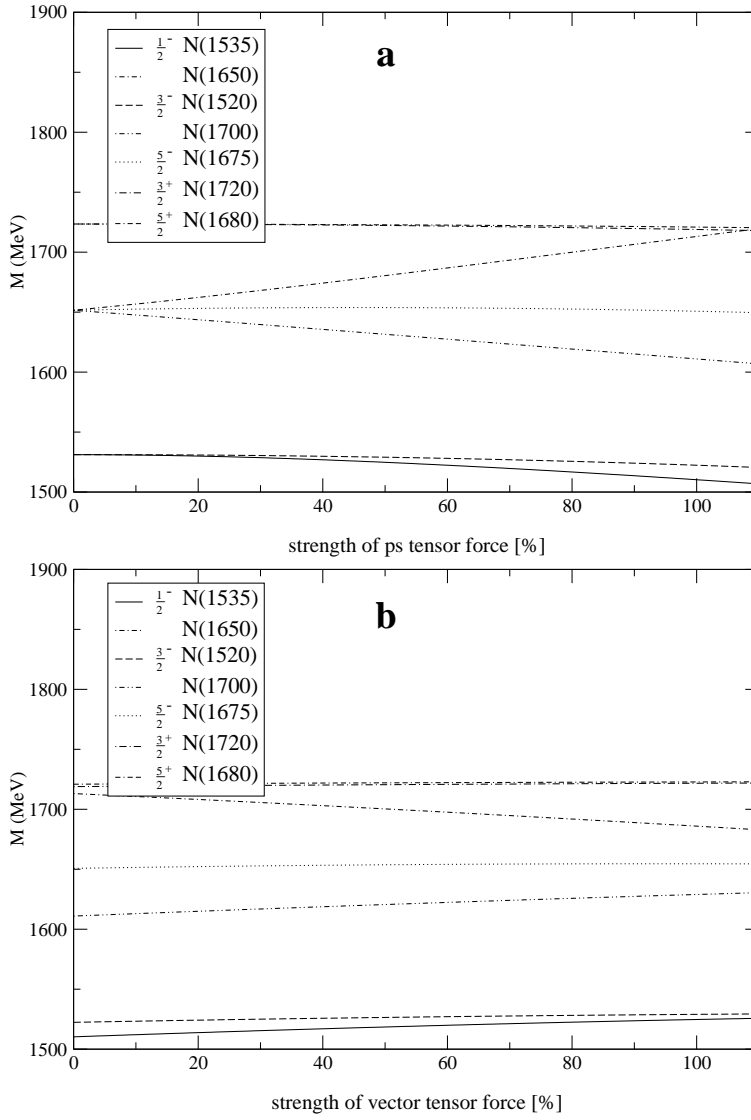


Fig. 2. Level shifts in the nucleon spectrum due to tensor forces: Starting from the case with no tensor force at all, we first turn on only the tensor forces from the pseudoscalar meson exchanges (a), and then in addition the tensor forces from the vector meson exchanges (b).

exchange tends to have a favourable influence on the level splittings of positive- and negative-parity states, however, with a much bigger strength.

4 Conclusion and Outlook

We have discussed the effective quark-quark interactions in baryons within CQMs. In particular, we reported evidences on the behaviour of various potential components along the CQM based on GBE dynamics. We started out from the original

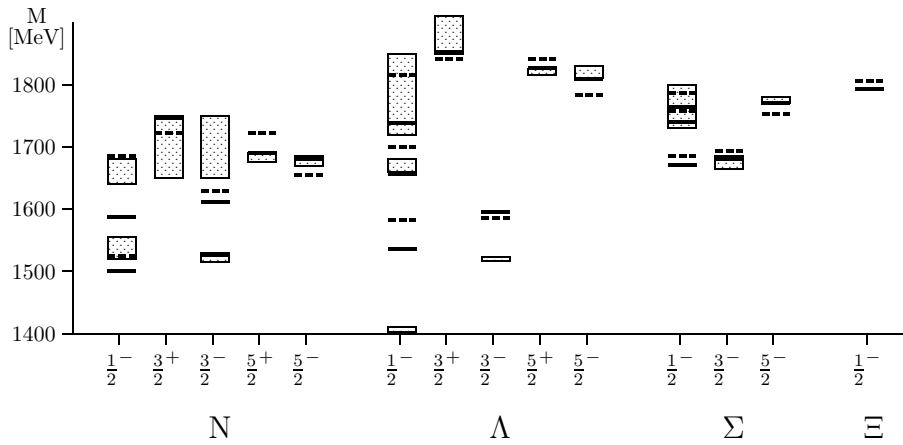


Fig. 3. Influence of spin-orbit forces on selected light and strange baryon states. The solid and dotted bars are the energy levels with and without spin-orbit forces, respectively.

version of the GBE CQM [4], which contains as the hyperfine interaction only the spin-spin component of the pseudoscalar-meson exchange. An extension of the GBE CQM to including vector- and scalar-meson exchanges is called for in order to take into account also multiple Goldstone-boson exchanges [7,8]. Thereby the favourable features of the GBE CQM are in general maintained and further improvements in the description of the spectra can be made [9]. Notably, one can reproduce the correct level orderings of the low-lying light and strange baryon spectra with about the same quality as in the original GBE CQM. It will be interesting to apply the extended GBE CQM with its additional force components in the investigation of the electromagnetic structure of the baryons, especially the nucleons, and in other studies of baryon reactions such as mesonic decays of resonances etc. Furthermore, the extended GBE CQM now also brings about the necessary force components for a microscopic derivation of the baryon-baryon interaction, which are missing in the pseudoscalar version [12]; it appears worthwhile to check if the N-N interaction can now be produced directly from the CQM.

Even though the GBE CQM has been quite successful in baryon spectroscopy and in first applications to the elastic electromagnetic and axial form factors of the nucleons [13], one must not forget that the description of the excited states as resonances with finite widths is still not achieved. This is obviously reflected in studies of mesonic N and Δ decays, which have recently been performed with the GBE CQM for the first time in a covariant framework (point form) [14]. One could (consistently) improve on that by extending the GBE CQM beyond $\{QQQ\}$ configurations to including higher Fock states such as $\{QQQ\pi\}$ or $\{QQQ\eta\}$ etc. One may be confident that a more adequate description of the resonances and their (decay) properties will then be achieved.

At this instance the GBE CQM is limited to the sector of light and strange flavors. One could think of extending it also to heavy flavors. Presumably new types of hyperfine interactions will be necessary for this purpose. One will not only need the light-light and heavy-heavy quark-quark forces but notably also

the light-heavy flavor interactions. Not much is known about the latter, what will make the attempt of creating a unified CQM of all baryons a rather difficult task.

References

1. A. de Rújula, H. Georgi, and S. L. Glashow, *Phys. Rev. D* **12**, 147 (1975).
2. L.Ya. Glozman, W. Plessas, K. Varga, and R.F. Wagenbrunn, *Phys. Rev. C* **57**, 3406 (1998).
3. U. Löring, B.C. Metsch, and H.R. Petry, *Eur. Phys. J.* **A10**, 395 (2001); *ibid.* **A10**, 447 (2001).
4. L. Ya. Glozman, W. Plessas, K. Varga, and R.F. Wagenbrunn, *Phys. Rev. D* **58**, 094030 (1998).
5. L.Ya. Glozman and D.O. Riska, *Phys. Rep.* **268**, 263 (1996).
6. D.O. Riska and G.E. Brown, *Nucl. Phys.* **A653**, 251 (1999).
7. R.F. Wagenbrunn, L.Ya. Glozman, W.Plessas, and K. Varga, *Nucl. Phys.* **A666&667**, 29c-32c (2000).
8. K. Glantschnig, Diploma Thesis, University of Graz, 2002, (unpublished).
9. B. Sengl, Diploma Thesis, University of Graz, 2003, (unpublished).
10. L.Ya. Glozman, arXiv hep-ph/9805345.
11. P. Stassart, Fl. Stancu, J.M. Richard, and L. Theussl, *J. Phys. G* **26**, 397 (2000).
12. D. Bartz and Fl. Stancu, *Phys. Rev. C* **60**, 055207 (1999).
13. S. Boffi, L.Ya. Glozman, W. Klink, W. Plessas, M. Radici, and R.F. Wagenbrunn, *Eur. Phys. J.* **A14**, 17 (2002).
14. *Few-Body Syst. Suppl.* **14**, 37 (2003).



The role of a three-body confinement interaction in pentaquarks

Fl. Stancu

Institute of Physics, B.5, University of Liege, Sart Tilman, B-4000 Liege 1, Belgium

Abstract. We discuss the role of a three-body confinement interaction in the stability of pentaquarks. For this purpose we derive a unitary transformation between asymptotic channels and adequate intermediate channels defined in the color space.

The recent observation of a narrow baryon resonance with strangeness $S = 1$ [1], referred to as Z^+ or Θ^+ , has prompted considerable interest in the theoretical study of pentaquarks. Due to its positive strangeness, this resonance must contain a strange antiquark. Thus Θ^+ cannot be interpreted as a q^3 system but rather as an exotic baryon with the minimal content $uudd\bar{s}$. In describing this resonance within constituent quark models one of the main issues is the parity quantum number. As shown in Ref. [2] the Goldstone boson exchange model supplemented by a quark-antiquark hyperfine interaction accommodates a stable positive parity $uudd\bar{s}$ pentaquark. In the case of heavy pentaquarks, containing \bar{c} or \bar{b} instead of \bar{s} , the Goldstone boson exchange interaction alone leads to stability [3].

Here we discuss a mechanism which could influence the stability of pentaquarks due the presence of a three-body confining interaction. Usually constituent quark models contain a two-body $F_i \cdot F_j$ interaction only. Based on the algebraic argument that QCD-inspired Hamiltonian models are invariant under a global $SU_C(3)$ symmetry Dmitrasinovic recently proposed [4] to express constituent quark model Hamiltonians in terms of every invariant operator of $SU(3)$. This implies that the Hamiltonian should contain both two- and three-body confining interactions. These can be expressed in terms of the quadratic (Casimir) operator and the cubic invariant of $SU(3)$ respectively. If added to the Hamiltonian, the three-body interaction has implications on the spectrum of ordinary baryons [4–6] and on the stability of tetraquarks [4,5,7]. Here we discuss its effect on the stability of pentaquarks. Although we deal with identical quarks, the conclusion also holds for heavy flavour pentaquarks because the confinement interaction is flavour independent.

Let us consider the Hamiltonian

$$H = \sum_i \frac{\mathbf{p}_i^2}{2m_i} - \frac{\mathbf{P}^2}{2M} + V_{2b} + V_{3b} \quad (1)$$

where \mathbf{p}_i and m_i are the momentum and the mass of the quark (antiquark) i , \mathbf{P} and M are the total momentum and the mass of the $q^4\bar{q}$ system and $V_{2b} + V_{3b}$ is

the confinement interaction. For the 2-body confinement interaction we take [4]

$$V_{2b} = \sum_{i<j} V_{ij} \left(\frac{7}{3} + F_i^a \cdot F_j^a \right) \quad (2)$$

where $F_i^a = \frac{1}{2}\lambda_i^a$ ($i=1,\dots,8$) is the color charge operator of the quark i . The three-body color confinement interaction has the form [4]

$$V_{3b} = V_{ijk} = \mathcal{V}_{ijk} \mathcal{C}_{ijk} \quad (3)$$

where \mathcal{V}_{ijk} is the radial part and \mathcal{C}_{ijk} is the three-body color operator. For a q^3 system or subsystem this is given by

$$\mathcal{C}_{ijk} = d^{abc} F_i^a F_j^b F_k^c, \quad (4)$$

where d^{abc} are some real constants, symmetric under any permutation of indices. The three-body color operator acting in a $q^2\bar{q}$ subsystem is defined as

$$\mathcal{C}_{ij\bar{k}} = -d^{abc} F_i^a F_j^b \bar{F}_k^c \quad (5)$$

where $\bar{F}_i^a = -\frac{1}{2}\lambda_i^{a*}$ ($i = 1,\dots,8$) is the color charge operator of an antiquark. These operators can be expressed in terms of the quadratic invariant $C^{(2)}$ and the cubic invariant $C^{(3)}$ of SU(3) as [4,5]

$$\mathcal{C}_{ijk} = \frac{1}{6} \left[C_{i+j+k}^{(3)} - \frac{5}{2} C_{i+j+k}^{(2)} + \frac{20}{3} \right] \quad (6)$$

and

$$\mathcal{C}_{ij\bar{k}} = -\frac{1}{6} \left[C_{i+j+\bar{k}}^{(3)} - \frac{5}{2} C_{i+j}^{(2)} + \frac{50}{9} \right] \quad (7)$$

For a given irrep of SU(3) labelled by $(\lambda\mu)$ the eigenvalues of these invariants are

$$\langle C^{(2)} \rangle = \frac{1}{3} (\lambda^2 + \mu^2 + \lambda\mu + 3\lambda + 3\mu) \quad (8)$$

and

$$\langle C^{(3)} \rangle = \frac{1}{18} (\lambda - \mu)(2\lambda + \mu + 3)(\lambda + 2\mu + 3). \quad (9)$$

Then for a q^3 system the expectation value of (6) is $10/9$ for a singlet $(\lambda\mu) = (00)$ and $-5/36$ for an octet $(\lambda\mu) = (11)$.

This is an exploratory study where a schematic form for the radial part of \mathcal{V}_{ijk} of (3) is assumed. This is

$$\langle \mathcal{V}_{ijk} \rangle = \frac{c}{3} (\langle V_{ij} \rangle + \langle V_{jk} \rangle + \langle V_{ki} \rangle). \quad (10)$$

where c represents the relative strength of the three-body over the two-body interaction, as in Refs. [4–6].

Now we discuss the basis states. For describing $q^4\bar{q}$ systems one can introduce various coupling schemes, each being convenient for a particular form of the interaction operator. For our discussion suppose that the particles 1, 2, 3 and

4 are quarks and 5 is an antiquark. Then one can first couple three quarks together and then couple this subsystem to a $q\bar{q}$ pair. In this way one introduces the so called asymptotic channels having a physical color singlet - color singlet state $|(123)_1(4\bar{5})_1\rangle$ and unphysical color octet - color octet states $|(123)_8(4\bar{5})_8\rangle$. This coupling scheme is useful to calculate matrix elements of the operator (4) and it gives the appropriate basis at large distances where only the singlet-singlet state must survive, the octet-octet states being pushed up by the quark-quark interaction. Asymptotic channels are common to all multiquark systems. The tetraquarks have one singlet-singlet and one octet-octet asymptotic channels. The pentaquarks have one singlet-singlet channel but two octet-octet channels. These are

$$\begin{aligned} |1\rangle &= |(123)_1(4\bar{5})_1\rangle \\ |2\rangle &= |(123)_8^\rho(4\bar{5})_8\rangle \\ |3\rangle &= |(123)_8^\lambda(4\bar{5})_8\rangle. \end{aligned} \tag{11}$$

where the ρ and λ superscripts correspond to the two linear independent basis vectors of the [21] irrep of the permutation group S_3 .

On the other hand in order to estimate the contribution of the three-body interaction (5) it is convenient first to couple two quarks, say 1 and 2 to the antiquark $\bar{5}$ and then to the subsystem of the remaining pair of quarks, 3 and 4, to get again total color singlets. One can construct the following normalized independent states

$$\begin{aligned} |\phi_1\rangle &= |[(12)^S \bar{5}]_{[211]} (34)_{[11]} \rangle \\ |\phi_2\rangle &= |[(12)^A \bar{5}]_{[211]} (34)_{[11]} \rangle \\ |\phi_3\rangle &= |[(12)^A \bar{5}]_{[22]} (34)_{[2]} \rangle. \end{aligned} \tag{12}$$

The first two contain an SU(3) triplet $q^2\bar{q}$ state denoted by [211] and the third contains an SU(3) antisextet state denoted by [22]. Of course, the states between different coupling schemes are related to each other. We found that the asymptotic channels are related to the intermediate coupling channels (12) by the following unitary transformation

	$ [(12)^A \bar{5}]_{[211]} (34)_{[11]} \rangle$	$ [(12)^A \bar{5}]_{[22]} (34)_{[2]} \rangle$	$ [(12)^S \bar{5}]_{[211]} (34)_{[11]} \rangle$
$ (123)_1(4\bar{5})_1\rangle$	$\sqrt{\frac{1}{3}}$	$\sqrt{\frac{2}{3}}$	0
$ (123)_8^\rho(4\bar{5})_8\rangle$	$-\sqrt{\frac{2}{3}}$	$\sqrt{\frac{1}{3}}$	0
$ (123)_8^\lambda(4\bar{5})_8\rangle$	0	0	1

(13)

The proof is given elsewhere [8]. The first two rows give transformation coefficients identical to those found for tetraquark systems [9]. This means that from permutation symmetry point of view the structure of the corresponding asymptotic basis vectors is the same in both cases. However the state $[[(12)^S \bar{5}]_{[211]} (34)_{[11]}]$ does not exist in tetraquarks, being incompatible with the definition of an anti-quark as an antisymmetric qq pair. Thus there is only one octet-octet state in tetraquarks.

In the basis (12) the expectation values of the operator (7) are

$$\begin{aligned} \langle \phi_1 | \mathcal{C}_{12\bar{5}} | \phi_1 \rangle &= 5/18 \\ \langle \phi_2 | \mathcal{C}_{12\bar{5}} | \phi_2 \rangle &= -5/9 \\ \langle \phi_3 | \mathcal{C}_{12\bar{5}} | \phi_3 \rangle &= 5/18 \end{aligned} \quad (14)$$

Here we first calculate the matrix elements of the color part of V_{2b} and V_{3b} and then discuss their contribution to the total energy of a $q^4\bar{q}$ system. Following Ref. [10] one has

$$\langle |F_i \cdot F_j| \rangle = \langle |F_i \cdot F_{\bar{j}}| \rangle = -\frac{1}{3} \quad (15)$$

Then the integration in the color space of (2) gives

$$\langle V_{2b} \rangle = 2 \sum_{i < j} V_{ij} \quad (16)$$

for any of the asymptotic states (11).

The matrix elements of the three-body interaction (3) can be written as

$$\langle i | V_{3b} | j \rangle = 4 \langle i | \mathcal{C}_{123} | j \rangle + 6 \langle i | \mathcal{C}_{12\bar{5}} | j \rangle \quad (17)$$

where \mathcal{C}_{123} and $\mathcal{C}_{12\bar{5}}$ are defined by (6) and (7) respectively. Using the expectation values of \mathcal{C}_{123} given below Eq. (9) and of $\mathcal{C}_{12\bar{5}}$, see Eq. (14), and the unitary transformation (13) we obtain the color part contribution of $V_{2b} + V_{3b}$ as given by the matrix

$$\begin{array}{c|ccc} & \langle 1|1 \rangle & \langle 2|2 \rangle & \langle 3|3 \rangle \\ \hline \langle 1|1 \rangle & 2 + \frac{4}{9}c & \frac{\sqrt{2}}{6}c & 0 \\ \langle 2|2 \rangle & \frac{\sqrt{2}}{6}c & 2 - \frac{2}{9}c & 0 \\ \langle 3|3 \rangle & 0 & 0 & 2 + \frac{1}{9}c \end{array} \quad (18)$$

where $i, j = 1, 2$ and 3 are the asymptotic states (11). The eigenvalues of this matrix are

$$e_{1,2} = 2 + \frac{c}{9} \pm \frac{c}{\sqrt{6}}, \quad e_3 = 2 + \frac{1}{9}c. \quad (19)$$

To get the full contribution of the confinement one must multiply each eigenvalue by $\sum_{i < j} V_{ij}$.

The eigenvector associated with e_1 is dominantly color singlet - color singlet (the state $|1\rangle$ appears with 91 % probability) and the eigenvector associated with e_2 is dominantly color octet - color octet (the state $|2\rangle$ appears with 91 % probability) irrespective of the value of c . In Ref. [4] the range proposed for the relative strength c was

$$-\frac{3}{2} < c < \frac{2}{5}. \quad (20)$$

Baryon spectroscopy favours negative values of c [4–6]. For c negative e_1 is the lowest eigenvalue and it decreases with decreasing c . When e_1 decreases the total energy of a $q^4\bar{q}$ system also decreases. Thus such system gets more stable.

In conclusion the three-body confining interaction (3) can increase the stability of pentaquarks provided its strength is negative. A similar conclusion results from the study of tetraquarks [7].

References

1. T. Nakano et al., LEPS collaboration, Phys. Rev. Lett. **91** (2003) 012002; S. Stepanyan et al., CLAS Collaboration, hep-ex/0307018; V. V. Barmin et al., DIANA Collaboration, hep-ex/0304040, to appear in Phys. Atom. Nucl.; J. Barth et al., SAPHIR Collaboration, hep-ex/0307083.
2. Fl. Stancu and D. O. Riska, Phys. Lett. B to appear, hep-ph/0307010.
3. Fl. Stancu, Phys. Rev. **D58** (1998) 111501.
4. V. Dmitrasinovic, Phys. Lett. **B499** (2001) 135.
5. S. Pepin and Fl. Stancu, Phys. Rev. **D65** (2002) 054032.
6. Z. Papp and Fl. Stancu, Nucl. Phys. **A726** (2003) 327.
7. D. Janc, V. Dmitrasinovic and M. Rosina, these proceedings.
8. Fl. Stancu, in preparation.
9. Fl. Stancu, *Group Theory in Subnuclear Physics*, Clarendon Press, Oxford, 1996.
10. M. Genovese, J. -M. Richard, Fl. Stancu and S. Pepin, Phys. Lett. **B425** (1998) 171.



$b\bar{b}b\bar{b}$ production in NN and NA interactions at the LHC ^{*}

A. Del Fabbro and D. Treleani

Dipartimento di Fisica Teorica dell'Università di Trieste and INFN, Sezione di Trieste,
Strada Costiera 11, Miramare-Grignano, I-34014 Trieste, Italy.

Abstract. The large parton luminosity will generate a sizable rate of events, in NN collisions at the CERN LHC, where several pairs of b-quarks are produced contemporarily by multiple parton interactions. The phenomenon is further enhanced in NA reactions, where nuclear structure will lead to a rather spectacular anti-shadowing effect.

1 Introduction

The large rates of production of heavy quarks, expected at high energies, may lead to a sizable number of events, at the CERN LHC, containing two or more pairs of b quarks, generated contemporarily by independent partonic collisions. An inclusive cross section of the order of $10 \mu\text{b}$ may in fact be foreseen for a double parton collision process, with two $b\bar{b}$ pairs produced in a pp interactions at 14TeV, while the cross section to produce two $b\bar{b}$ pairs by a single collision at the same c.m. energy may be one order of magnitude smaller[1]. All production rates are significantly enhanced in proton-nucleus collisions, which may offer considerable advantages for studying multiparton collision processes[2].

2 $b\bar{b}b\bar{b}$ production

Quite in general[3], with the only assumption of factorization of the hard component of the interaction, the expression of the double parton scattering cross section to produce two $b\bar{b}$ pairs in proton-nucleon and proton-nucleus collisions is given by

$$\sigma_{(N,A)}^D(b\bar{b}, b\bar{b}) = \frac{1}{2} \sum_{ij} \int \Gamma_p(x_i, x_j; s_{ij}) \hat{\sigma}(x_i, x'_i) \hat{\sigma}(x_j, x'_j) \Gamma_{(N,A)}(x'_j, x'_j; s_{ij}) dx_i dx'_i dx_j dx'_j d^2 s_{ij}, \quad (1)$$

where the indices N, A refer to the cases where the target is an isolated nucleon or a nucleus, i, j refer to the different kinds of partons which annihilate to produce a $b\bar{b}$ pair and the factor 1/2 is a consequence of the symmetry of the expression

^{*} Talk delivered by D. Treleani

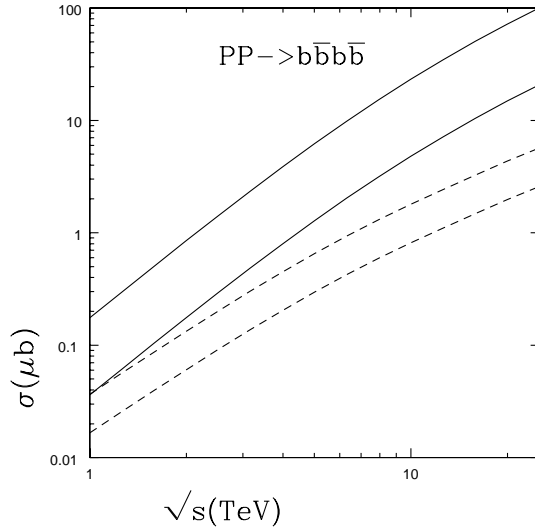


Fig. 1. $b\bar{b}b\bar{b}$ production cross section as a function of center of mass energy, by double parton scattering (continuous curves) and by single parton scattering (dashed curves). To keep higher order corrections into account the cross sections are multiplied by the ‘K-factor’, $K = 2.5$ for the lower curves and $K = 5.5$ for the higher curves.

for exchanging i and j . The non-perturbative input of a double parton collision is the two-body parton distribution function $\Gamma(x_1, x_2, s_{1,2})$, which depends not only on the fractional momenta $x_{1,2}$, but also on the relative distance in transverse space $s_{1,2}$. The cross section is simplest when the target is a nucleon and partons are not correlated in fractional momenta, which may be not be an unreasonable approximation in the limit of small x . In such a case the two-body parton distribution may be factorized as $\Gamma_p(x_i, x_j; s_{ij}) = G(x_i)G(x_j)F(s_{ij})$, where $G(x)$ are the usual (one-body) parton distributions and $F(s)$ a function normalized to 1 and representing the parton pair density in transverse space. In this limit one obtains

$$\sigma_N^D(b\bar{b}; b\bar{b}) = \frac{1}{2} \sum_{ij} \Theta^{ij} \sigma_i(b\bar{b}) \sigma_j(b\bar{b}) \quad (2)$$

where $\sigma_i(b\bar{b})$ is the inclusive cross sections to produce a $b\bar{b}$ pair in a hadronic collision (the index i labelling a definite parton process) while the factors Θ^{ij} have dimension an inverse cross section and result from integrating the products of the two-body parton distributions in transverse space. In this simplified case the factors Θ^{ij} provide a direct measure of the different average transverse distances between different pairs of partons in the hadron structure.

The simplest possibility, in the case of NA interactions, is when the nuclear parton distributions are additive in the nucleon parton distributions. In such a case one may express the nuclear parton pair density, $\Gamma_A(x'_i, x'_j; s_{ij})$, as the sum

of two well defined contributions, where the two partons are originated by either one or by two different parent nucleons, namely

$$\Gamma_A(x'_i, x'_j; s_{ij}) = \Gamma_A(x'_i, x'_j; s_{ij})\Big|_1 + \Gamma_A(x'_i, x'_j; s_{ij})\Big|_2 \quad (3)$$

and correspondingly $\sigma_D^A = \sigma_D^A|_1 + \sigma_D^A|_2$. By introducing the transverse parton coordinates $B \pm \frac{s_{ij}}{2}$, where B is the impact parameter of the hadron-nucleus collision, one may write

$$\Gamma_A(x'_i, x'_j; s_{ij})\Big|_{1,2} = \int d^2B \gamma_A\left(x'_i, x'_j; B + \frac{s_{ij}}{2}, B - \frac{s_{ij}}{2}\right)\Big|_{1,2} \quad (4)$$

where $\gamma_A|_{1,2}$ are given by

$$\begin{aligned} \gamma_A\left(x'_i, x'_j; B + \frac{s_{ij}}{2}, B - \frac{s_{ij}}{2}\right)\Big|_1 &= \Gamma_N(x'_i, x'_j; s_{ij})T(B) \\ \gamma_A\left(x'_i, x'_j; B + \frac{s_{ij}}{2}, B - \frac{s_{ij}}{2}\right)\Big|_2 &= G_N(x'_i)G_N(x'_j)T\left(B + \frac{s_{ij}}{2}\right)T\left(B - \frac{s_{ij}}{2}\right) \end{aligned} \quad (5)$$

with $T(B)$ is the nuclear thickness function, normalized to the atomic mass number A and G_N nuclear parton distributions divided by the atomic mass number.

The first term in Eq.(3) obviously gives a simple rescaling of the double parton distribution of an isolated nucleon:

$$\Gamma_A(x'_i, x'_j; s_{ij})\Big|_1 = \Gamma_N(x'_i, x'_j; s_{ij}) \int d^2BT(B) \quad (6)$$

and the resulting contribution to the cross section is the same as in a nucleon-nucleon interaction, apart from the enhancement nuclear flux factor, so one obtains $\sigma_A^D|_1 = A\sigma_N^D$. In the $\sigma_A^D|_2$ term the integration on s_{ij} involves the projectile and two different target nucleons:

$$\int ds_{ij} \Gamma_p(x_i, x_j; s_{ij})T\left(B + \frac{s_{ij}}{2}\right)T\left(B - \frac{s_{ij}}{2}\right) \quad (7)$$

In the limit $r_p \ll R_A$ one may approximate $T\left(B \pm \frac{s_{ij}}{2}\right) \simeq T(B)$, which gives:

$$\sigma_A^D|_2 = \frac{1}{2} \sum_{ij} \int G_p(x_i, x_j) \hat{\delta}(x_i, x'_i) \hat{\delta}(x_j, x'_j) G_N(x'_i) G_N(x'_j) dx_i dx'_i dx_j dx'_j \int d^2BT^2(B), \quad (8)$$

where

$$G_p(x_i, x_j) = \int d^2s_{ij} \Gamma_p(x_i, x_j; s_{ij}) \quad (9)$$

The two terms $\sigma_A^D|_1$ and $\sigma_A^D|_2$ have hence very different properties. While in the simplest case presently considered $\sigma_A^D|_1$ scales as A^1 , $\sigma_A^D|_2$ scales as $A^{4/3}$. The effects induced by the presence of the nucleonic degrees of freedom, in double parton scattering, cannot hence be reduced to the simple shadowing corrections of the nuclear parton structure functions, whose effect is to decrease the cross

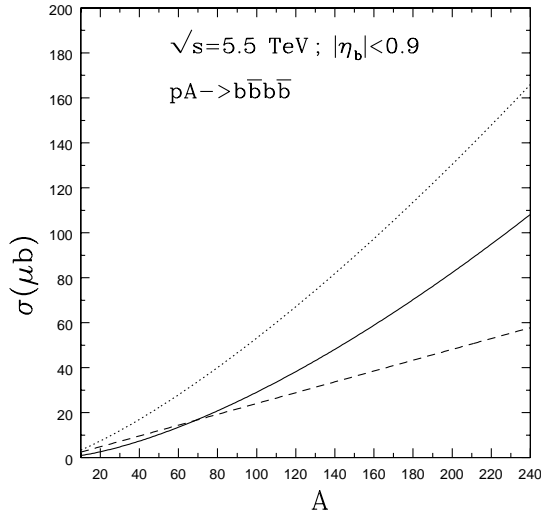


Fig. 2. Different contributions to the cross section for $b\bar{b}b\bar{b}$ production, in a central calorimeter as a function of A of the one-nucleon (dashed line) and of the two nucleons (continuous line) terms. The dotted line is the sum of the two terms.

section as a function of A . Rather the main effect of the nuclear structure is due to the presence of the $\sigma_A^D|_2$ term in the cross section, which grows much more rapidly with the atomic mass number, as compared to the single scattering term, giving rise to a sizable additive contribution to the cross section.

3 Summarizing:

- The cross section of $b\bar{b}b\bar{b}$ production in hadron-nucleus collisions at the LHC is rather large, reaching values of the order of hundreds of μb .
- A rather direct feature is the "anomalous" dependence of the process on A . The presence of the nucleonic degrees of freedom do not lead, in this case, to the 'usual' shadowing corrections to the nuclear structure functions, which cause a limited *decrease* (of the order of 20%) of the cross section. On the contrary the dominant effect of the nuclear structure is due to the presence of the $\sigma_A^D|_2$ term in the cross section, which scales as $A^{4/3}$, giving rise to a correction with opposite sign, namely to an *increase* of the cross section which may become larger than 100% for a heavy nucleus.

References

1. A. Del Fabbro and D. Treleani, Phys. Rev. **D66** (2002) 074012.
2. M. Strikman and D. Treleani, Phys. Rev. Lett. **88**, 031801 (2002).
3. N. Paver and D. Treleani, Nuovo Cim. A **70**, 215 (1982).



Covariant electromagnetic and axial form factors in a constituent quark model

R.F. Wagenbrunn

Institut für Theoretische Physik, Karl-Franzens-Universität Graz, Universitätsplatz 5,
A-8010 Austria

Abstract. I discuss several aspects of electromagnetic and axial form factors of the nucleons predicted within constituent quark models. In particular I address the problem of covariance, current conservation, many-body currents.

Recently predictions for electromagnetic and axial form factors of the nucleons were given [1–3] for the GBE constituent quark model [4]. The results were obtained within the point form of relativistic quantum mechanics [5]. While in this form all Lorentz transformation are left kinematical, the dynamics enters in all four components of the momentum operator [6]. It is introduced along the Bakamjian Thomas (BT) construction [7]. Eigenstates of all four components of the momentum operator are obtained by solving one eigenvalue problem for a mass operator which in this respect plays the same role as the Hamiltonian in nonrelativistic quantum mechanics. For calculation of the form factors electromagnetic and axial current operators in the so called point form spectator approximation (PFSA) were applied. For more details I refer to [8]. Manifest covariance must hold since the boosts are kinematical and the results for the form factors are indeed frame independent.

The so obtained results (see Fig. 1) [1–3] are in a surprisingly close agreement with the data. This is particularly remarkable because there are no free (fit) parameters in these calculations. The GBE constituent quark model does have some parameters but they were fitted only to the baryon spectra. Then the resulting nucleon wave function goes into the calculation of the form factors.

It is at the time not yet clear why such a successful description of the electromagnetic and axial structure of the nucleons is possible within this formalism. The ultimate goal is thus to better understand the formalism and its physical contents. A starting point for such an investigation is the issue of current conservation which must be satisfied for the electromagnetic current. As a consequence the third component of the current must vanish in the Breit frame (with momenta $P(st)$ and $P'(st)$ of the incoming and outgoing nucleon) which can explicitly be checked for the PFSA current. It turns out that the matrix element $\langle P'(st)|J^3(0)|P(st) \rangle \neq 0$, i.e., that the electromagnetic current in PFSA is not

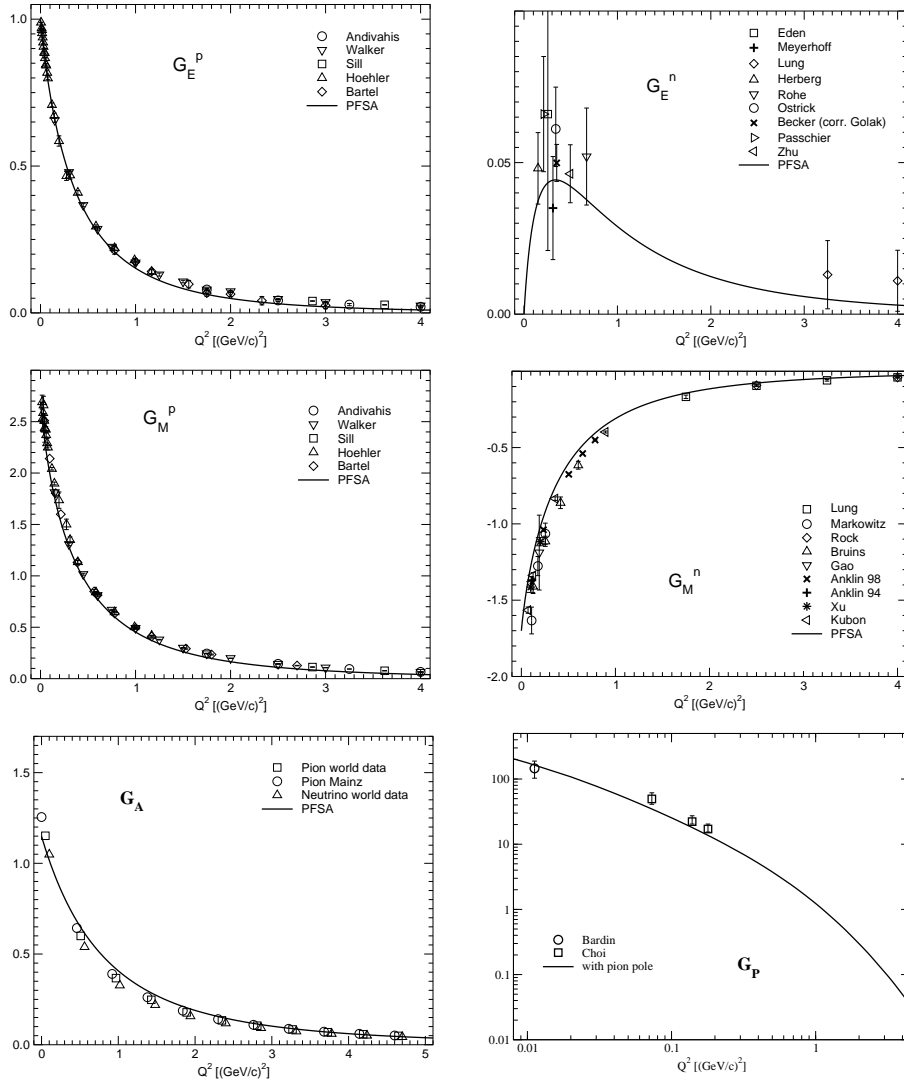


Fig. 1. Predictions for the proton electric (top left), neutron electric (top right), proton magnetic (middle left), neutron magnetic (middle right), and nucleon axial (bottom left), and induced pseudoscalar (bottom right) form factors for the GBE constituent quark model in PFSA.

conserved. A comparison to the zero-component of the current shows however, that the size of the third component is much smaller. This is demonstrated in Fig. 2 where I plot the absolute value of the ratio of $\langle P'(st)|J^3(0)|P(st) \rangle$ to $\langle P'(st)|J^0(0)|P(st) \rangle$ for the proton. It is smaller than 1% for momentum transfers q^μ with $Q^2 = -q^2 < 4 \text{ GeV}^2$. In this sense one can call the violation of current conservation small. In order to restore it one can redefine the electromagnetic current by just projecting it on its transverse components, i.e., one uses the current $\tilde{J}^\mu(0) = J^\mu(0) - \frac{J^\nu(0)q_\nu}{q^2}q^\mu$. This current has some problem if one con-

siders electromagnetic transitions to resonances since there would be a pole for $Q^2 = 0$. There have been suggested two different ways out. Either one can add an additional purely transverse current having also a pole at $Q^2 = 0$ which just cancels the one in the original $\tilde{J}(0)$ [10]. This term must not be taken into account, however, in case of elastic form factors. Alternatively an a priori conserved current operator was recently constructed [11] which reduces to $\tilde{J}^\mu(0)$ for the elastic case but can also be used for transitions without having a pole at $Q^2 = 0$.

In nonrelativistic physics current conservation can be achieved by a proper choice of two-body currents which can be related to the microscopic picture behind a model. Until now we have not yet succeeded to find an analogon in the point form relativistic quantum mechanics. Modifying the current as described above to establish current conservation means that one adds some two- or three-body currents. In this way it is however not so clear how to connect them with the underlying microscopic picture (i.e., the interaction added to the mass operator in the BT construction). In general current conservation is only a constraint on the longitudinal component of the current. This freedom (which exists also in a nonrelativistic theory) can be utilized to add additional purely transverse terms to the current. A possible way of introducing such currents was suggested in Ref. [10]. Finally it must be mentioned that in relativistic quantum-mechanics the separation into one- and many-body currents becomes ambiguous. In principle, the different forms of dynamics must yield the same results since the forms are unitary equivalent. A one-body current in one form, however, becomes a many-body current in the other form. The spectator approximations in two different forms are therefore not equivalent. Thus it becomes clear why the results in PFSA and in a corresponding instant form spectator approximation can become very different [8]. Big differences between results obtained in different forms of dy-

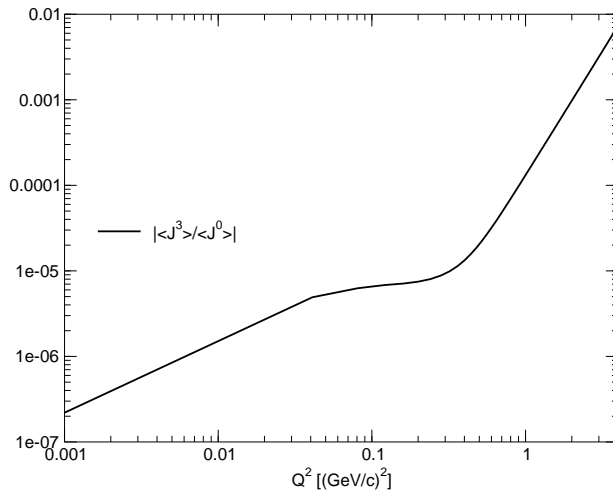


Fig. 2. Ratio of the matrix elements of J^3 and J^0 for the proton in the Breit frame.

namics were also found for form factors of bound states of two spinless particles by the Grenoble group [9].

Contrary to the electromagnetic current, the axial current is not conserved. From the definition of the axial current for a spin- $\frac{1}{2}$ particle it follows that the matrix element of its zero component must vanish in the Breit frame $\langle P'(st)|A^0(0)|P(st) \rangle = 0$. So even though the axial current is not conserved there is also a constraint which turns out to be violated in case of the PFSA. Similarly as in the case of the electromagnetic current one could introduce a modified axial current by projecting away its component in the direction of $\mathbf{p} = P'(st) + P(st)$, i.e., introduce a current $\tilde{A}^\mu(0) = A^\mu(0) - \frac{A^0(0)p_\nu}{p^2} p^\mu$, which then fulfills the constraint by construction. In the Breit frame (where $\mathbf{p} = (2P(st)^0, 0, 0, 0)$) it makes $\langle P'(st)|\tilde{A}^0(0)|P(st) \rangle = 0$ without changing the other three components. Since the axial and the induced pseudoscalar form factors are determined only from the latter components our results remain unchanged.

This work was supported by the Austrian Science Fund (Project P14806).

References

1. R.F. Wagenbrunn, S. Boffi, W. Klink, W. Plessas and M. Radici, Phys. Lett. B **511**, 33 (2001).
2. L.Ya. Glozman, M. Radici, R.F. Wagenbrunn, S. Boffi, W. Klink and W. Plessas, Phys. Lett. B **516**, 183 (2001).
3. S. Boffi, L.Ya. Glozman, W. Klink, W. Plessas, M. Radici and R.F. Wagenbrunn, Eur. Phys. J. A **14**, 17 (2002).
4. L.Ya. Glozman, W. Plessas, K. Varga and R.F. Wagenbrunn, Phys. Rev. D **58**, 094030 (1998).
5. B.D. Keister and W.N. Polyzou, Adv. Nucl. Phys. **20**, 225 (1991).
6. P.A.M. Dirac, Rev. Mod. Phys. **21**, 392 (1949).
7. B. Bakamjian and L.H. Thomas, Phys. Rev. **92**, 1300 (1953).
8. K. Berger, these proceedings.
9. A. Amghar, B. Desplanques, and L. Theußl, Nucl. Phys. A **714**, 213 (2003).
10. W. Klink, unpublished.
11. F. Coester and D.O. Riska, Nucl. Phys. A **728**, 439 (2003).



Calculation of electroproduction amplitudes in the K-matrix formalism

Bojan Golli

Faculty of Education, University of Ljubljana, and J. Stefan Institute, Ljubljana, Slovenia

Abstract. We present the K-matrix approach to calculate pion electroproduction amplitudes in the framework of chiral quark models. We derive the relation between the K-matrix and the experimentally measured T-matrix and show how to separate the resonant contribution to the amplitudes from the background.

The work is being done in collaboration with Manuel Fiolhais (Coimbra), Pedro Alberto (Coimbra), Ze Amoreira (Covilha) and Simon Širca (Ljubljana).

1 Motivation

In our previous work [1] on electroweak excitations we have shown that different versions of chiral quark models may successfully describe the properties of the low lying nucleon resonances. In these calculations the excited states have been treated as bound states which is justified if we are interested only in the resonant part of the production amplitudes. The total amplitudes as measured in the experiment however include also non-resonant (background) processes related to the outgoing pion. Incorporating the decaying channel in the model calculation may therefore represent a stringent test for the model as well as yield interesting information on the production mechanism and in particular on the role of non-quark degrees in freedom in baryons.

In several models such as the linear σ -model or the chromodielectric model, which include nonlinear effects and in which the interplay between quark and non-quark degrees of freedom is treated in a self-consistent way, the calculation is only feasible in a variational approach. While such an approach can be easily implemented in the bound state calculations its application to the description of scattering processes is much more complicated. In [2] the Kohn variational approach has been adopted to calculate the πN phase shifts and the structure of the resonant state in the Cloudy-Bag-type models. In this work we extend the approach to be able to calculate also the electroproduction amplitudes for pions.

We shall limit ourself to the description of the Δ resonance.

2 The variational approach to the K-matrix

We shall be interest in the class of models in which the pion is coupled linearly to the quark source:

$$H = \int dk \sum_{mt} \left[\omega_k a_{mt}^\dagger(k) a_{mt}(k) + V_{mt}(k) a_{mt}(k) + V_{mt}^\dagger(k) a_{mt}^\dagger(k) \right] + \sum_B E_B^0 c_B^\dagger c_B \quad (1)$$

where

$$V_{mt}(k) = -V(k) \sum_{i=1}^3 \tau_t^i \sigma_m^i, \quad V_{mt}^\dagger(k) = (-1)^{t+m} V_{-m-t}(k). \quad (2)$$

Here $a_{mt}(k)$ and $a_{mt}^\dagger(k)$ are annihilation and creation operators for the $l = 1$ pions with the third component of the spin m and isospin t ; c_B and c_B^\dagger are annihilation and creation operators for the "bare" baryons made up of three quarks, E_B^0 are the corresponding bare energies, $V(k)$ is the source function determined from the quark profiles. We shall limit here only to two state, the nucleon N , and the Δ . In the present stage we do not include meson self-interactions.

In the variational approach to the K-matrix when only a single channel is opened (such as the resonant scattering in the P33 channel below the 2 pion threshold) the resonant state is assumed in the form:

$$|\Psi\rangle = c_\Delta |\Phi_\Delta\rangle + \int dk \eta(k, k_0) \left[a_{mt}^\dagger(k) |\Phi_N^E\rangle \right]^{\frac{3}{2}\frac{3}{2}}. \quad (3)$$

Here $|\Phi_N^E\rangle$ and $|\Phi_\Delta\rangle$ represent the nucleon and the Δ bound states normalized as $\langle \Phi_N^E | \Phi_N^E \rangle = 1$ and $\langle \Phi_\Delta | \Phi_\Delta \rangle = 1$, respectively; $\eta(k, k_0)$ describes the scattering pion and \square^{ST} denotes the coupling of spin and isospin of the pion and the bare quark core to the quantum numbers of the Δ . Asymptotically the pion wave function behaves as

$$\eta(r, k_0) = k_0 j_1(k_0 r) - \tan \delta k_0 y_1(k_0 r), \quad r \rightarrow \infty. \quad (4)$$

Note that in the K-matrix approach the standing waves rather than outgoing (and incoming) waves are used. In k -space this leads to

$$\eta(k, k_0) = \sqrt{\frac{\pi}{2}} \delta(k - k_0) + \frac{\chi(k, k_0)}{\omega_k - \omega_0}, \quad K \equiv \tan \delta = \sqrt{2\pi} \frac{\omega_0}{k_0} \chi(k_0, k_0). \quad (5)$$

The nucleon state $|\Phi_N^E\rangle$ in (3), modified in presence of the scattering pion, i.e. it depends on k and k_0 of the pion, should asymptotically go over to the ground states, $|\Phi_N^E\rangle \rightarrow |\Phi_N\rangle$ for $k \rightarrow k_0$.

Before introducing the variational principle which determines the parameters of the trial function of the type (3), i.e. the pion wave function $\eta(k, k_0)$, the parameter c_Δ as well as structure of the states Φ_Δ and Φ_N^E , we first prove an important relation which hold in this type of models:

$$\chi(k_0, k_0) = \langle \Psi | (H - E) \left[a_{mt}^\dagger(k_0) |\Phi_N\rangle \right]^{\frac{3}{2}\frac{3}{2}}. \quad (6)$$

We assume that both $|\Psi\rangle$ and $|\Phi\rangle$ are exact states, i.e. $H|\Psi\rangle = E|\Psi\rangle$ and $H|\Phi\rangle = E_N|\Phi\rangle$. We should keep in mind that H is *not Hermitian* since Ψ is not a square integrable function, hence $\langle\Psi|H \neq \langle\Psi|E$, and the above expression does not vanish. We write $H = H^\dagger + (H - H^\dagger)$:

$$\langle\Psi|(H - E) \left[a_{m't}^\dagger(k_0)|\Phi_N\rangle \right]^{\frac{3}{2}\frac{3}{2}} = \langle\Psi|(H - H^\dagger) \left[a_{m't}^\dagger(k_0)|\Phi_N\rangle \right]^{\frac{3}{2}\frac{3}{2}}. \quad (7)$$

The non-Hermitian part of H is the pion kinetic energy term:

$$H_{kin} = \int d\mathbf{r} \sum_t (-1)^t \pi_{-t}(\mathbf{r}) \left[-\overrightarrow{\Delta}_r \right] \pi_t(\mathbf{r}). \quad (8)$$

Only those terms in Ψ that asymptotically ($r \rightarrow \infty$) behave as r^{-1} contribute to (7), i.e. the terms involving $\eta(k, k_0)$. Expression (7) yields

$$\int dk \eta(k, k_0) \int d\mathbf{r} \sum_t \left[\langle\Phi_N^E|a_{m't'}(k) \right]^{\frac{3}{2}\frac{3}{2}} \pi_t^\dagger(\mathbf{r}) \left[\overleftarrow{\Delta}_r - \overrightarrow{\Delta}_r \right] \pi_t(\mathbf{r}) \left[a_{m't}^\dagger(k_0)|\Phi_N\rangle \right]^{\frac{3}{2}\frac{3}{2}}. \quad (9)$$

We now commute a and a^\dagger through the pion field; only the commutators produce a non vanishing contribution. We next perform the k -integration yielding the pion wave function in r -space (4). After performing the angular integration we end up with the following integral

$$\frac{k_0^2}{2\omega_0} \sqrt{\frac{2}{\pi}} \int dr \left(j_1(k_0 r) - \sqrt{2\pi} \frac{\omega_0}{k_0} \chi(k_0, k_0) y_1(k_0 r) \right) \left[\overleftarrow{\frac{d}{dr}} r^2 \overleftarrow{\frac{d}{dr}} - \overrightarrow{\frac{d}{dr}} r^2 \overrightarrow{\frac{d}{dr}} \right] j_1(k_0 r). \quad (10)$$

The first term in () vanishes. We perform an integration *per partes* and we are left with the Wronskian of j_1 and y_1 , $W(j(k_0 r), y_1(k_0 r)) = 1/(k_0 r)^2$, multiplied by $k_0^2 r^2 \chi(k_0, k_0)$. The resulting integral is finite for $r \rightarrow \infty$ and equal to $\chi(k_0, k_0)$ which proves (6). Relation (6) holds quite generally since the only assumption in the derivation was on the asymptotic form of the wave function Ψ .

For the class of models (2) we can derive another useful relation by commuting a^\dagger in (6) through (2): $(H - E)a_{m't}^\dagger(k_0) = \omega_0 a_{m't}^\dagger(k_0) + V_{m't}(k_0) + a_{m't}^\dagger(k_0)(H - E)$. Since $(H - E)|\Phi\rangle = -\omega_0|\Phi\rangle$ the last term cancels the first one and we are left only with the matrix element of (2):

$$K_{\pi\pi} \equiv K(k_0, k_0) = \sqrt{2\pi} \frac{\omega_0}{k_0} \chi(k_0, k_0) = -\sqrt{2\pi} \frac{\omega_0}{k_0} \langle\Psi| \sum \sigma\tau |\Phi\rangle V(k_0). \quad (11)$$

This is an exact relation since in the derivation we have not made any assumption about the structure of the resonant state or the ground state; we have only referred to the form of the pion field far away from the source. The result is similar to the expression derived by Chew and Low for the T-matrix [3].

We now sketch a more general derivation of the Kohn variational principle for the K-matrix in the case of pion scattering compared to the derivation given in [2]. It is valid for a more general class of Hamiltonians than (2); we only require that the exact solution (as well as the trial state) has the form of (3) where the pion field asymptotically behaves as (4).

We start by observing that the matrix element between the exact wave function Ψ_e and a trial wave function Ψ_t , satisfying the boundary condition (4) with an approximate phase shift δ_t , can be written in the form

$$\langle \Psi_e | H - E | \Psi_t \rangle = -\frac{k_0}{2\omega_0} (\tan \delta_e - \tan \delta_t). \quad (12)$$

The proof goes similarly as from (7) to (10), the only difference is that in (10) the expression $\sqrt{2/\pi}(j_1(k_0 r) - \tan \delta_t y_1(k_0 r))$ appears instead of the second $j_1(k_0 r)$. Introducing $\delta\Psi = \Psi_t - \Psi_e$ and taking into account $(H - E)|\Psi_e\rangle = 0$ we can write

$$\tan \delta_e = \tan \delta_t - \frac{2\omega_0}{k_0} (\langle \Psi_t | H - E | \Psi_t \rangle - \langle \delta\Psi | H - E | \delta\Psi \rangle) \quad (13)$$

which means that the functional

$$\mathcal{F}_K(\Psi_t) = \tan \delta_t - \frac{2\omega_0}{k_0} \langle \Psi_t | H - E | \Psi_t \rangle \quad (14)$$

is stationary with respect to variations of Ψ_t .

3 The K-matrix for the pion production

We may now extend the model by introducing the coupling to the photon, $H \rightarrow H + H_\gamma$, where H_γ has the usual form of the EM Hamiltonian with the minimal coupling to the hadronic EM current. Then the resonant state will include the emission and absorption of the M1 and E2 photons (denoted by the common index \mathcal{M}) which will modify our ansatz (3) in the following way:

$$\begin{aligned} |\Psi\rangle &= c_\Delta |\Phi_\Delta\rangle + \left[a_{\text{mt}}^\dagger(k_0) |\Phi_N\rangle \right]^{\frac{3}{2} \frac{3}{2}} + \int dk \frac{\chi_{\pi\pi}(k, k_0)}{\omega_k - \omega_0} \left[a_{\text{mt}}^\dagger(k) |\Phi_N^E\rangle \right]^{\frac{3}{2} \frac{3}{2}} \\ &+ \sum_{\mathcal{M}} \int dq \frac{\chi_{\gamma\pi}^{\mathcal{M}}(q, k_\gamma)}{\omega_q - \omega_\gamma} \left[a_{\mathcal{M}}^\dagger(q) |\Phi_N\rangle \right]^{\frac{3}{2} \frac{3}{2}}. \end{aligned} \quad (15)$$

We make the standard assumption that the EM coupling is much weaker compared to the strong coupling and does not modify the structure of the resonant state. The functions $\chi^{\text{M}1}$ and $\chi^{\text{E}2}$ are related to the corresponding K-matrices for the pion electroproduction. The proof of these relations is analogous to the derivation of the K-matrix for the elastic pion scattering. We find:

$$\frac{k_\gamma}{\sqrt{2\pi}\omega_\gamma} K_{\gamma\pi}^{\mathcal{M}} \equiv \chi_{\gamma\pi}^{\mathcal{M}}(k_\gamma, k_\gamma) = -\langle \Psi | (H - E) \left[a_{\mathcal{M}}^\dagger(k_\gamma) |\Phi_N\rangle \right]^{\frac{3}{2} \frac{3}{2}} \quad (16)$$

leading to

$$K_{\gamma\pi}^{\mathcal{M}} = -\sqrt{2\pi} \frac{\omega_\gamma}{k_\gamma} \langle \Psi | \left[H_\gamma, a_{\mathcal{M}}^\dagger(k_\gamma) \right] | \Phi \rangle. \quad (17)$$

4 Splitting the amplitudes in the resonant and the non resonant part

The K-matrix calculated in a model as discussed above exhibits a typical resonant behavior (provided of course the bare Δ -N splitting is sufficiently large). The energy at which the phase goes through 90° corresponds to the energy of the physical Δ , E_Δ . It can be parametrized in the form suggested by Davidson et al.[5]:

$$K_{\pi\pi} \equiv \tan \delta = \frac{C}{E_\Delta - E} + D \equiv \tan \delta_\Delta^K + \tan \delta_b. \quad (18)$$

Here δ is the full phase shift, δ_Δ^K is called the resonant phase shift and δ_b the background phase shift (BPS), which – as shown below – is identical to the BPS in the T-matrix approach. Note that both, δ and δ_Δ^K go through 90° at the same E , (e.g. $E = 1232$ MeV for Δ). The width of the resonance is simply related to the parameter C by $\Gamma_\Delta^K = 2C$.

The T-matrix which is directly related to experimentally measured amplitudes is related to the K-matrix as

$$T = \frac{K}{1 - iK} = \frac{C + (E_\Delta - E)D}{(E_\Delta - E) - i(C + (E_\Delta - E)D)}. \quad (19)$$

In contradistinction to the K-matrix which is a real quantity the T-matrix is complex. The position of the pole in the complex plain can be easily determined if we assume that the coefficients C and D do not depend on the energy. Then the above expression can be brought in the familiar form:

$$T_{\pi\pi}(E) = e^{2i\delta_b} \frac{\Gamma_\Delta^T/2}{M_\Delta - E - i\Gamma_\Delta^T/2} + \sin \delta_b e^{i\delta_b} \quad (20)$$

with

$$M_\Delta = E_\Delta + \frac{CD}{1 + D^2} = E_\Delta + \frac{1}{2}\Gamma_\Delta^T \tan \delta_b, \quad \Gamma_\Delta^T = \frac{2C}{1 + D^2} = \Gamma_\Delta^K \cos^2 \delta_b. \quad (21)$$

From the experimental phase shift in the P33 channel the following values are extracted $M_\Delta = 1210$ MeV, $\Gamma_\Delta^T = 100$ MeV and $\delta_b \approx -23.5^\circ$.

Turning to the T-matrix matrix for the electroproduction, $T_{\gamma\pi}$, we note that the effect of the EM coupling to the photon has a negligible effect on the structure of the state (15). The position and the width of the pole is not changed with respect to the pure π N channel; the phase shift of the amplitudes is that of the π N scattering. This is the so called *Watson theorem* which in our case can be expressed in the form [5]

$$T_{\gamma\pi} = K_{\gamma\pi}(1 + iT_{\pi\pi}) = \frac{K_{\gamma\pi}}{1 - iK_{\pi\pi}}. \quad (22)$$

Using the popular parametrization

$$K_{\gamma\pi} = \frac{A}{E_\Delta - E} + B \quad (23)$$

we can express (22) in the form:

$$T_{\gamma\pi} = \frac{A + B(E_\Delta - E)}{(E_\Delta - E) - i[C + D(E_\Delta - E)]}. \quad (24)$$

Assuming again that the parameters A, B, C and D do not depend on the energy, we can relate our result to the parametrization of $T_{\gamma\pi}$ used in parameterizing the experimental data [4]:

$$T_{\gamma\pi} = re^{i\phi} T_{\pi\pi}^R + \beta e^{i\delta_b}, \quad T_{\pi\pi}^R = \frac{\Gamma_\Delta^T/2}{M_\Delta - E - i\Gamma_\Delta^T/2}. \quad (25)$$

We obtain:

$$re^{i\phi} = \frac{A}{C} - 2 \frac{B}{D} \frac{D^2}{1+D^2} + iD \left(\frac{A}{C} + \frac{B}{D} \frac{1-D^2}{1+D^2} \right) \quad \text{and} \quad \beta = \frac{B}{D} \sin \delta_b. \quad (26)$$

We have to comment on the above assumption of constant parameters. If we identify the parameters in (18) and (23) with what comes out from a model calculation it turns out that the parameters exhibit a strong dependence on the pion momenta k_0 and therefore also on the energy. This can be seen already from the lowest order expression for the scattering matrix which takes the form:

$$K_{\pi\pi} = \pi \frac{\omega_0}{k_0} V(k_0)^2 \left[\frac{\langle \Delta \| \sum \sigma\tau \| N \rangle^2}{E_\Delta - E} + \frac{4}{9} \frac{\langle N \| \sum \sigma\tau \| N \rangle^2}{E_N + 2\omega_0 - E} + \frac{1}{9} \frac{\langle \Delta \| \sum \sigma\tau \| N \rangle^2}{E_\Delta + 2\omega_0 - E} \right] \quad (27)$$

where we immediately identify the parameter C in (18) with the numerator of the first term and D with the other two terms corresponding to the crossed processes with either the nucleon or the Δ in the intermediate state. Since the pions are p-waves, $V(k_0) \propto k_0^2$, and $K_{\pi\pi}$ behaves as k_0^3 close to the threshold – as it should. The resulting background phase shift δ_b is positive for all k_0 .

In the analysis of experimental data it is more convenient to parametrize the resonant T matrix using the familiar form (25) with constant Γ and M . A consequence of such an assumption is that the background phase shift δ_b stays negative for the whole energy range. We should be aware that the negative δ_b does not correspond to any physical process; it is merely a convenient tool to analyze the experimental data. In order to extract the parameters M , Γ , r , and δ_b from the model calculation we should therefore numerically fit the calculated $K_{\pi\pi}$ and $K_{\gamma\pi}$ to the forms (18) and (23) and use (21) and (26) to relate them to the values of A, B, C and D obtained from the fit.

References

1. M. Fiolhais, B. Golli and S. Širca, Phys. Lett. **B 373** (1996) 229; L. Amoreira, P. Alberto, M. Fiolhais, Phys. Rev. C **62** (2000) 045202; P. Alberto, P., M. Fiolhais, B. Golli, J. Marques, Phys. Lett. **B 523** (2001) 273; B. Golli, S. Širca, L. Amoreira, M. Fiolhais, Phys. Lett. **B 553** (2003) 51.
2. B. Golli, M. Rosina, J. da Providência, Nucl. Phys. **A436** (1985) 733
3. G. F. Chew and F. E. Low, Phys. Rev. **101** (1956) 1570
4. Th. Wilbois, P. Wilhelm and H. Arenhövel, Phys. Rev. C **57** (1998) 295
5. R.M. Davidson, N.C. Mukhopadhyay, Phys. Rev. D **42** (1990) 20



Double Charmed Tetraquarks *

Damijan Janc^a and Mitja Rosina^{a,b}

^bJ. Stefan Institute, P.O. Box 3000, 1000 Ljubljana, Slovenia

^aFaculty of Mathematics and Physics, University of Ljubljana, 1000 Ljubljana, Slovenia

Abstract. We present a detailed four-body calculation in a basis which is also adequate for a weakly bound state of two mesons. The $T_{cc} = cc\bar{u}\bar{d}$ state with quantum numbers $IS = 01$ and positive parity is analyzed. The influence of a weak three-body force is studied.

The bound state of two mesons is now a very hot topic due to new experimental discoveries. The $c\bar{c}$ resonance [1] and the $D_s(2430)$ state [2] detected this year can be explained in the constituent quark model as two-quark two-antiquark bound states. Here we present some numerical results on the $cc\bar{u}\bar{d}$ system. We use a basis which also contains asymptotic channels of two free mesons so that we are able to treat also weakly bound states. The aim of this talk is to explain numerics involved in the calculations, while the motivation for this subject was presented by Mitja Rosina (these Proceedings).

1 Basis

We are interested only in $L=0$ states, so we expand the orbital part of the tetraquark wave function in terms of gaussians with different widths. We do not use Jacobi coordinates but we rather choose coordinates which are more natural for the two-quark two-antiquark system. This coordinate systems (Fig. 1) were already introduced in [3] but were not fully applied. The use of all systems is important since although the total angular momentum is zero, one can by using e.g. system b) in Fig. 1 have a nonzero relative angular momenta between two quarks l_{12} or between two antiquarks l_{34} resulting in a more complete Hilbert space.

When we have a strong quark mass asymmetry we expect diquark-antidiquark clustering [3] so that the first coordinate system on Fig 1 is more suitable and the dominant color configuration has the diquark in antitriplet and the antidiquark in triplet color state. On the other hand, if the binding is weak, the direct and exchange meson-meson channels are more adequate. For these channels we need also the sextet-antisextet color configuration as can be seen by the recoupling

$$|1_{13}1_{24}\rangle = \sqrt{\frac{1}{3}}|\bar{3}_{12}\bar{3}_{34}\rangle + \sqrt{\frac{2}{3}}|6_{12}\bar{6}_{34}\rangle,$$

$$|8_{13}8_{24}\rangle = -\sqrt{\frac{2}{3}}|\bar{3}_{12}\bar{3}_{34}\rangle + \sqrt{\frac{1}{3}}|6_{12}\bar{6}_{34}\rangle.$$

* Talk delivered by D. Janc.

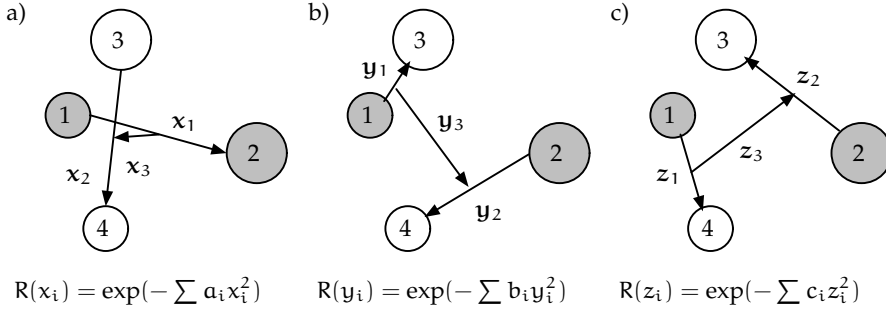


Fig. 1. Two quarks (dashed circles) and two antiquarks (empty circles) in three different relative coordinate systems: a) diquark-antidiquark, b) direct and c) exchange meson-meson channels. The orbital part of the wave function is expanded in Gaussians of relative coordinates $\psi = \sum d_n R^n$ using all three systems.

The important configuration is singlet-singlet while the octet-octet configuration does not make a significant contribution. Similarly one can use different coupling schemes for the spin part of the wave function. To solve the problem as accurately as possible we use all color and spin types of configuration.

2 Binding energy of tetraquarks

We search for solutions of our Hamiltonian with the variational method, where we use a general diagonalization of the Hamiltonian spanned by the nonorthogonal basis functions $R^n = e^{-\sum a_i^n x_i^2}$ or $e^{-\sum b_i^n y_i^2}$ or $e^{-\sum c_i^n z_i^2}$, $n = 1 \dots N$. We have built the basis functions step by step by adding the best configurations from Fig. 1 with the best color-spin configurations allowed for our quantum numbers ($IS=01$, positive parity and color singlet) after optimizing the corresponding widths. To obtain 1 MeV accuracy we constructed in this way basis with up to $N_{\max} = 40$ functions. This basis states can also accommodate two asymptotically free mesons if the four-body problem have no bound state.

In our calculations we use nonrelativistic potential model with the Bhaduri potential [4] which is very successful in reproducing the ground state of almost all mesons. The calculation in harmonic oscillator basis [5] has shown that the T_{cc} tetraquark in this model is not bound. Similarly a phenomenological estimate of the mass [6] also suggest that the system is not bound. This estimate is built on the assumption that one can neglect contributions from the sextet-sextet configuration and from direct and exchange meson-meson channels in Fig. 1. In our approach our ground state is a state of two free color singlet mesons so that the mass of the tetraquark is equal to the sum of masses of the D and D^* mesons. For this it is crucial to use in the expansion also states b) and c) from Fig. 1. Since we are interested how the results are changed if we slightly modify the parameters in the Bhaduri potential or add some new weak three-body interaction which would not spoil the meson spectroscopy and will have only minor effects also for baryons. We investigate the possibility of weak binding of T_{cc} and we need a good description also of asymptotic states with respect to which we are calculat-

ing the binding energy. This is why we find our basis more suitable than the basis used in [5].

To get some deeper understanding of our four-quark system we calculate the masses of the tetraquarks in a basis where we do not optimize all widths of Gaussian functions, but keep one of them fixed. The most natural choice is to keep the width which define the wave functions between two two-body cluster fixed ($1/d^2=a_3, b_3, \text{ or } c_3$). If this width are very large the mass of the system should be equal to the sum of the masses of the two mesons. since our basis states do include this asymptotical configurations. On the other hand if the plot of the mass of the tetraquark as a function of this parameter has a local minimum with the mass lower than the asymptotic value, we have a four-body bound state. In this way we can get some information about interaction between two two-body clusters in tetraquark although this mass at fixed d should not be confused with effective potential in Born–Oppenheimer approximation.

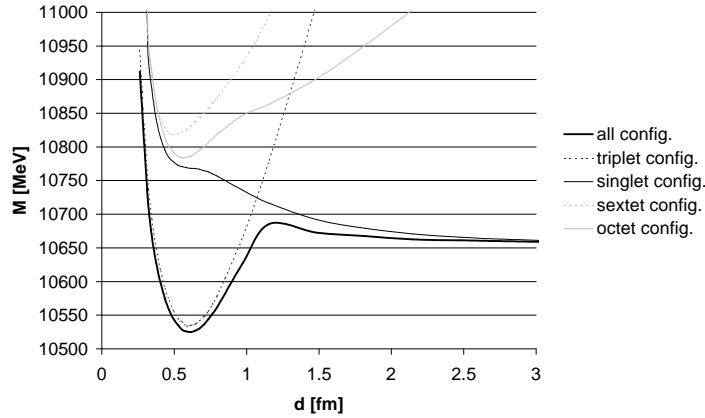


Fig. 2. The mass of T_{bb} as a function of the width between two clusters. Different curves present results of the calculations where only some type of color wave function were used in expansion of the tetraquark wave function (e.g. dotted curve for results with only $|\bar{3}_{12}3_{34}\rangle$ configurations.)

We illustrate this on the $bb\bar{u}\bar{d}$ tetraquark which was already rigorously solved with Bhaduri potential in [5] in harmonic oscillator basis. Results are shown in Fig. 2. The masses of free B and B^* mesons obtained with Bhaduri potential are 5301 MeV and 5350 MeV respectively. We see that for large d the energy of the system approaches this value. But at $d \sim 0.6$ fm we have a minimum which indicate that the T_{bb} is bound in our model. On the same figure are presented the results of calculations with only some type of color wave function used in expansion of the tetraquark wave function. We see that for the minimum at $d \sim 0.6$ fm the $|\bar{3}_{12}3_{34}\rangle$ configurations are far the most important. Using only this configurations the mass of the tetraquark is 10531 MeV which is only 6 MeV above the energy obtained if we use all color configurations and do minimization without fixing any of the widths. This then means that by ignoring few percents in the bind-

ing energy that the ground state of the T_{bb} tetraquark is the antiquark in color triplet state and the diquark in color antitriplet between which the relative motion can be described by $e^{-x_3^2/(0.6\text{fm})^2}$. Thus the T_{bb} tetraquark can be described as the harmonic oscillator built out of the heavy diquark and light antiquark.

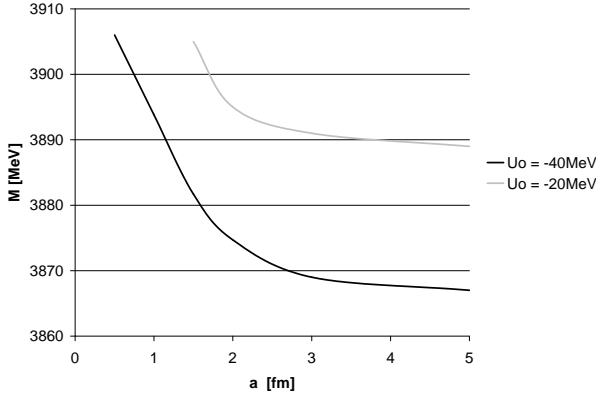


Fig. 3. The mass of T_{cc} as a function of the smearing of three body potential for two different strengths. The asymptotic mass of D plus D^* is 3906 MeV in our model.

As expected, we have clustering in color singlet states for large d (Fig. 3), while due to confinement the energy of colored configurations rises sharply. The rise for small d ($d < 0.5$ fm) is due to the kinetic energy between two clusters.

3 Three-body interaction

The T_{cc} tetraquark in the nonrelativistic constituent quark model with the Bhaduri potential is above the $D D^*$ threshold. But as one can see on Fig 3 that the mass of T_{cc} as a function of the width between two clusters has a significant minimum at $d \sim 0.7$ fm which indicates a diquark-antidiquark clustering. Now we investigate how close to binding this system is in this model. We do this by introduction a SU(3) color invariant three body interaction. The origin and influence of such interaction on three and four quark state was studied in [7]. We present the results of detailed four-body calculations with Bhaduri potential extended with the tree-body interaction of the form

$$V_{qqq}^{3b}(\mathbf{r}_i, \mathbf{r}_j, \mathbf{r}_k) = -\frac{1}{8} d^{abc} \lambda_i^a \lambda_j^b \lambda_k^{c*} U_0 \exp[-(r_i^2 + r_j^2 + r_k^2)/a^2],$$

$$V_{qqq}^{3b}(\mathbf{r}_i, \mathbf{r}_j, \mathbf{r}_k) = \frac{1}{8} d^{abc} \lambda_i^a \lambda_j^{b*} \lambda_k^{c*} U_0 \exp[-(r_i^2 + r_j^2 + r_k^2)/a^2].$$

Here r_i is the distance of the i -th quark from the center of the triangle formed by i -th, j -th and k -th quark, and similarly for r_j and r_k . λ_a are the Gell-Mann color matrices and d^{abc} are the SU(3) structure constants ($\{\lambda^a, \lambda^b\} = 2d^{abc}\lambda^c$).

The diagonal matrix elements of the color part of the three body interaction between two quarks and an antiquark are $-5/18$ and $5/9$ for $|\bar{3}_{12}3_{34}\rangle$ and $|\bar{6}_{12}\bar{6}_{34}\rangle$ color states, respectively. If the strength of this interaction U_0 is negative it will lower the states with diquark-antidiquark configuration. This can be seen on Fig. 4. The dependence of the mass of the T_{cc} tetraquark on the strength of the potential U_0 and on the smearing of this potential is shown in Fig. 3. When $a = 3$ fm and $U_0 = -20$ MeV the system is bound with the energy of -15 MeV, while as it can be seen on Fig. 4 it is unbound if we fix one of the parameters in orbital wave function. The system still possesses clustering of quarks into diquark and antiquark but the simple picture where the diquark and the antiquark form a harmonic oscillator is not accurate anymore. The effective interaction between clusters has now more complicated form. Since $d^{abc}\lambda_i^a\lambda_j^b\lambda_k^c/8$ in color singlet baryons is $10/9$ this interaction will lower the masses of the baryons for about U_0 if $a \gg 1$ fm (the size of the baryon) and less for smaller a . Since the Bhaduri potential gives ~ 10 MeV too large masses of baryons this interaction would also improve baryon spectroscopy. But we wish to keep the effect of this new interaction as small as possible, so we prefer weaker three-body force ($U_0 \sim -10$ MeV).

The main result therefore is that while T_{cc} is not bound with the Bhaduri potential we can change the situation with a modification of this potential. Just by changing the parameters (strength of confinement, masses) one can not achieve this goal since it is not possible just to reduce the mass of the tetraquark without reducing masses of mesons and thus lowering the threshold. But a weak three-body force whose color factor is zero in the asymptotic channel can lead to the binding.

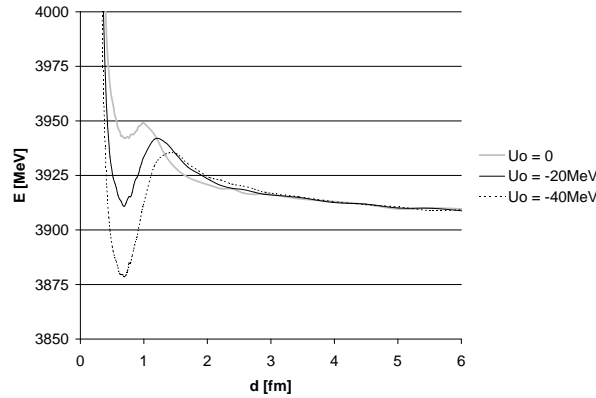


Fig. 4. The mass of T_{cc} as a function of the width between two clusters. The results of the calculations for three different strengths of the tree-body potential are shown. The smearing of this potential is $a = 3$ fm.

References

1. S.-K. Choi et al. (Belle Collaboration), hep-ex/0309032;
S.-K. Choi et al. (Belle Collaboration), hep-ex/0308029.
2. B. Aubert et al. (BABAR Collaboration) Phys. Rev.Lett. **90** (2003) 242001.
3. D.M. Brink, Fl. Stancu, Phys.Rev. D **57** (1998) 6778.
4. R.K. Bhaduri, L.E. Cohler, Y. Nogami, Nuovo Cimento A **65** (1981) 376.
5. B. Silvestre-Brac, C. Semay, Z. Phys. C **57** (1993) 273.
6. D. Janc, M. Rosina, Few-Body Systems **31** (2001) 1.
7. V. Dmitrasinovic, Phys. Lett. B **499** (2001) 135.



A simplified collective model of pion *

Borut T. Oblak

Faculty of Mathematics and Physics, University of Ljubljana, Jadranska 19, P.O. Box 2964, SI-1001 Ljubljana, Slovenia

Abstract. In order to test the accuracy of the approximate methods commonly used for the Nambu – Jona-Lasinio model we study a simpler model which can be solved exactly. We find that the Random Phase Approximation gives reasonably good results if used in combination with the Hartree ground state (vacuum). On the other hand, the Tamm-Dancoff and Hermitian Operator Methods give even better results, but for the price of requiring a better approximation of the ground state.

1 Introduction

In the Nambu – Jona-Lasinio model (NJL), the vacuum properties and the pion excitation are usually calculated using the Hartree-Fock (HF) and Random Phase Approximations (RPA). We propose a simplified version of NJL which is appropriate to test the accuracy of these approximate methods. The model preserves the main features of NJL and is simple enough to be solved exactly. For simplicity we limit ourselves to one flavour of quarks.

Since we shall deal with a finite number of quarks, it is convenient to start with the one-flavour NJL Hamiltonian written in the first-quantized form [1] and with a momentum cutoff Λ

$$\begin{aligned}
 H = & \sum_{k=1}^N (\gamma_5(k)h(k)p(k) + m_0\beta(k)) \\
 & - \frac{g}{2} \sum_{k=1}^N \sum_{\substack{l=1 \\ l \neq k}}^N \left(\beta(k)\beta(l) + (i\beta(k)\gamma_5(k)) \cdot (i\beta(l)\gamma_5(l)) \right) \cdot \\
 & \cdot \sum_{\mathbf{p}'_k}^{\Lambda} \sum_{\mathbf{p}'_l}^{\Lambda} \sum_{\mathbf{p}_k}^{\Lambda} \sum_{\mathbf{p}_l}^{\Lambda} \delta_{\mathbf{p}'_k + \mathbf{p}'_l, \mathbf{p}_k + \mathbf{p}_l} |\mathbf{p}'_k, \mathbf{p}'_l\rangle \langle \mathbf{p}_k, \mathbf{p}_l| \quad .
 \end{aligned}$$

* Outline of the Diploma Thesis presented at the University of Ljubljana (Mentor: Mitja Rosina)

2 The simple model

We made four approximations:

1. We confined quarks in a finite volume \mathcal{V} with periodic boundary conditions so that their momenta become discrete. Because the absolute values of momenta are limited, there is only a finite number of momenta available. Therefore we have only a finite number $2N$ of single-particle states occupied by a finite number N of quarks.
2. In the kinetic term of the Hamiltonian we take an average absolute value of momenta ($P = \frac{3}{4}\Lambda$) instead of their true values.
3. The interaction changes only the quark's chirality and preserves its helicity, color and momentum which then label the quark. Therefore the quarks can be treated as distinguishable and Hartree is equivalent to Hartree-Fock.
4. We include a quark selfinteraction so that the double summations can be replaced by two single summations. This contributes a trivial constant $-gN$.

The simplified Hamiltonian is:

$$H = \sum_{k=1}^N \left(\gamma_5(k) h(k) P + m_0 \beta(k) \right) - \frac{g}{2} \left(\sum_{k=1}^N \beta(k) \sum_{l=1}^N \beta(l) + \sum_{k=1}^N i\beta(k) \gamma_5(k) \sum_{l=1}^N i\beta(l) \gamma_5(l) \right) .$$

We can introduce the operators:

$$j_x = \frac{1}{2}\beta, \quad j_y = \frac{1}{2}i\beta\gamma_5, \quad j_z = \frac{1}{2}\gamma_5,$$

which obey (quasi)spin commutation relations and allow us to make full use of the angular momentum algebra.

Also separate sums over quarks with right and left helicity

$$L_\alpha = \sum_{k=1}^N \frac{1+h(k)}{2} j_\alpha(k), \quad S_\alpha = \sum_{k=1}^N \frac{1-h(k)}{2} j_\alpha(k)$$

as well as the total sum

$$J_\alpha = L_\alpha + S_\alpha = \sum_{k=1}^N j_\alpha(k)$$

obey the (quasi)spin commutation relations ($\alpha = x, y, z$).

The model Hamiltonian can then be written as

$$H = 2P(L_z - S_z) + 2m_0 J_x - 2g(J_x^2 + J_y^2) .$$

It commutes with \mathbf{L}^2 and \mathbf{S}^2 but not with L_z and S_z . Nevertheless, it is convenient to work in the basis $|L, S, L_z, S_z\rangle$. The Hamiltonian matrix elements can be

easily calculated using the angular momentum algebra. By diagonalisation we then obtain the energy spectrum of the system.

The model has three model parameters: P , m_0 and g . Instead of g we prefer to take $G = g\mathcal{V}/2$ where $\mathcal{V} = \pi^2 N/\Lambda^3$ is the normalization volume since g decreases with increasing number of quarks while G stabilizes at large N .

We want to study the simple model in a physically interesting regime. Therefore we choose the three model parameters so that we fit three observable

1. We calculate the *mass of dressed quark* ($M = 335$ MeV) from the difference between the ground state energies (E_g) of the systems of N and $N - 1$ quarks. For the momentum of quark we take the average value (P) and we obtain

$$M = \sqrt{(E_g(N) - E_g(N - 1))^2 - P^2}.$$

2. The *mass of pion* m_π should be 138 MeV. The pion corresponds to the first excited state of the system,

$$E_\pi = E_1 - E_g \Rightarrow m_\pi = \sqrt{E_\pi^2 - p_\pi^2},$$

where E_1 is the energy of the first excited state and E_π is the pion energy. We determined the effective pion momentum p_π by the requirement, that the pion behaves as a Goldstone boson in the chiral limit and that p_π does not change much when the small quark mass term is introduced:

$$p_\pi = E_1(m_0 = 0) - E_g(m_0 = 0).$$

3. Instead of the *pionic decay constant* ($f_\pi = 93$ MeV) we prefer to fit the *chiral condensate* Q which is related to f_π through the Gell-Mann – Oakes – Renner relation

$$-Q = f_\pi^2 m_\pi^2 / m_0.$$

In this way we avoid the ambiguity how to introduce f_π in a one-flavour model, as well as the ambiguities with the effective momentum of the pion in a finite volume. In our model, the chiral condensate is

$$Q = \frac{1}{\mathcal{V}} \langle g | \sum_{i=1}^N \beta_i | g \rangle = \frac{2}{\mathcal{V}} \langle g | J_x | g \rangle.$$

We compare the fitted values of model parameters for several values of N (Table 1). It is amusing that they are rather close to NJL parameters corresponding to two flavours and infinite number of quarks in the system [2].

3 Test of approximate methods – the vacuum

We compare the ground state (vacuum) energy E_g and the chiral condensate Q of the Hartree approximation with the exact solution.

The vacuum energy (Table 2) for $N=48$ and for the physically interesting value $G = 40.1$ MeV fm³ deviates only by 1.2%. The deviation decreases with

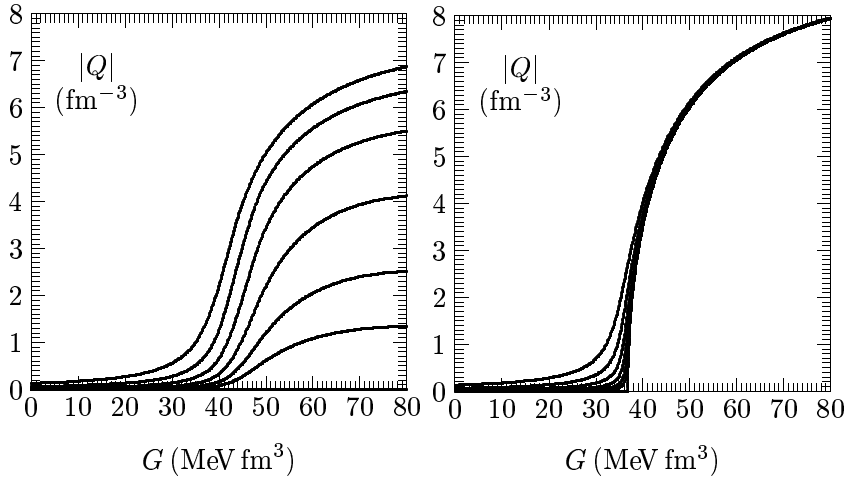
Table 1. Model parameters (above) fitted to reproduce the observables (below).

N	12	24	36	48	NJL	exper.
G (MeV fm ³)	69.9	55.9	46.5	40.1	42.2	
m ₀ (MeV)	26.0	15.9	11.8	9.6	5.5	
P (MeV)	484	557	613	659	473	
M (MeV)	335	335	335	335	335	335
m _π (MeV)	138	138	138	138	138	138
f _π (MeV)	93.0	93.0	93.0	93.0	93.0	93.0

Table 2. The energies E_g of the ground state for 48 quarks for P = 659 MeV and m₀ = 9.6 MeV and three values of G.

G (MeV fm ³)	20.0	40.1	60.0
Exact	-32058.96	-32970.80	-37028.30
Hartree	-31991.62	-32586.51	-36565.25

increasing N which hints that Hartree is a good large-N limit (we could not test it yet for large enough N). One should take some care, however, since in spite of the good agreement the Hartree ground state is still above the first (few) exact excited states in some of the studied cases.

**Fig. 1.** Dependence of absolute value of the chiral condensate on the strength of interaction for 48 particles and P = 659 MeV. From above follow the lines for m₀ = 9.6, 4.8, 2.4, 1.2, 0.6, 0.3 and 0 MeV. Exact (left) and Hartree (right) results are compared.

For a finite system we do not expect a sharp transition from the chirally symmetric to the chirally broken phase as a function of the interaction strength G. As a matter of fact, for m₀ = 0 the system remains chirally symmetric, the order parameter Q remains zero. For a small but finite explicit symmetry breaking term m₀ the system responds first with a small Q proportional to m₀. For G larger than

some critical value, however, Q starts to rise sharply (Fig.1). This is the analogue for spontaneous symmetry breaking in the case of a finite system. One expects a sharp phase transition if one makes the limit $N \rightarrow \infty$ faster than the limit $m_0 \rightarrow 0$.

On the other hand, one gets in the Hartree approximation a sharp phase transition already in the chiral limit $m_0 = 0$ and a slightly larger chiral condensate for $m_0 > 0$. This shows that the Hartree approximation strongly exaggerates the chiral symmetry breaking and in this way immitates the situation at $N \rightarrow \infty$ even at smaller N .

4 Test of approximate methods – π and σ mesons.

The first excited state (negative parity) corresponds to pion and the second excited state (positive parity) corresponds to sigma meson. As approximate methods we study several *particle-hole methods* in which the ground state is excited by a one-body (“particle-hole”) excitation operator.

In our case the low-lying states are symmetric under permutation of quark labels. Therefore the one-body excitation operators can be expressed as combination of quasispin operators $L_x, S_x, iL_y, iS_y, L_z$ and S_z which we denote jointly by $B_i, i = 1, \dots, 6$. Then we expand the excited states in the basis $|i\rangle$

$$|\text{exc}\rangle = \sum_i c_i |i\rangle, \quad |i\rangle = B_i^\dagger |g\rangle.$$

The calculation is formulated in terms of a secular equation for the excitation energy ω and expansion coefficients c_i

$$\underline{\mathcal{H}} \underline{c} = \omega \underline{\mathcal{N}} \underline{c}.$$

Different approximate methods differ in the proposition for the hamiltonian and overlap matrices

1. In the *Tamm-Dancoff method* (TD) the basis $|i\rangle$ is taken literally and one obtains

$$\begin{aligned} \mathcal{H}_{j i} &= \langle j | (H - E_g) | i \rangle = \langle g | B_j (H - E_g) B_i^\dagger | g \rangle \quad \text{and} \\ \mathcal{N}_{j i} &= \langle j | i \rangle = \langle g | B_j B_i^\dagger | g \rangle. \end{aligned}$$

2. The *Hermitian Operator Method* (HOM) [3] is an approximation to TD which restricts the excitation operator to be either hermitian or antihermitian and relies on $|g\rangle$ being an exact ground state. This simplifies the evaluation of the matrix elements, but it makes a restriction to a smaller model space by decoupling the spaces generated by real hermitian (L_x, S_x, L_z and S_z) and real antihermitian (iL_y and iS_y) operators.

$$\begin{aligned} \mathcal{H}_{j i} &= \frac{1}{2} \langle g | [B_j, [H, B_i^\dagger]] | g \rangle \quad \text{and} \\ \mathcal{N}_{j i} &= \begin{cases} \langle j | i \rangle &= \langle g | B_j B_i^\dagger | g \rangle \\ 0 & \end{cases}, \end{aligned}$$

where the upper line in $\mathcal{N}_{j,i}$ applies if B_i and B_j^\dagger are both hermitian or both antihermitian and the lower line (0) otherwise.

3. The *Simple Operator Method* (SOM) is even a more restrictive approximation to TD, it chooses only one of the listed one-body operators, iJ_y . Its success in the description of the pion is based on the observation that such state is very close to the pionic excitation: $\langle \pi | iJ_y | g \rangle / \sqrt{\langle g | J_y^2 | g \rangle} = 0.990$ (for $N = 48$). It is even useful to calculate the two-pion excitation $|2\pi\rangle = -J_y^2 |g\rangle - \langle g | -J_y^2 | g \rangle |g\rangle$.
4. In the *Random Phase Approximation* one makes a risky but often successful assumption that there exists an excitation operator $A^\dagger = \sum_i c_i B_i^\dagger$ whose adjoint kills the ground state

$$A^\dagger |g\rangle = |\text{exc}\rangle, \quad A |g\rangle = 0.$$

The inspiration comes from the creation and annihilation operators of the harmonic oscillator and it is a promising approximation when one observes harmonic vibrational spectra. One then gets

$$\begin{aligned} \mathcal{H}_{j,i} &= \langle g | [B_j, [H, B_i^\dagger]] | g \rangle \quad \text{and} \\ \mathcal{N}_{j,i} &= \langle g | [B_j, B_i^\dagger] | g \rangle. \end{aligned}$$

5 Conclusion

We found that although the Hartree ground state energy differs from the exact ground state energy only by a small percentage for realistic model parameters, the energy difference between the Hartree and the exact ground state is comparable to the energy differences between the lowest exact excited states and the exact ground state. In spite of this, the Random Phase Approximation (RPA) gives a rather good approximation of the pion energy if used with the Hartree ground state (Table 3); as a matter of fact, it gives better results when used with the Hartree ground state than when used with the exact ground state. The condition $A|g\rangle = 0$ for a one-body operator A is namely better fulfilled in the case of the Hartree ground state than in the case of the exact ground state. On the other hand, the Hermitian Operator Method (HOM), the Simple Operator Method (SOM) and the Tamm-Dancoff (TD) method fail for the Hartree ground state, but give very good results when used with the exact ground state.

Acknowledgement. Part of this work has been done at the *Jožef Stefan Institute* within the Research Programme PO517 financed by the Ministry of Education, Science and Sport of Slovenia.

Table 3. Exact excitation energies compared to several approximate methods for 48 quarks, $P = 659$ MeV and $m_0 = 9.6$ MeV and three values of G .

G (MeV fm ³)		20.0		40.1		60.0	
	state	ω (MeV)	parity	ω (MeV)	parity	ω (MeV)	parity
exact solutions							
		1870.76	1.00	879.21	1.00	947.76	-1.00
		1870.76	-1.00	788.36	-1.00	647.98	1.00
		1848.51	1.00	788.33	1.00	579.88	-1.00
	$ \sigma\rangle$	916.91	1.00	365.20	1.00	401.18	1.00
	$ \pi\rangle$	916.46	-1.00	319.65	-1.00	214.59	-1.00
	$ g\rangle$	0.00	1.00	0.00	1.00	0.00	1.00
approximations of low-lying states computed from the exact ground state							
RPA	$ \sigma\rangle$	917.06	1.00	538.36	1.00	1630.42	1.00
	$ \pi\rangle$	916.59	-1.00	423.80	-1.00	591.55	-1.00
TD	$ \sigma\rangle$	917.00	1.00	423.54	1.00	1365.81	1.00
	$ \pi\rangle$	916.53	-1.00	337.51	-1.00	246.99	-1.00
	$ g\rangle$	0.48	1.00	4.74	1.00	9.01	1.00
HOM	$ \sigma\rangle$	916.96	1.00	413.93	1.00	1223.81	1.00
	$ \pi\rangle$	916.49	-1.00	333.98	-1.00	243.37	-1.00
	$ g\rangle$	0.48	1.00	4.76	1.00	9.07	1.00
SOM	$ 2\pi\rangle$	1859.35	1.00	843.56	1.00	609.14	1.00
	$ \pi\rangle$	916.49	-1.00	333.98	-1.00	243.37	-1.00
approximations of low-lying states computed from the Hartree ground state							
RPA	$ \sigma\rangle$	908.25	1.00	656.92	1.00	1691.41	1.00
	$ \pi\rangle$	907.75	-1.00	260.35	-1.00	229.05	-1.00
TD	$ \sigma\rangle$	976.01	1.00	886.01	1.00	1744.26	1.00
	$ \pi\rangle$	975.67	-1.00	760.63	-1.00	1083.67	-1.00
	$ g\rangle$	0.00	1.00	0.00	1.00	0.00	1.00
HOM	$ \sigma\rangle$	975.70	-0.01	763.78	0.11	1881.07	-0.34
	$ \pi\rangle$	773.19	0.55	584.56	0.40	1097.31	0.00
	$ g\rangle$	0.00	1.00	0.00	1.00	0.00	1.00
SOM	$ 2\pi\rangle$	1965.87	1.00	1540.17	1.00	2156.63	1.00
	$ \pi\rangle$	975.67	-1.00	760.63	-1.00	1083.67	-1.00

References

1. J. da Providência, M. C. Ruivo and C. A. de Sousa, Phys. Rev. D **36**, 1882 (1987).
2. M. Fiolhais, J. da Providência, M. Rosina and C. A. de Sousa, Phys. Rev. C **56**, 3311 (1997).
3. M. Bouten, P. van Leuven, M. V. Mihailović and M. Rosina, Nucl. Phys. **A202**, 127 (1973).



Is the $cc\bar{u}\bar{d}$ tetraquark bound? *

M. Rosina^{a,b} and D. Janc^b

^aFaculty of Mathematics and Physics, University of Ljubljana, Jadranska 19, P.O. Box 2964, 1001 Ljubljana, Slovenia

^bJ. Stefan Institute, 1000 Ljubljana, Slovenia

Abstract. The lightest $cc\bar{u}\bar{d}$ tetraquark ($J^P=01^+$) is supposed to be above the DD^* threshold. We show, however, that it is possible to stretch the quark model parameters so that it might get bound.

1 Introduction

In previous Bled Workshop we were very enthusiastic about the $bb\bar{u}\bar{d}$ tetraquark which according to our [1–4] and other [5,6] estimates should be bound by about 100 MeV with respect to the BB^* threshold. We strongly advertised to preparation for its search, possibly at LHC. However, our estimate of its production rate at LHC [3,4] is only about 5 events/hour, and its decay is not very characteristic.

This year, we turned our attention to the $cc\bar{u}\bar{d}$ tetraquark, in spite of our pessimistic estimates [1,2] that it is not bound. The motivation is threefold.

- It would be *more abundant*, possibly 10^4 events/hour if the same mechanism applies as for the bb -tetraquark [3,4,7], namely a double gluon fusion in two $c\bar{c}$ pairs so that the two charm quarks join in a cc -diquark which gets later dressed with two light antiquarks.
- It might be *easier to detect*, for example by $cc\bar{u}\bar{d} \rightarrow D^+ + K^- + \pi^+$ (in analogy with the SELEX ccd signal [8] $ccd \rightarrow \Lambda_c^+ + K^- + \pi^+$).
- If it exists its discovery would be *more revolutionary*. We would have to modify the effective quark-quark interaction, and/or introduce many-quark forces.

2 Mechanisms for stronger binding

It is difficult to stretch the parameters in the OGE+linear confinement so as to bind cc -meson without spoiling the fit to mesons and baryons. At first sight it seems that smaller quark masses could do the job if the $V_{QQ} = \frac{1}{2}V_{Q\bar{Q}}$ rule applies. In this case it has been shown [1] that the diquark binding energy is $E_{cc}(m_{\text{red}}) = \frac{1}{2}E_{c\bar{c}}(m_{\text{red}}/2)$. For Bhaduri masses, half of reduced mass of the cc diquark ($m_c/4 = 467$ MeV) coincides with the reduced mass of D_s , $m_c m_s / (m_c + m_s) = 454$ MeV so

* Talk delivered by M. Rosina

that $E_{cc} = \frac{1}{2}E_{c\bar{s}}$. If we decrease all quark masses by 200 MeV, the reduced mass of D_s would decrease by 132 MeV and $m_c/4$ only by 50 MeV. Higher reduced mass of cc compared to D_s means better binding of cc (by about 40 MeV). However, this would spoil the spectra of single mesons.

A three-body interaction of the type

$$V_{qq\bar{q}}(\mathbf{r}_i, \mathbf{r}_j, \mathbf{r}_k) = -\frac{1}{8}d^{abc}\lambda_i^a\lambda_j^b\lambda_k^{c*}U_0 \exp(-(\mathbf{r}_i^2 + \mathbf{r}_j^2 + \mathbf{r}_k^2)/a^2)$$

with $U_0 < 20$ MeV and $a > 2.3$ fm would bind. Due to the combinatorics, a three-body interaction is more effective for tetraquarks than for baryons and the proposed one spoils baryons only by about 10 MeV. Details are presented in the talk of Damijan Janc (these Proceedings).

The $cc\bar{u}\bar{d} = DD^*$ offers a coulomb-like long-range force because the exchanged pion is almost on the mass shell [9]: ($D^* \rightarrow D + \pi$), ($D + \pi \rightarrow D^*$). (Note that $m_{D^{*+}} - m_{D^+} - m_{\pi^0} = 5.6$ MeV, $m_{D^{*0}} - m_{D^0} - m_{\pi^0} = 7.1$ MeV, $m_{D^{*+}} - m_{D^0} - m_{\pi^+} = 5.8$ MeV.)

Assuming Coulomb binding similar to that in the hydrogen atom, but with $g \approx 0.6$, (" α " = $g^2/4\pi \approx 1/35$) we get a loose system bound by only $E = -\frac{1}{2}\frac{m}{2}\frac{1}{35^2} = -0.4$ MeV. However, this effect might help in the asymptotic channel.

3 Important information will come from double-charm baryons

Recent SELEX experiments and analyses [8] gave some more and some less convincing signals about the ccu (3460 and 3541) and ccd (3443 and 3520) baryons.

We first show that the more established ccd resonance at 3520 MeV is consistent with our phenomenological expectations if it is the ground state. Then we discuss the dramatic deviation from our expectations if the other three resonances are confirmed so that the ground state is at 3450 MeV (the isodoublet average) and the isodoublet average 3530 would then be the excited state of the double-charm baryon.

A phenomenological estimate following the same lines as we have used for the $cc\bar{u}\bar{d}$ tetraquark [1–3] gives for $s=1/2$ (assuming an $S=1$ cc -diquark) the value

$$m_{ccq} = \frac{1}{2}m_{J/\psi} + E_{cc} - \frac{1}{2}E_{c\bar{c}} + \frac{3}{4}m_D + \frac{1}{4}m_{D^*} = 3584 \text{ MeV}$$

Here we have imitated the ccq baryon by a $\bar{c}q$ meson and estimated the cc binding energy to be [1] $E_{cc} - \frac{1}{2}E_{c\bar{c}} = 134$ MeV. We also took the appropriate averages of the spin-spin interaction. Actually, the cc -dimeson has a mass inbetween the \bar{c} and \bar{b} masses and the ccq mass could be as low as

$$\begin{aligned} m_{ccq} &= \frac{1}{2}m_{J/\psi} + E_{cc} - \frac{1}{2}E_{c\bar{c}} + m_c - m_b \\ &+ \frac{1}{4}m_B + \frac{3}{4}m_{B^*} - \frac{1}{2}(m_{D^*} - m_D) = 3535 \text{ MeV} \end{aligned}$$

or inbetween both values.

The predicted spin 3/2 state lies higher by $m_{\text{ccq}(3/2)} - m_{\text{ccq}(1/2)} = \frac{3}{4}(m_{D^*} - m_D) = 106 \text{ MeV}$. Such spin-spin splitting is noticeably larger than the difference 80 MeV between the 3530 and 3450 MeV SELEX levels and it will be some surprise if the 3450 level is confirmed as a ground state and the 3530 level gets an 3/2 assignment. The surprise would be even more evident in the need for a major revision of quark model parameters in order to obtain the ccq ground state as low as 3450 MeV.

Then follows a phenomenological estimate for the cc-dimeson. If the 3530 level is the ground state

$$\begin{aligned} \Delta E_{\text{cc}\bar{u}\bar{d}} &= m_{\text{ccu}} - \left(\frac{3}{4}m_D + \frac{1}{4}m_{D^*} \right) \\ &+ m_{\Lambda_c} - m_D - m_{D^*} = +38 \text{ MeV} \end{aligned}$$

or, alternatively

$$\begin{aligned} \Delta E_{\text{cc}\bar{u}\bar{d}} &= m_{\text{ccu}} - \left(\frac{1}{4}m_B + \frac{3}{4}m_{B^*} \right) \\ &+ \frac{1}{2}(m_{D^*} - m_D) + m_{\Lambda_b} - m_D - m_{D^*} = +35 \text{ MeV} \end{aligned}$$

If, however, the 3450 level is confirmed as the ground state, the corresponding estimates would give -42 (or - 45) MeV binding ! Such confirmation would strongly encourage the search for the cc-tetraquark.

4 Conclusion

There are several subtle effects each of which separately is not likely to bind the cc $\bar{u}\bar{d}$ tetraquark with respect to the DD* threshold. However, their cooperative effect might just bind it or just fail to bind it. We emphasise the importance of the search for the cc $\bar{u}\bar{d}$ tetraquark as a crucial experiment.

References

1. D. Janc and M. Rosina, *Few-Body Systems* **31**, 1 (2001).
2. D. Janc and M. Rosina, *Bled Workshops in Physics* **1**, No.1, 90 (2000).
3. M. Rosina, D. Janc, D. Treleani, and A Del Fabbro, *Bled Workshops in Physics* **3**, No.3, 63 (2002).
4. D. Janc, M. Rosina, D. Treleani, and A. Del Fabbro, *Few-Body Systems Suppl.* **14** (2003) 25.
5. B. Silvestre-Brac and C. Semay, *Z. Phys.* **C57**, 273 (1993).
6. D. M. Brink and Fl. Stancu, *Phys. Rev.* **D57**, 6778 (1998).
7. A. Del Fabbro and D. Treleani, *Phys. Rev.* **D61**, 077502 (2000); *Phys. Rev.* **D63**, 057901 (2001); *Nucl. Phys. B* **92**, 130 (2001).
8. M. Mattson et al. (SELEX Collaboration), *Phys. Rev. Lett.* **89**, 112001 (2002); J. S. Russ (on behalf of the SELEX Collaboration), hep-ex/0209075
9. J-M. Richard, *Double Charm Physics*, hep-ph/0212224 (2002).



Structure of the nucleon and the Δ from pion electro-production experiments at MAMI

S. Širca^{a,b}

^aFaculty of Mathematics and Physics, University of Ljubljana, 1000 Ljubljana, Slovenia

^bJožef Stefan Institute, 1000 Ljubljana, Slovenia

Abstract. Recent pion electro-production experiments of the A1 Collaboration at MAMI are presented. The threshold data in the $p(e, e'p)\pi^0$ and $d(e, e'd)\pi^0$ channels reveal the chiral dynamics of the pion-nucleon system at low energies. Measurements of the neutral channel in the Δ region address the issue of nucleon and/or Δ deformation and of the pion cloud, while the $p(e, e'\pi^+)n$ channel gives access to the axial structure of the nucleon.

1 Introduction

Electro-production of neutral or charged pions off nucleons close to the pion production threshold is an important tool to explore the structure of protons and neutrons at low energies. The s - and p -wave partial amplitudes in the $p\pi^0$ channel are bench-mark tests for predictions of the Chiral Perturbation Theory (ChiPT) which is believed to be a good low-energy approximation to QCD involving nucleon and pion degrees of freedom. Its validity can also be examined in the $n\pi^+$ channel which offers a possibility to extract the axial and induced pseudo-scalar form-factors of the proton. The threshold coherent π^0 production on the deuteron, used as an effective neutron target, is a sensitive probe of the chiral dynamics of the pion-neutron system. Experiments in the region of the Δ resonance probe the multipole structure of the $N \rightarrow \Delta$ transition by isolating interferences of small quadrupole transition amplitudes with the dominant magnetic dipole amplitude, and provide a quantitative measure for the deformation of the nucleon and/or the Δ . In addition, many observables in the $N \rightarrow \Delta$ transition exhibit large sensitivities to the effects of the pion cloud.

2 Testing ChiPT with $p(e, e'p)\pi^0$ and $d(e, e'd)\pi^0$ reactions

2.1 The proton

The first photo-production measurements $p(\gamma, p)\pi^0$ at threshold were designed to access the s -wave electric dipole amplitude E_{0+} [1] and thereby test the early low-energy theorems [2]. The severe disagreement between these theorems and the experiments was subsequently resolved by refined calculations in ChiPT [3], which also gave predictions for the p -wave multipole combinations P_i . Soon experimental work at MAMI extended to electro-production in order to study the

evolution of low-energy theorems of ChiPT [6]. In the first Mainz experiment at $Q^2 = 0.1 \text{ (GeV/c)}^2$, the s -wave amplitudes E_{0+} and L_{0+} were extracted by using *calculated* p -waves. In the transverse, longitudinal, and the interference terms in the cross-section, which can be decomposed by measuring the complete distributions in the azimuthal angle, the p -waves appear in specific combinations,

$$\begin{aligned} P_1 &= 3E_{1+} + M_{1+} - M_{1-} , \\ P_2 &= 3E_{1+} - M_{1+} + M_{1-} , \\ P_3 &= 2M_{1+} + M_{1-} , \\ P_4 &= 4L_{1+} + L_{1-} , \\ P_5 &= L_{1-} - 2L_{1+} . \end{aligned}$$

All multipoles are functions of the pion energy and of Q^2 . Neglecting multipoles with $l \geq 2$, the structure functions can be expressed in terms of the multipoles as follows:

$$\begin{aligned} R_T &= |E_{0+} + P_1 \cos \theta|^2 + \frac{1}{2} (|P_2|^2 + |P_3|^2) \sin^2 \theta , \\ R_L &= |L_{0+} + P_4 \cos \theta|^2 + |P_5|^2 \sin^2 \theta , \\ R_{TL} &= -\sin \theta \operatorname{Re} [(E_{0+} + P_1 \cos \theta) P_5^* + (L_{0+} + P_4 \cos \theta) P_2^*] , \\ R_{TT} &= \frac{1}{2} (|P_2|^2 - |P_3|^2) \sin^2 \theta , \end{aligned} \quad (1)$$

where θ is the pion centre-of-mass angle.

For the experiment at $Q^2 = 0.1 \text{ (GeV/c)}^2$, the predictions for P_i were considered to be reliable because the one-pion-loop contributions are much smaller than those of the tree diagrams, contrary to the s -wave amplitudes E_{0+} and L_{0+} which pick up large pion-loop corrections even at threshold and at $Q^2 \rightarrow 0$. The low-energy parameters of ChiPT were fitted to the partial cross-sections of [5], and the photo-production data, the electro-production data, and the theory seemed consistent. However, the value of Q^2 was believed to be too high for the convergence of ChiPT.

Therefore, another experiment at $Q^2 = 0.05 \text{ (GeV/c)}^2$ was recently performed at MAMI [7], in which a model-independent extraction of the multipoles was attempted. Because the transverse-transverse interference term in the cross-section (1) was consistent with zero within the experimental uncertainty, only the s -wave multipoles and the combinations P_1 , P_4 , P_5 were extracted, while the P_2 and P_3 terms could not be separated: only their combination $P_{23} = \frac{1}{2} (|P_2|^2 + |P_3|^2)$ could be determined. The experiment showed large discrepancies with respect to the calculations. For example, the measured Q^2 -dependence of the total cross-section, which is dominated by systematical uncertainties, strongly deviates from the prediction of ChiPT (see Fig. 1). Furthermore, there are large discrepancies between ChiPT and the MAID model [8]. Similar large disagreements were observed in the differential (and partial) cross-sections. While the resolution of the experiment was not good enough to perform a complete separation of the multipoles, it seems that the deviation is hidden in the P_{23} term which is constrained by photo-production and is not free to be re-adjusted to fit the new data set.

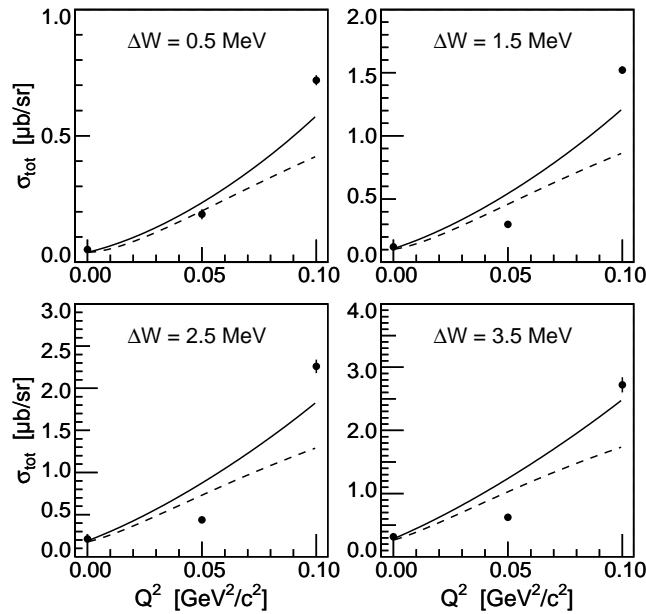


Fig. 1. The Q^2 -dependence of the total cross-section for $p(e, e' p)\pi^0$ at four energies above threshold ΔW , at the virtual photon polarisation of $\varepsilon = 0.8$. The solid (dashed) curves are the prediction of ChiPT (MAID).

Since the discrepancy is large and seems to persist, this subject urgently needs further investigation. An experiment is planned at MAMI to scan the pertinent Q^2 -region. Parts of the experimental programme have been performed in the Spring of 2003. An independent experiment, using the large-acceptance spectrometer BigBite, is being prepared at JLab [9] with extended kinematical coverage up to 20 MeV above threshold.

2.2 The deuteron

In the absence of free neutron targets, coherent π^0 electro-production from the deuteron has proven to be a promising way to obtain information on the electro-production amplitude off a free neutron. In the impulse approximation, the full production amplitude is a coherent isoscalar sum of the free proton and neutron amplitudes. The nuclear binding effects are typically accounted for by means of deuteron form-factors. Interpreted in terms of ChiPT, the $d(e, e' d)\pi^0$ process establishes a connection to the pion-nucleon chiral dynamics in the proton channel: once the low-energy constants of ChiPT are optimally adjusted to describe the pion photo- and electro-production data sets on the proton, the measured deuteron threshold s -wave amplitudes E_d and L_d (analogs of E_{0+} and L_{0+} of the proton case) can be used to extract the predictions for the neutron amplitudes without introducing new or readjusting old low-energy parameters.

A cross-section measurement with real photons was performed at SAL, using coincidence detection of the π^0 -decay photons in the IGLOO detector [10]. Since the missing-mass resolution was insufficient to separate the coherent channel from the deuteron breakup, the breakup contribution was subtracted by using a model, yielding $E_d = (-1.45 \pm 0.09) \times 10^{-3}/m_\pi$. This value is about 20% below the prediction of ChiPT, $E_d = (-1.8 \pm 0.6) \times 10^{-3}/m_\pi$ [11], but it is within the error bars.

The first experiment at finite Q^2 and close to threshold was recently performed at MAMI [12]. In this experiment, a magnetic spectrometer was used to detect the deuterons, thereby cleanly separating the coherent from the breakup channel. However, the detection of the low-energy deuterons suffering from large energy loss and multiple scattering, limited the Q^2 range to 0.1 (GeV/c)^2 . The complete centre-of-mass solid angle was covered up to 4 MeV above threshold, and a Rosenbluth separation was performed. We extracted a value of $|L_d| = (0.50 \pm 0.11) \cdot 10^{-3}/m_\pi$ for the longitudinal s -wave amplitude at threshold, and an upper limit of $|E_d| \leq 0.42 \cdot 10^{-3}/m_\pi$. The results are shown in Fig. 2.

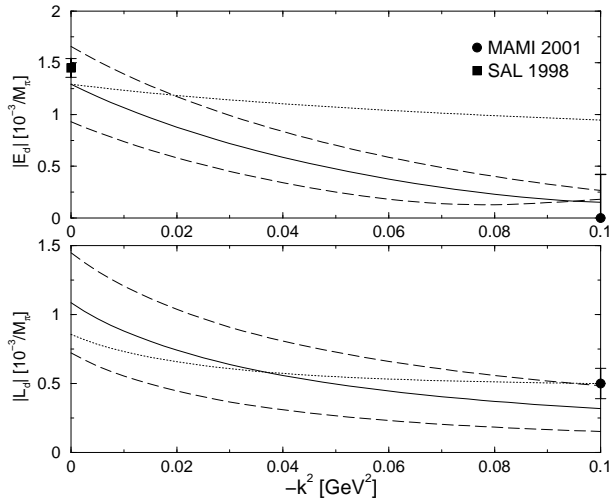


Fig. 2. The Q^2 -dependence of the threshold s -wave multipoles E_d and L_d for $d(e, e'd)\pi^0$. The solid (dotted) curves represent fits 2 (1) of ChiPT (see [13] for details). The band between the dashed lines centered around fit 2 corresponds to a variation of the single-scattering amplitudes $E_{0+}^{(n)}$ and $L_{0+}^{(n)}$ by $\pm 1 \cdot 10^{-3}/m_\pi$.

The calculation of the threshold amplitude within ChiPT [13] showed that in order to understand the present data set, it is necessary to calculate the single-scattering (nucleon) amplitudes and three-body interactions in a consistent chiral scheme. A similar conclusion was reached in Ref. [14]. Since in the charged channel, the E_{0+} amplitude exceeds the one in the neutral channel by an order of magnitude (typically $|E_{0+}(n\pi^+)| \approx 20 |E_{0+}(p\pi^0)|$), strong rescattering effects (involving pion loops) are anticipated, as illustrated in Fig. 3.

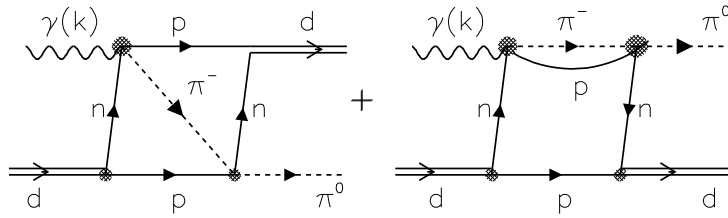


Fig. 3. Rescattering mechanisms in the $d(e, e'd)\pi^0$ process. (Figure adopted from [14].)

Considerations of rescattering effects in Ref. [14] show that it is most crucial to ensure proper anti-symmetrisation in the intermediate state, to apply correctly parity and angular momentum conservation, and to prevent double-counting. It was shown that rescattering effects cancel out, indicating that indeed the coherent π^0 production off the deuteron is a good way to access the elementary neutron amplitude. One of the observations supporting this conclusion is that also the unitary cusp observed in the $p\pi^0$ channel at the π^+ threshold disappears. However, the calculations in the framework of ChiPT also demonstrate that the p-wave multipoles are substantial and that the amplitudes possess a more complex momentum dependence than postulated in the original data analysis. Thus, even though consistency between data and theory seems to have been achieved (within the relatively large systematic uncertainties), more precise measurements at lower Q^2 would be beneficial to test these concepts accurately.

3 Nucleon axial and induced pseudo-scalar form-factors

Close to threshold, the transverse and longitudinal cross-sections for $p(e, e'\pi^+)n$ in parallel kinematics depend predominantly on the electric (E_{0+}) and the longitudinal (L_{0+}) multipoles, respectively. The E_{0+} amplitude is sensitive to the axial form-factor G_A , while the L_{0+} amplitude depends on the pion charge form-factor F_π and the induced pseudo-scalar form-factor G_P . Rosenbluth separations of the transverse and longitudinal cross-sections were performed in recent experiments at MAMI at an invariant mass of $W = 1125$ MeV and several values of Q^2 (see Fig. 4 for kinematics coverage).

For the transverse cross-section, the s-wave dominance is known to persist to relatively high energies above the threshold. Thus the axial mass parameter M_A (a cut-off in the dipole parameterisation of G_A) has been extracted from the Q^2 -dependence of transverse cross-section by using an effective Lagrangian model [15] in which G_A was the only adjustable form-factor while the electro-magnetic form-factors were assumed to be well-known.

One of the key difficulties in this extraction which directly translates into the variation in M_A is the value of the transverse cross-section in the real-photon limit. This value needs to be determined by extrapolation of angular distributions for photo-production $p(\gamma, \pi^+)n$ to zero, a procedure with a large systematical uncertainty (see Fig. 5).

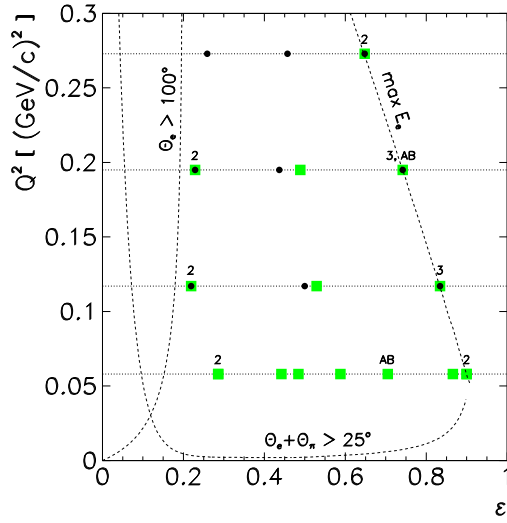


Fig. 4. Kinematics coverage for the Rosenbluth separations in the $p(e, e' \pi^+)n$ channel at $W = 1125 \text{ MeV}/c$. Circles: published data [15]; squares: recently acquired data. The symbols '2' and '3' denote measurements repeated in different time periods, while 'AB' indicates spectrometer swaps which were performed to control systematics.

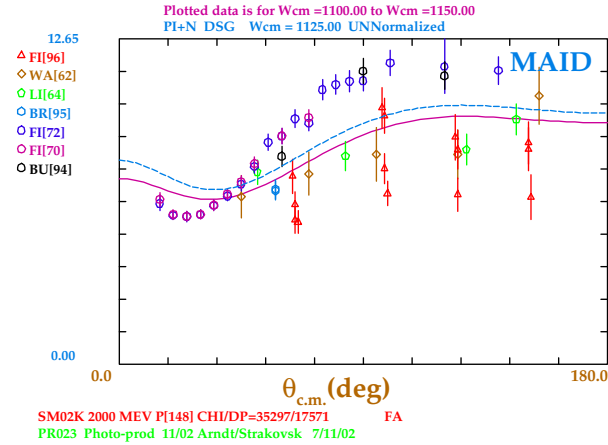


Fig. 5. Extrapolation of the photo-production angular distributions to zero in order to obtain the transverse cross-section at $Q^2 = 0$. The results of a partial-wave analysis SAID (full curve) and the Mainz Unitary Isobar Model MAID (dashed curve) are shown.

We have used a weighted-average cross-section at the photon point of $(7.22 \pm 0.36) \mu\text{b}/\text{sr}$ (The corresponding value of $E_{0^+}(n\pi^+)$ is also well supported by the studies of the GDH sum rule and by the low-energy (Kroll-Ruderman) limit.) The extracted value of $M_A = (1.077 \pm 0.039) \text{ GeV}$ is $(0.051 \pm 0.044) \text{ GeV}$ larger than the axial mass $M_A = (1.026 \pm 0.021) \text{ GeV}$ known from neutrino scattering

experiments. This ‘axial mass discrepancy’ is consistent with the prediction of ChiPT [16] which originates in pion-loop corrections to the electro-production process exemplified in Fig. 6.

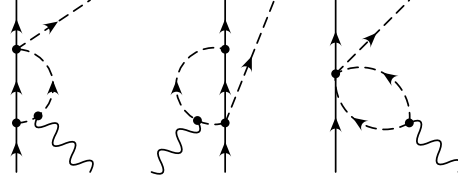


Fig. 6. Pion-loop corrections to the $p(e, e' \pi^+)n$ process which induce a modification of M_A . (Figure adopted from [16].)

Unfortunately, the kinematics range of the presently acquired data was too high for a direct application of the ChiPT result. The model-dependent terms, especially in the L_{0+} multipole, are of a size which does not allow to distinguish the pion form-factor from the induced pseudo-scalar form-factor. Even closer to threshold, however, also the longitudinal cross-section will be dominated by the s -wave, and we shall have

$$E_{0+}(q^2) = \frac{c}{\sqrt{2}f_\pi} \left[G_A(q^2) + \frac{q^2}{4M^2} G_A(0)G_M^v(q^2) + \dots \right],$$

$$L_{0+}(q^2) = c \left[D(t) - 2MG_A(0) \right] \frac{\omega F_\pi(k_\pi^2)}{\sqrt{2}m_\pi f_\pi (2M + m_\pi)} + \frac{\omega}{m_\pi} E_{0+}(m_\pi^2).$$

Here the divergence form-factor

$$D(t) = \frac{2f_\pi g_{\pi NN} m_\pi^2}{m_\pi^2 - t} + 2 \left[MG_A(0) - f_\pi g_{\pi NN} \right] \frac{\lambda^2}{\lambda^2 - t}$$

measures the deviation of the induced pseudo-scalar form-factor G_P from its pion-pole dominance ($1/(m_\pi^2 - t)$) form. This allows one, by fitting λ to the data, a simultaneous extraction of G_A and G_P . To access very low Q^2 and pion momenta in the vicinity of the threshold, a dedicated short-orbit spectrometer is being commissioned in Mainz, and is expected to take data soon [17].

4 The $N \rightarrow \Delta$ transition

One of the main goals of the $N \rightarrow \Delta$ experiments is to measure the Q^2 -dependence of the transition amplitudes. The non-vanishing electric (E2) and Coulomb (C2) quadrupole amplitudes, which are much smaller than the leading magnetic dipole amplitude (M1), are an indication that the nucleon and/or the Δ deviate from spherical symmetry. Several mechanisms have been proposed to explain the nature of this deviation. In models involving explicit pion degrees of freedom, relatively large contributions to M1 and dominant contributions to E2 and

C2 originate in the coupling of the virtual photon to the p-wave pion field. The motivation behind the recent $N \rightarrow \Delta$ program at MAMI is to map out the M1, E2, and C2 multipoles in the region of low Q^2 where the pion-cloud effects are expected to play the most important role.

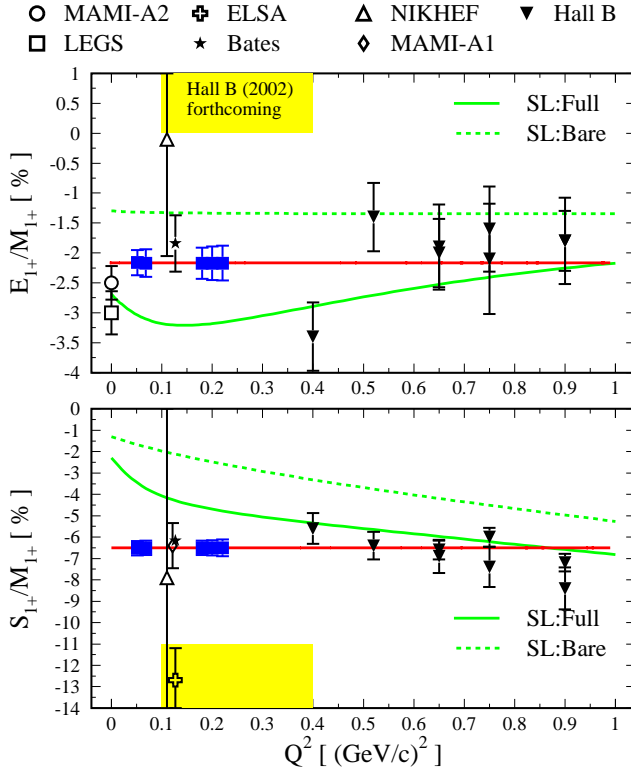


Fig. 7. Recent experimental data on the E2/M1 and C2/M1 ratios compared to the predictions of the model of Sato and Lee [18] (dashed curves: bare nucleon, full curves: including pion cloud) and MAID [8] (constant values of -2.2% and -6.5% , respectively). The anticipated MAMI data (taken in the Spring of 2003) are shown with full squares.

The small quadrupole amplitudes E2 and C2 can be accessed through specific terms in the cross-section which contain interferences of the electro-production multipoles E_{1+} and S_{1+} with the dominant M_{1+} :

$$\begin{aligned} \sigma_{0\pi}(\theta_\pi^*) &= \sigma_0(\theta_\pi^*) + \sigma_{\text{TT}}(\theta_\pi^*) - \sigma_0(180^\circ) \\ &\sim 2(\cos\theta_\pi^* + 1) \text{Re}[E_{0+}^* M_{1+}] - 12 \sin^2\theta_\pi^* \text{Re}[E_{1+}^* M_{1+}], \\ \sigma_{\text{LT}}(\theta_\pi^*) &\sim \sin\theta_\pi^* \text{Re}[S_{0+}^* M_{1+}] - 6 \cos\theta_\pi^* \sin\theta_\pi^* \text{Re}[S_{1+}^* M_{1+}], \\ \sigma_{\text{LT}'}(\theta_\pi^*) &\sim -\sin\theta_\pi^* \text{Im}[(-6 \cos\theta_\pi^* S_{1+} + S_{0+})^* M_{1+}], \end{aligned}$$

where θ_π^* is the emission angle of the pion in the centre-of-mass frame of the πN system and $\sigma_0 = \sigma_T + \varepsilon\sigma_L$. The $\sigma_{0\pi}$ and σ_{LT} terms exhibit large sensitivities to the $E2/M1 \sim \text{Re}[E_{1+}^* M_{1+}]$ and the $C2/M1 \sim \text{Re}[S_{1+}^* M_{1+}]$ ratios, respectively, while the $\sigma_{LT'}$ is sensitive to the imaginary part of the $S_{1+}^* M_{1+}$ interference.

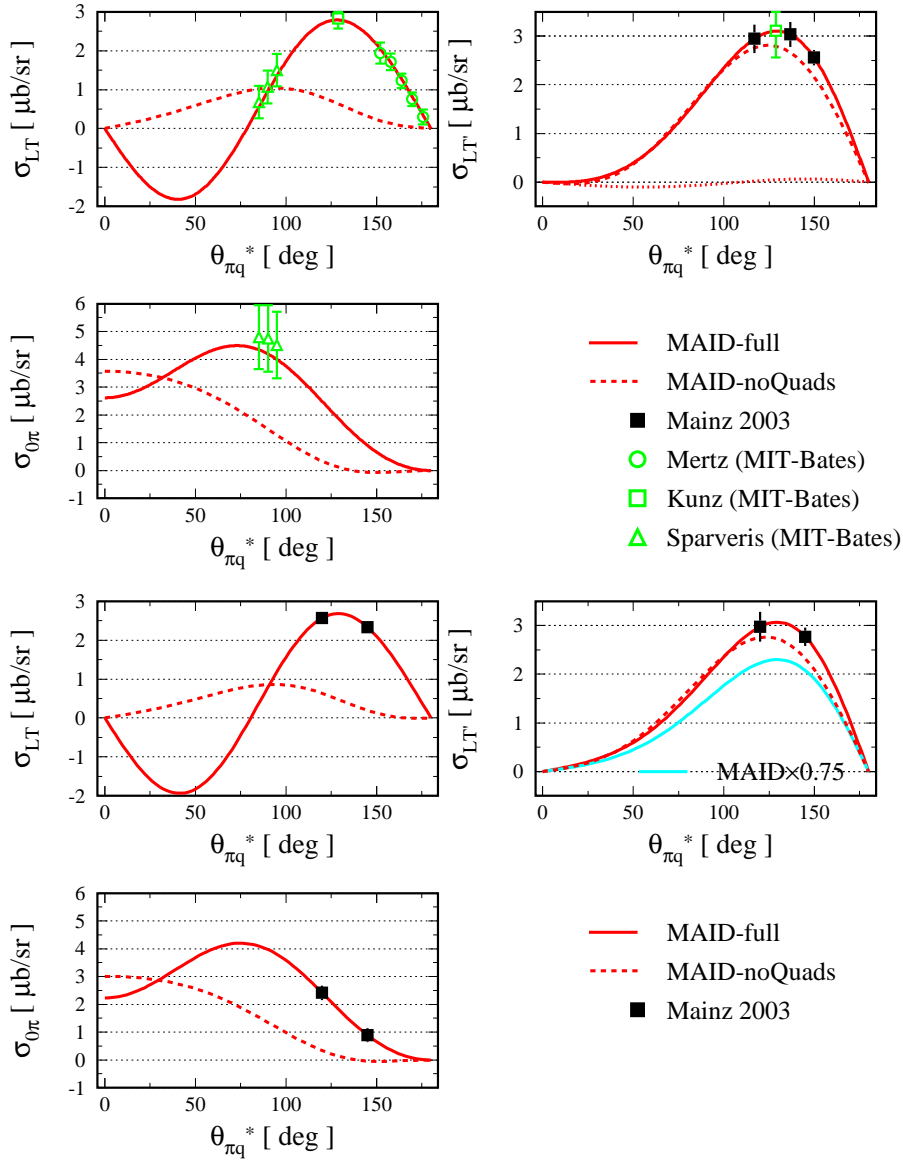


Fig. 8. Angular distributions of σ_{LT} , $\sigma_{LT'}$, and $\sigma_{\pi 0}$ for $Q^2 = 0.127$ (upper three panels) and 0.200 (GeV/c^2) (lower three panels). The full curves indicate full MAID predictions, the dashed curves correspond to the MAID prediction without the quadrupole amplitudes. For details, see text.

In the Spring of 2003, new high-precision data in the $p(e, e'p)\pi^0$ channel were acquired at MAMI in the region of the Δ resonance, at four-momentum transfers of -0.06 , -0.127 , and -0.2 $(\text{GeV}/c)^2$. The anticipated results for the $E2/M1$ and $C2/M1$ ratios as a function of Q^2 are shown in Fig. 7.

In addition to our primary goal, the extractions of $E2/M1$ and $C2/M1$ ratios at different Q^2 , the present data set will try to answer several open questions arising from previous experiments at MIT-Bates and MAMI. For example, the measurement of $\sigma_{LT'}$ at $Q^2 = 0.2$ $(\text{GeV}/c)^2$ will address the significant disagreement between MAID and the $A_{LT'}$ result from Mainz, which is underestimated by MAID by about 25% [19]. The measurement of $\sigma_{LT'}$ at $Q^2 = 0.127$ $(\text{GeV}/c)^2$ which overlaps with Bates will try to yield more insight into the apparent inability of the models to simultaneously describe the polarisation components obtained in the recoil-polarisation measurements [20]. At present, it is unclear where the violation of the consistency relation between P'_x , P'_z , and P'_y comes from. The multipole structure of $\sigma_{LT'}$ resembles that of P'_y , so we expect new data to help resolve this issue. The expected data points in the angular distributions of σ_{LT} , $\sigma_{LT'}$, and $\sigma_{0\pi}$ at $Q^2 = 0.127$ and 0.200 $(\text{GeV}/c)^2$ are shown in Fig. 8.

References

1. E. Mazzucato et al., Phys. Rev. Lett. **57** (1986) 3144;
R. Beck et al., Phys. Rev. Lett. **65** (1990) 1841.
2. P. de Baenst, Nucl. Phys. B **24** (1970) 633;
I.A. Vainshtein, V.I. Zakharov, Nucl. Phys. B **36** (1972) 589.
3. V. Bernard, N. Kaiser, J. Gasser, U.-G. Meißner, Phys. Lett. B **268** (1991) 291 (1991);
V. Bernard et al., Nucl. Phys. B **383** (1992) 442;
V. Bernard, N. Kaiser, U.-G. Meißner, Z. Phys. C **70** (1996) 483.
4. H.B. van den Brink et al., Phys. Rev. Lett. **74** (1995) 3561;
T.P. Welch et al., Phys. Rev. Lett. **69** (1992) 2761.
5. M.O. Distler et al. (A1 Collaboration), Phys. Rev. Lett. **80** (1998) 2294.
6. V. Bernard, N. Kaiser, U.-G. Meißner, Nucl. Phys. A **607** (1996) 379;
erratum ibid. **633** (1998) 695.
7. H. Merkel et al. (A1 Collaboration), Phys. Rev. Lett. **88** (2002) 012301.
8. D. Drechsel, O. Hanstein, S. S. Kamalov, L. Tiator, Nucl. Phys. A **645** (1999) 145.
9. R. Lindgren, D.W. Higinbotham, J.R.M. Annand, V. Nelyubin (spokespersons), JLab Experiment E01-014.
10. J.C. Bergstrom et al., Phys. Rev. C **57** (1998) 3203.
11. S.R. Beane et al., Nucl. Phys. A **618** (1997) 381.
12. I. Ewald et al. (A1 Collaboration), Phys. Lett. B **499** (2001) 238.
13. H. Krebs, V. Bernard, U.-G. Meißner, Nucl. Phys. A **713** (2003) 405.
14. M.P. Rekalo, E. Tomasi-Gustafsson, Phys. Rev. C **66** (2002) 015203.
15. A. Liesenfeld, A.W. Richter, S. Širca et al. (A1 Collaboration), Phys. Lett. B **468** (1999) 20.
16. V. Bernard, L. Elouadrhiri, U.-G. Meißner, J. Phys. G: Nucl. Part. Phys. **28** (2002) R1.
17. R. Neuhausen (spokesperson), A1 Collaboration Proposal A1/1-98.
18. T. Sato, T.-S.H. Lee, Phys. Rev. C **63** (2001) 055201.
19. P. Bartsch et al. (A1 Collaboration), Phys. Rev. Lett. **88** (2002) 142001.
20. Th. Pospischil et al. (A1 Collaboration), Phys. Rev. Lett. **86** (2001) 2959.

BLEJSKE DELAVNICE IZ FIZIKE, LETNIK 4, ŠT. 1, ISSN 1580-4992

BLED WORKSHOPS IN PHYSICS, VOL. 4, NO. 1

Zbornik delavnice 'Quarks and Hadrons', Bled, 7. – 14. julij 2003

Proceedings of the Mini-Workshop 'Quarks and Hadrons', Bled, July 7-14, 2003

Uredili in oblikovali Bojan Golli, Mitja Rosina, Simon Širca

Publikacijo sofinancira Ministrstvo za šolstvo, znanost in šport

Tehnični urednik Andreja Čas

Založilo: DMFA – založništvo, Jadranska 19, 1000 Ljubljana, Slovenija

Natisnila Tiskarna MIGRAF v nakladi 100 izvodov

Publikacija DMFA številka 1550
